



Universitat Autònoma de Barcelona

ADVERTIMENT. L'accés als continguts d'aquesta tesi queda condicionat a l'acceptació de les condicions d'ús establertes per la següent llicència Creative Commons:  http://cat.creativecommons.org/?page_id=184

ADVERTENCIA. El acceso a los contenidos de esta tesis queda condicionado a la aceptación de las condiciones de uso establecidas por la siguiente licencia Creative Commons:  <http://es.creativecommons.org/blog/licencias/>

WARNING. The access to the contents of this doctoral thesis it is limited to the acceptance of the use conditions set by the following Creative Commons license:  <https://creativecommons.org/licenses/?lang=en>

UNIVERSITAT AUTÒNOMA DE BARCELONA

DOCTORAL THESIS

**Random walks under stochastic
resetting from a renewal
perspective**

Author:

Axel MASÓ-PUIGDELLOSAS

Supervisor:

Dr. Vicenç MÉNDEZ

*A thesis submitted in fulfillment of the requirements
for the degree of Physics PhD programme*

in the

Unitat de Física Estadística
Department de Física

November 4, 2022

Declaration of Authorship

I, Axel MASÓ-PUIGDELLOSAS, declare that this thesis titled “Random walks under stochastic resetting from a renewal perspective” and the work presented in it are my own. It is submitted as a compendium of four articles published in peer-reviewed journals with an international scope.

Axel Masó-Puigdellosas, Daniel Campos, and Vicenç Méndez, *Transport properties and first arrival statistics of random motion with stochastic reset times*, *Phys. Rev. E* **99**, 012141

Axel Masó-Puigdellosas, Daniel Campos, and Vicenç Méndez, *Stochastic movement subject to a reset-and-residence mechanism: transport properties and first arrival statistics*, *J. Stat. Mech.* (2019) 033201

Axel Masó-Puigdellosas, Daniel Campos, and Vicenç Méndez, *Transport properties of random walks under stochastic non-instantaneous resetting*, *Phys. Rev. E* **100**, 042104

Axel Masó-Puigdellosas, Daniel Campos, and Vicenç Méndez, *Conditioned backward and forward times of diffusion with stochastic resetting: A renewal theory approach*, *Phys. Rev. E* **106**, 034126

Axel MASÓ-PUIGDELLOSAS
Universitat Autònoma de Barcelona, **November 4, 2022**

Other works

Vicenç Méndez, Michael Assaf, **Axel Masó-Puigdellosas**, Daniel Campos and Werner Horsthemke, *Demographic stochasticity and extinction in populations with Allee effect*, *Phys. Rev. E* **99**, 022101

Axel Masó-Puigdellosas, Daniel Campos and Vicenç Méndez, *Anomalous Diffusion in Random-Walks With Memory-Induced Relocations*, *Frontiers in Physics* **7**, 112

Viktor Domazetoski, **Axel Masó-Puigdellosas**, Trifce Sandev, Vicenç Méndez, Alexander Iomin and Ljupco Kocarev, *Stochastic resetting on comblike structures*, *Phys. Rev. Research* **2**, 033027

Andreu Riera-Campenya, Jan Ollé and **Axel Masó-Puigdellosas**, *Measurement-induced resetting in open quantum systems*, [arXiv:2011.04403](https://arxiv.org/abs/2011.04403)

Vicenç Méndez, **Axel Masó-Puigdellosas**, Trifce Sandev and Daniel Campos, *Continuous time random walks under Markovian resetting*, *Phys. Rev. E* **103(2)**, 022103

Vicenç Méndez, **Axel Masó-Puigdellosas** and Daniel Campos, *Nonstandard diffusion under Markovian resetting in bounded domains*, *Physical Review E* **105(5)**, 054118

“Visc a un planeta ple d’ecosistemes. No és del tot rodó: el va escriure un moro que tenia mala lletra. Sa rotació gairebé no se nota. Ningú no ha vist sa translació perquè ens aplega en haver dinat quan feim horeta.”

Antònia Font

UNIVERSITAT AUTÒNOMA DE BARCELONA

Abstract

Facultat de Ciències

Department de Física

Physics PhD programme

Random walks under stochastic resetting from a renewal perspective

by Axel MASÓ-PUIGDELLOSAS

Stochastic models including resetting have attracted interest from the physics community due to their simple formulation, their wide range of applicability, and the properties emerging on the systems when restarted stochastically (e.g. the formation of non-equilibrium steady states and the optimization of the completion time of stochastic processes). In the articles composing this thesis, we investigate in what manner renewal theory provides an advantageous scheme to study stochastic processes with resets. We predominantly focus on diffusive random walks and, in some cases, on other types of stochastic motion, though most of the results can be straightforwardly generalized to other systems. We employ renewal equations to generalize some features of diffusion under Markovian resetting and to introduce novel elements to the previous models, such as an inactive period after resets and finite velocity resetting. Using the knowledge from renewal theory, we propose two novel magnitudes to study stochastic processes under resets: the conditioned backward and forward times. These are, respectively, the times since the last and until the upcoming reset given that we know the current state of the system (e.g. the position).

Acknowledgements

First of all, I would like to thank my supervisor Vicenç for his guidance and helpful advice in such an active research field as stochastic resetting is. Navigating through the enormous quantity of published works in such a dynamic topic and developing original ideas would have been impossible without his expertise.

To Daniel for the fruitful discussions during these years. Thank you for those ideas and suggestions which have by all means left a footprint on the results of this thesis. Likewise, to the collaborators of the papers which are not included in the thesis for expanding the horizons of this work. Thank you Viktor, Trifce, Andreu and Jan.

To my office colleagues (those who have left, those who will leave), as well as all the people in the department with whom I have exchanged more than a "*Hola, bon dia*", thank you for making this journey more pleasant.

Last but not least, I would like to thank Leo Messi, Arthur Melo, Aki Kaurismaki, Albert Serra and Gaspar Noé. Thanks to Laura Palmer, Miguel Noguera and one of the two Vengamonjas, to the people from the bar and some people in the E3 bus for making me happy every once in a while. And also to you all -you know who you are-, thanks for making me happy every single day. I owe you everything.

Contents

Declaration of Authorship	iii
Abstract	ix
Acknowledgements	xi
1 Introduction	1
1.1 Brief introduction to CTRWs	1
1.1.1 Diffusion equation	6
1.1.2 First passage time	6
1.2 Historical introduction to stochastic resetting	7
1.2.1 Early models. Population dynamics	8
1.2.2 Computer science. Algorithm optimisation	9
1.2.3 Recent models. Physics perspective	11
1.3 State of the art	13
1.4 Objectives	16
2 Results	19
2.1 First model	20
2.1.1 Transport properties	21
2.1.2 First passage time	22
2.1.3 Summary	24
2.2 Second model	24
2.2.1 Transport properties	25
2.2.2 First passage time	27
2.2.3 Summary	29
2.3 Third model	29
2.3.1 Markovian resetting	30
2.3.2 Pareto resetting	32
2.3.3 Return time PDF	33
2.3.4 Summary	34
2.4 Conditioned backward and forward times	35

2.4.1	Markovian resetting	36
2.4.2	Pareto resetting with $\gamma_R > 1$	37
2.4.3	Pareto resetting with $0 < \gamma_R < 1$	38
2.4.4	Summary	40
3	Conclusions	43
3.1	Open questions and further work	44
	Bibliography	45
A	First Article	51
B	Second Article	61
C	Third Article	79
D	Fourth Article	89

List of Abbreviations

CTRW	Continuous-Time Random Walk
FPT	First Passage Time
FPTD	First Passage Time Distribution
MSD	Mean Squared Displacement
MFAT	Mean First Arrival Time
MFPT	Mean First Passage Time
NESS	Non-Equilibrium Steady State
PDF	Probability Density Function

Ja està, mama.

Chapter 1

Introduction

There are countless systems in nature which suffer from sudden and often random changes on its behaviour. It may be the case of the extinction of a local population of animals due to a natural disaster, a drastic computer shut-down or the cease/activation of some metabolic processes in our body when we fall sleep. Resetting can be seen as a particular type of this wide class of phenomena. It consists on interrupting a process to readily start it again from its initial condition. There have been numerous attempts from the physical and mathematical community to model these type of phenomena. In this chapter we follow the path to which nowadays has become a field by itself: stochastic processes with resetting. In the articles composing this thesis, the focus is put on random walks under resets, so, in Section 1.1 of this introduction, relevant results from *Continuous-Time Random Walk* (CTRW) theory are introduced. In Section 1.2 we present an historical excursion through different perspectives on the problem of stochastic resetting, and the current state of the field is summarized in Section 1.3. Finally, in Section 1.4 the objectives of the further investigation are exposed. After introducing the context and the purpose of the thesis, Chapter 2 is devoted to summarize the articles included in Appendices. The conclusions and new perspectives on the field are proposed in Chapter 3.

1.1 Brief introduction to CTRWs

The continuous version of a random walk was firstly introduced by Montroll and Weiss in 1965 [1] as a generalisation of discrete random walks. There, time is considered as a continuous random variable starting at $t = 0$. After a stochastic time $t = t_1$ the walker jumps to the next position, waiting there until the second jump at $t = t_2$, and so on and so forth. The times between jumps ($\Delta t_1 = t_1 - 0$, $\Delta t_2 = t_2 - t_1, \dots$, $\Delta t_n = t_n - t_{n-1}$) are independent, identically distributed (*iid*) random variables called *waiting times*,

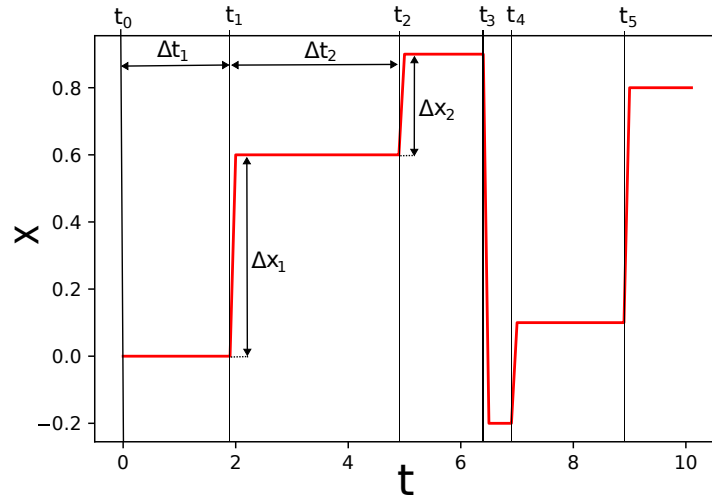


FIGURE 1.1: Illustrative trajectory of a CTRW from $t = 0$ to $t = 10$. The stochastic jump times t_i , the two first waiting times Δt_i and the two first jump lengths Δx_i have been represented. The value of x is the addition of the jump lengths up to the time t as expressed by Eq. (1.1).

their distribution being $\phi(\Delta t_i)$. The *jump length* Δx_n for each step $n = 1, 2, \dots$ is an *iid* random variable too with distribution $\Phi(\Delta x_n)$ (for a discrete lattice, $\Phi(\Delta x_n) = \delta(\Delta x_n)$, with $\delta(\cdot)$ the Dirac delta). In such a case, defining $N(t)$ as the number of jumps until time t , the position of the walker can be expressed as

$$x = \sum_{n=1}^{N(t)} \Delta x_n. \quad (1.1)$$

See Figure 1.1 for a sample trajectory.

Since the temporal and spatial variables are statistically independent, they can be treated separately to obtain the *probability density function* (PDF) of the process $P(x, t)$. This is, being $q_n(t)$ the probability of exactly n jumps happening *until* t and $p_n(x)$ the PDF of reaching x with n jumps, we have that

$$P(x, t) = \sum_{n=0}^{\infty} q_n(t) p_n(x), \quad (1.2)$$

where the sum is over all the possible number of jumps.

Starting by $p_n(x)$, it accounts for all the paths the walker may take to go from the initial position to x by jumping n times. Since the jump lengths are

iid random variables, one has that

$$p_n(x) = \begin{cases} \delta(x - x_0) & \text{for } n = 0 \\ \int_{-\infty}^{\infty} dx_1 \Phi(x_1 - x_0) \dots \int_{-\infty}^{\infty} dx_n \Phi(x_n - x_{n-1}) \delta(x - x_n) & \text{for } n \geq 1, \end{cases} \quad (1.3)$$

where x_0 is the initial position of the walker. The last integral ensures that the walker is at position x after n jumps. Defining the Fourier transform of a function $f(x)$ as

$$\tilde{f}(k) = \int_{-\infty}^{\infty} dx e^{-ikx} f(x), \quad (1.4)$$

with i the imaginary unit number and the initial position $x_0 = 0$ for simplicity, by the convolution theorem for the Fourier transform one finds (from Eq. (1.3))

$$\tilde{p}_n(k) = \tilde{\Phi}(k)^n \quad (1.5)$$

in the Fourier space.

Let us now compute $q_n(t)$ from Eq. (1.2) in terms of the waiting time distribution $\phi(t)$. Before doing so, it is convenient to compute the probability $Q_n(t)$ of the n -th jump being exactly *at* t . It can be written in terms of $Q_{n-1}(t)$ as

$$Q_n(t) = \int_0^t d\Delta t Q_{n-1}(t - \Delta t) \phi(\Delta t). \quad (1.6)$$

This is, the particle jumps for the $(n - 1)$ -th time at $t - \Delta t$ and waits a time Δt drawn from $\phi(\Delta t)$ before jumping once again. Defining the Laplace transform of a function $f(t)$ with $t \geq 0$ as

$$\mathcal{L}_s[f(t)] = \hat{f}(s) = \int_0^{\infty} dt e^{-st} f(t) \quad (1.7)$$

and using the convolution theorem for the Laplace transform on Eq. (1.6), one readily arrives to the recurrent relation

$$\hat{Q}_n(s) = \hat{Q}_{n-1}(s) \hat{\phi}(s) \quad (1.8)$$

in the Laplace space. One can find the expression for $n = 1$ by seeing that the first jump comes from the waiting time distribution, i.e. $Q_1(t) = \phi(t)$. Under this condition,

$$\hat{Q}_n(s) = \hat{\phi}(s)^n. \quad (1.9)$$

For further convenience. At this point, one can define the rate function $Q(t)$, being the total probability of the last event happening at time t , through its Laplace transform:

$$\hat{Q}(s) = \sum_{n=0}^{\infty} \hat{Q}_n(s) = \sum_{n=0}^{\infty} \hat{\phi}(s)^n = \frac{1}{1 - \hat{\phi}(s)}. \quad (1.10)$$

Now, we are interested in knowing the probability $q_n(t)$ of the walker having performed exactly n jumps *before* t . This, in terms of the above, reads

$$q_n(t) = \int_0^{\infty} d\Delta t Q_n(t - \Delta t) \phi^*(\Delta t), \quad (1.11)$$

where

$$\phi^*(\Delta t) = \int_{\Delta t}^{\infty} d\Delta t' \phi(\Delta t') \quad (1.12)$$

is the survival probability of $\phi(\Delta t)$, i.e. the probability of not jumping in the interval Δt . Using the convolution theorem on Eq. (1.11) and introducing Eq. (1.9), one gets

$$\hat{q}_n(s) = \hat{\phi}(s)^n \hat{\phi}^*(s). \quad (1.13)$$

Due to the stochastic independence of the spatial and temporal variables in Eq. (1.2), one can apply the Laplace transform on t and the Fourier transform on x to have the propagator of the CTRW in the Fourier-Laplace space:

$$\hat{P}(k, s) = \sum_{n=0}^{\infty} \hat{q}_n(s) \tilde{p}_n(k). \quad (1.14)$$

Finally, introducing both the results from Eq. (1.5) and Eq. (1.13) and summing over n , one gets the Montroll-Weiss equation, i.e.

$$\hat{P}(k, s) = \frac{\hat{\phi}^*(s)}{1 - \hat{\phi}(s) \tilde{\Phi}(k)}. \quad (1.15)$$

Now, depending on the waiting time and the jump length distributions, the propagator may take myriad forms with different properties and characteristics. Consider only symmetric processes with $\Phi(x) = \Phi(-x)$ (i.e. all the odd moments of $\Phi(x)$ are null). The arising processes can then be generally classified in three types in terms of the behaviour of its *mean-square displacement* (MSD) $\langle x^2(t) \rangle$: sub-diffusive, diffusive and Lévy flights.

- If the first moment $\langle \Delta t \rangle_{\phi}$ of $\phi(\Delta t)$ and the second moment $\langle \Delta x^2 \rangle_{\Phi}$ of $\Phi(\Delta x)$ are finite, then the process is diffusive, meaning that $\langle x^2(t) \rangle \sim t$. See an example in Figure 1.2. In such a case, in the small s (long t) and

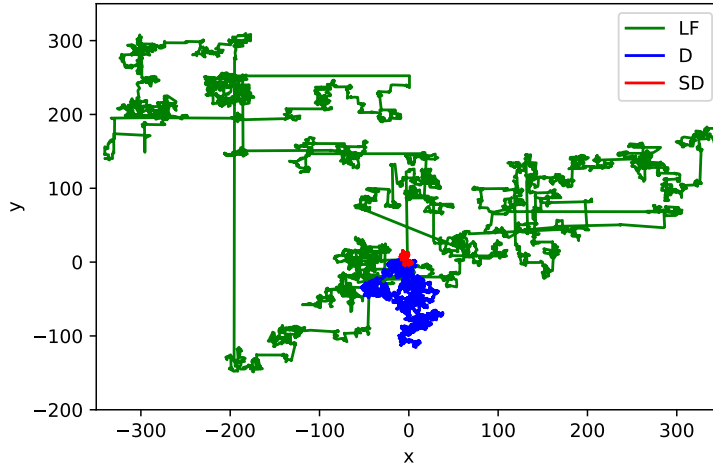


FIGURE 1.2: Sample trajectories for a diffusive CTRW (blue, D in the plot), a sub-diffusive CTRW (red, SD in the plot) and a Lévy flight (green, LF in the plot) for $t = 10^4$. With respect to the first and during the same amount of time, the sub-diffusive trajectory remains closer to the initial position, while the Lévy flight performs long jumps and explores remote regions.

small k (large x) limit, Eq.(1.15) reduces to the Gaussian propagator in the position and time space, i.e.

$$P(x, t) = \frac{1}{\sqrt{4\pi Dt}} e^{-\frac{x^2}{4Dt}}, \quad (1.16)$$

with $D = \frac{\langle x^2 \rangle_{\Phi}}{2\langle t \rangle_{\phi}}$. See [2] for further details.

- If the first moment of $\phi(\Delta t)$ diverges while the second moment of $\Phi(\Delta x)$ is finite, the process is sub-diffusive, meaning that $\langle x^2(t) \rangle \sim t^{\theta}$, $\theta < 1$. See an example in Figure 1.2.
- If the second moment of $\Phi(\Delta x)$ diverges, the process is a Lévy flight and its MSD is infinite too. See an example in Figure 1.2.

Note that, independently of the waiting times and the jump lengths, this CTRW model does not reach a stationary state. The propagator in Eq. (1.15) may evolve fast or slow in time but, in all cases, the walker moves away from the origin. For a more exhaustive dissemination on the topic we refer the interested reader to Chapter 3 from [2].

1.1.1 Diffusion equation

The above derivation for the propagator of the CTRW is based on the use of renewal theory. Nonetheless, for some particular types of walkers, $P(x, t)$ can be found by other means, e.g. for diffusive motion it is the solution of a partial differential equation

$$\frac{\partial P(x, t)}{\partial t} = D \frac{\partial^2 P(x, t)}{\partial x^2}, \quad (1.17)$$

which also corresponds to the Fokker-Planck equation for the propagator of a Brownian particle. A detailed derivation of the equation and its properties can be found in [3]. In the right hand side, D is the diffusion constant. Diffusion equations can be found for other types of motion (e.g. sub-diffusive random walks -see Chapter 6 from [2]) and give a different perspective for the understanding of random walks.

The solution of Eq. (1.17) for $x \in \mathbb{R}$ with initial condition $P(x, 0) = \delta(x)$ is the Gaussian propagator

$$P(x, t) = \frac{1}{\sqrt{4\pi Dt}} e^{-\frac{x^2}{4Dt}}, \quad (1.18)$$

which is the very same result obtained in Eq.(1.16) from a renewal perspective in the diffusive limit.

1.1.2 First passage time

The time spent to reach a particular position, i.e. the *first passage time* (FPT), is another interesting property of random walks. It is a stochastic variable itself, so it can be characterized by the *first passage time distribution* (FPTD) and its first moment, i.e. the *mean first passage time* (MFPT). Along with the propagator, the study of the first passage will be central in the course of the thesis. For this reason it is briefly introduced in this section.

When the random walk is diffusive with propagator in Eq. (1.18), then the FPTD reads

$$f(t; x_t) = \frac{|x_t|}{\sqrt{4\pi Dt^3}} e^{-\frac{|x_t|^2}{4Dt}} \sim \frac{1}{t^{3/2}}, \quad (1.19)$$

where x_t is the position of the target. Asymptotically, the FPTD decays as a power-law with exponent $3/2$, which is a well-known result related to the Sparre Andersen theorem [2, 4]. Since the exponent is lesser than 2, the MFPT

is infinite, i.e. the walker may get lost in the state space and never find the target. This divergence can be addressed, for instance, by confining the walker to a finite region [5, 6] or adding a bias to the motion [7].

Similarly to the diffusive case, sub-diffusive random walks and Lévy flights also have an infinite MFPT [8]. Actually, let us point out that it would be more accurate to call it mean first *arrival* time (MFAT). This is because, while for sub-diffusive and diffusive random walks the MFAT and the MFPT are equivalent, they differ in the case of Lévy flights as a consequence of longer jump lengths making the walker jump over the target. Nevertheless, MFPT will be used in the following pages as a general rule to remain true to the original term, while MFAT will be used when necessary only.

At this point, let us introduce a formula which will be of great importance in the articles of the compendium. There, the survival probability instead of the PDF will be often used to compute the MFPT. This is the probability of not having reached the target at time t , i.e.

$$S_{x_t}(t) = \int_t^\infty dt' f(t'; x_t). \quad (1.20)$$

Now, from the Laplace transform of the survival probability one can readily compute the MFPT to be

$$\langle t \rangle_{x_t} = \int_0^\infty t f(t; x_t) dt = \int_0^\infty [t S_{x_t}(t)]_0^\infty + \int_0^\infty S_{x_t}(t) dt = \hat{S}_{x_t}(s=0). \quad (1.21)$$

In the second equality, integration by parts have been applied. The first term cancels at both limits, while the second one is the Laplace transform of the survival probability for $s = 0$.

1.2 Historical introduction to stochastic resetting

Numerous attempts on describing stochastic dynamics with resetting have been made during the last decades from different perspectives. Here we present the three main approaches to the problem in a chronological order. The first resetting models were developed within the mathematical community, in the context of population dynamics during the 1970s (Section 1.2.1). In Section 1.2.2 we briefly introduce some investigations on the benefits of resetting stochastic algorithms and, finally, in Section 1.2.3 we present the recent developments made by the physics community.

1.2.1 Early models. Population dynamics

Population dynamics have been extensively studied from a mathematical point of view due to the simplicity of its models, but also because it leads to results which can be readily compared with reality [9]. A first example of these models is a birth-death process. It describes the evolution of an initial population of $n_0 \geq 0$ individuals, each of which may reproduce themselves with rate λ and die with rate μ . Thus, the overall population n evolves according to the following transition rates, starting from $n = n_0$:

Transition	Rate	Condition
$n \rightarrow n + 1$	λn	$n \geq 1$
$n \rightarrow n - 1$	μn	$n \geq 0$

For this class of models, the focus is often put on studying the extinction properties of the dynamics, as for instance the mean time to extinction or the probability of extinction. The time-dependent transition probabilities from a population of n individuals to a population of m individuals are also studied in some cases, as well as the existence of an equilibrium distribution [9].

The simplicity of the set-up permits the straight-forward introduction of further features to the model. For instance, a population-independent rate can be introduced to the $n \rightarrow n + 1$ transition to model immigration [10]. Also, catastrophes can be considered by introducing an additional, independent rate γ to model a sudden decrease in the population, such that $n \rightarrow n - m$, with $m \leq n$. This could be either a natural disaster causing the decrease of many individuals or a mass emigration of the population from a certain region [11, 12, 13, 14]. There, the population decrease in a catastrophe m is considered to be stochastic. This type of event is called to be a *partial* catastrophe. The main objective in these works is usually to compute the mean time to extinction or the extinction probability. Even for deterministic growth models, sudden catastrophes may provoke the extinction of the population [15, 16, 17].

Partial catastrophes may lead to the extinction of a population, but still can not be considered a resetting process. In [18], Kyriakidis and Abakuks developed an immigration-birth model with *total* catastrophes, which always reduce the population size to zero. After that, the number of individuals may rise again due to immigration. The transition rates of this process are summarized in the following table: where λ is the birth rate, α the immigration rate and γ the catastrophe rate. The aim of the study was to determine an optimal pest control protocol, minimizing the damage caused by the plague

Transition	Rate	Condition
$n \rightarrow n + 1$	$\lambda n + \alpha$	$n \geq 0$
$n \rightarrow 0$	γ	$n \geq 1$

and the cost of the protocol. This process, with the catastrophes being the complete annihilation of the plague, may be considered the first model of stochastic dynamics with resets.

Following the article by Kyriakidis and Abakuks, numerous authors have studied population models which may suffer total catastrophes and reborn afterwards [19, 20, 21, 22, 23, 24, 25]. The main interest there is to obtain the transient probabilities of the process and its stationary state. In [20, 23], the dynamics are studied by solving the Chapman-Kolmogorov master equation of the process, whilst in [19, 21, 22, 24, 25] a renewal equation perspective is employed. This dichotomy between differential equation models and a renewal formalism during the 2000s augurs what was to come during the 2010s within the physics community studying stochastic processes under resetting (see details in Section 1.3). The results by Economou and Fakinis in [24] are particularly interesting. There, a general formalism based on renewal equations is presented, which may be used to study a wide class of stochastic models with total catastrophes, among others.

These models may appear unreal due to the improbable chance of the total extinction of a group of individuals. Nevertheless, they start to gain practicality when considering a queue model instead of population dynamics. Parallel to the aforementioned articles, various works studied queue models with total catastrophes [26, 27], which may be applicable to solve task processing problems in electronic devices. There, catastrophes/resetting would correspond to the freezing or sudden breakdown of the processor.

1.2.2 Computer science. Algorithm optimisation

The study of stochastic processes has been historically approached from a mathematical perspective. Nevertheless, since the appearance of the first electronic programmable computer in the early 40s and the subsequent development of randomized algorithms, the concepts of probability and stochasticity began to gain more practical relevance in computer sciences [28]. Randomized algorithms are usually employed to solve problems with a large set of solutions. In these kind of problems, randomness is beneficial with respect to deterministic methods due to its capacity to optimally explore the

full solution space. Problem-solving randomized algorithms can be generally divided in two different groups:

- **Las Vegas algorithms** give either the solution or its non-existence as an outcome. Thus, their running time is a stochastic variable which depends on the structure of the solution space and the strategy to be employed.
- Contrarily, **Monte Carlo algorithms** give an approximated solution to the problem and its running time remains more controllable.

The performance of randomized algorithms have been usually enhanced by employing different techniques. For instance, by employing Guided Random Search Techniques (see Chapter 5 from [29]) or building dynamic schemes that can learn from the already visited set of solutions. In [30] a method to optimize Las Vegas algorithms by *restarting* it at stochastic times is developed. Their method starts by running the random algorithm for a number of steps t_1 . If the solution is not found at this point, the algorithm is restarted from the beginning with an independent seed, and it runs again for a number of steps t_2 , and so on. It turns out that if $t_1 = t_2 = \dots = t^*$, where t^* is a carefully chosen reset time, then the mean running time of any Las Vegas algorithm is minimized. This is, restarting may be beneficial to optimize a stochastic search. The very same result was found by Alt et al. [31] from a different perspective. They found that Las Vegas algorithms with heavy-tailed running time distributions could be turned into algorithms with short-tailed running time distributions by sequentially restarting them.

The capacity of restarts to reduce the running time of an algorithm may be surprising at first sight. Nevertheless, randomized algorithms may occasionally get lost in the solution space, searching far away from the actual solution to the problem. In these scenarios, a fresh restart of the process can bring the algorithm closer to the solution, avoiding long and fruitless searches (see Figure 1.3).

The results from [30] and [31] provide a universal restart strategy to enhance the performance of randomized algorithms, assuming previous knowledge about the running time distribution. This enables to find some general, theoretical results, but the method is not practical when dealing with most of the problems, which are often confronted with no previous knowledge about the running time distribution. This issue was approached some years later with the so called dynamic restart strategies (see [32], [33] and references therein). They consist on restarting the algorithm depending on whether it

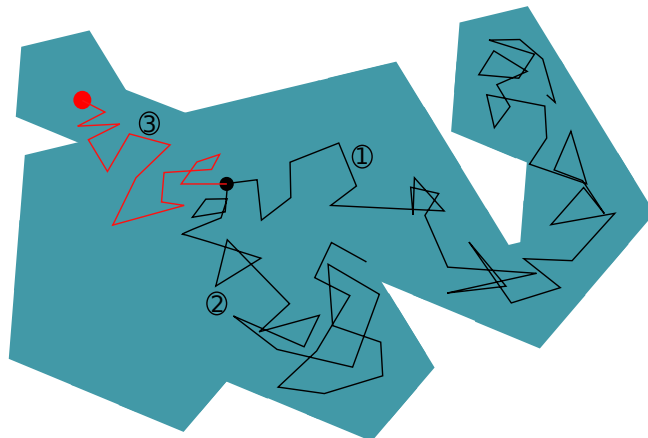


FIGURE 1.3: Schematic example of an exploration of the solution space (blue region). From the initial condition (black dot), in the first (1) attempt the algorithm explores a region far from the solution (red dot). By restarting, the algorithm is able to avoid being stuck in the dead end. After a second (2) attempt, the solution to the problem is found in the third (3) attempt.

may be beneficial or not, given the knowledge accumulated during its current execution. It is worth mentioning that restarting has been proven to enhance the performance of other processes in Computer Science. For instance, it can minimize the time required to retrieve a page in the world wide web [34] or improve the performance of clause learning to solve Boolean satisfiability problems (SAT) [35].

1.2.3 Recent models. Physics perspective

Resetting models firstly captured the attention of physicists in 1999 [36], when Manrubia and Zanette studied resetting on a stochastic multiplicative process, i.e. the variable n evolves according to the following rules:

Transition	Probability
$n \rightarrow \mu n$	$1 - p$
$n \rightarrow n_0$	p

where μ and n_0 may (or may not) be stochastic variables. This process resembles the ones studied many years before by mathematicians as seen in Section 1.2.1. Nevertheless, in their article, Manrubia and Zanette are interested in this process for the capacity to generate power-law stationary distributions for n .

The physics community, however, remained unaware of the potential of stochastic resetting until some years later, when Evans and Majumdar [37]

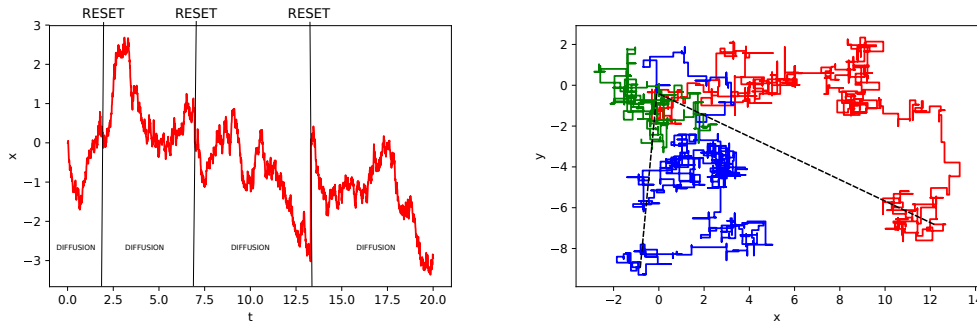


FIGURE 1.4: On the left, the plot shows the position of the diffusion process with resets described by Eq. (1.22), starting at $x_0 = 0$ and for particular values of r and D . Resets happen at $t = 2.1, 6.9, 13.1$. Between them, the motion can be described by the usual diffusion equation (see Eq. (1.17)). On the right, the trajectory of a two-dimensional random walk with resets is shown. The walker resets its position twice (dashed black lines), performing three different trajectories starting at the origin (sequentially: red, blue and green traces) during the simulation time.

developed an easy-to-operate model of diffusion with Markovian resetting. To do so, they built the Fokker-Planck equation for the dynamics of a Brownian particle initially located at point x_0 under a resetting Poisson process of its location to the initial position with a rate r . The propagator $\rho(x, t|x_0)$ of the particle follows

$$\frac{\partial \rho(x, t|x_0)}{\partial t} = D \frac{\partial^2 \rho(x, t|x_0)}{\partial x^2} - r\rho(x, t|x_0) + r\delta(x - x_0). \quad (1.22)$$

This corresponds to the usual Fokker-Planck equation for diffusion (see Eq. (1.17)) with two additional elements. The second term in the right hand side annihilates particles from any position at rate r , while the third reintroduces them to x_0 at the same rate. With this, they found a *non-equilibrium steady state* (NESS) to be

$$\rho_s(x) = \sqrt{\frac{r}{4D}} e^{-\sqrt{\frac{r}{D}}|x-x_0|} \quad (1.23)$$

and also an optimal, finite MFPT. This model is remarkable due to its capacity of capturing the two features of resetting previously observed by the mathematical and computer science communities separately. This is, the existence of a NESS and the ability of resetting to optimize the accomplishment of certain processes (see Figure 1.3 above) as the mean first passage time.

The simple manner these results were presented in [37] gave rise to many open questions (see Figure 1.4 for two examples of stochastic processes under

resets). For instance, does the existence of a NESS and an optimal MFPT hold for non-Markovian resetting? Does it hold for stochastic dynamics different than diffusion? What happens if the resetting is inherent to the motion (e.g. triggering when reaching a boundary) instead of an external element? Do the main features significantly change? Are there other magnitudes which could contribute to understand the details of stochastic processes under resets?

Some of these questions have been addressed during the last few years, yielding a considerable amount of works devoted to stochastic resetting. The existence of a non-equilibrium steady state (NESS) has been found to be non-exclusive of diffusion with Markovian resetting. For instance, a NESS is reached in various CTRW models [38, 39, 40, 41, 42] or variations of diffusion processes such as multi-dimensional diffusion [43], reaction-diffusion dynamics [44] and diffusion in potential landscapes [45] or bounded domains [46]. Also, non-Markovian resetting has been shown to be able to generate NESSs [42, 47, 48].

The optimization ability of resetting has been deeply studied from a physical perspective as well. In [49] the authors broadened the analyses of the optimal first passage time of a diffusing particle made in [37] by introducing a space dependent reset rate and randomizing the resetting position, as well as the position of the target. Other works have shown that different processes can be optimized when restarted, as for instance [50, 51, 52]. A general framework to study the mean completion time of a process with resets has been proposed in [50] from a Michaelis-Menten reaction scheme and in [53] by using renewal equations. Interestingly, in the latter they find that the optimal resetting strategy is a sharp reset (i.e. deterministic reset), which was also found in [30] for randomized algorithms with restart, as mentioned in the previous section.

These features have attracted a lot of attention from the scientific community and different techniques have been employed to describe stochastic processes with resets, most of which have been recently reviewed in [54]. In the following, the current state of the field is presented to frame the objectives of the thesis.

1.3 State of the art

In the recent literature, there are two main frameworks to model stochastic processes under resets: via the Fokker-Planck equation of the system or

from a renewal perspective. The first lets an intuitive, straightforward introduction of resetting to any process with a Fokker-Planck equation which is already known. The latter allows to build a much more detailed and versatile model.

Since the beginning, both frameworks have been equally used, depending on the purpose of the investigation. On one hand, in [37], resetting was smartly introduced to the Fokker-Planck equation for diffusion and its transport and first passage properties were derived. On the other hand, two years later, in [38], renewal equations were used to model a monotonous continuous-time random walk with drifts. The latter is beneficial, in the context of this thesis, because it allows for a much more detailed modelling of the process. By using renewal equations, one can control each of the elements conforming the model. An appropriate example to illustrate this point can be found in [51], where resetting is subordinated to motion, in the sense that the relocation of the walker is limited to when it is not moving. This degree of detail in the modelling of stochastic processes with resets can only be achieved by using renewal equations.

The advantage of modelling resetting using renewal equations lies in the fact that one can describe the entire process by considering the dynamics until the first reset only. After that, everything starts again. Thus, all the information about the process is contained in the initial excursion, which is repeatedly concatenated along time (see Figure 1.4 above). This has been employed by scientists to model many types of stochastic processes with resets, some of which have been already mentioned in Section 1.2.3. In [39, 55] renewal equations are used to study the existence of a NESS for stochastic dynamics under resets and in [40] the Sisyphus random walk is modelled with them. A renewal framework also allows to consider time-dependent reset rates [47], power-law reset times [48], or different types of stochastic processes such as run-and-tumble random walks [56] and ballistic motion [57].

The vast possibilities of the renewal perspective finds its splendour when modelling the first completion time of stochastic processes [53, 58, 59]. Since they allow for a general formulation, one can ask the question about the conditions under which resetting renders an optimal completion time. In such a case, the process can be modelled as follows. Consider the completion time without the presence of resetting to be a random variable T and the reset time to be another random variable R . If the process is completed before the reset happens ($T < R$), then the objective is accomplished in the first attempt.

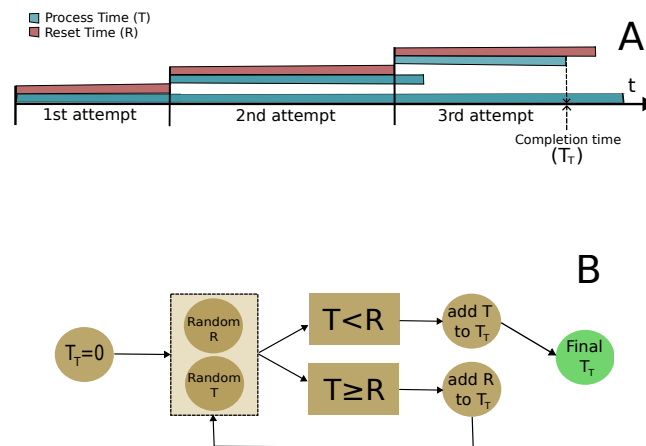


FIGURE 1.5: Panel A. In this example the process completes after three resets at time T_T . In the first attempt, resetting prevents the process to take a long time to complete since $R \ll T$. The process must restart again ($R < T$ in the second attempt to), before completing in the third attempt when $T < R$. Overall, the process is optimal because the time it would have taken to complete without resetting (first blue bar) is longer than the time considering resets (first two red bars and last blue bar). **Panel B.** Scheme for computing the total completion time T_T of a process with resets. If the reset time is shorter than the time required by the process to complete $T \geq R$, it restarts and the reset time is added to the total time. Otherwise $T < R$, the process is completed.

Otherwise, if $R \leq T$, the process restarts before finishing and it starts anew (see Figure 1.5). Therefore, the problem becomes to know how many times this competition must be repeated so that the first possibility happens. It is worth mentioning that this formulation allowed Pal and Reuveni to demonstrate that deterministic restart is optimal among all the possible strategies [53], answering an important question in the field.

Renewal equations and renewal theory appear as a magnificent framework to study stochastic processes under resets. Its versatility allows to consider very particular processes and, at the same time, general features of the dynamics. Thus, in light of the above, the starting point of the present thesis is to investigate the general properties of stochastic processes and, in particular, random walks under resets from a renewal perspective. Let us state the hypothesis to be tested in the course of the thesis.

1.4 Objectives

In the basis of what have been exposed in the sections above, let us present the main purposes of the thesis. The two ideas to be explained here gather the objectives that have been pursued in the four articles summarized in Chapter 2. The *first objective* refers to the connection between resetting and renewal theory. By the nature of the first, the latter appears as a suitable framework to study its properties. Therefore:

O1. *Employ renewal theory as a natural scheme to model the resetting of stochastic processes and, in particular, random walks.*

Renewal equations allow to build very detailed stochastic models. In the context of resetting, this feature is shown in [51], for instance, where the resets are subordinated to the motion of the walker. An objective derived from the previous is, thus:

O1'. *Employ renewal equations to introduce new elements to the resetting model.*

The vast majority of stochastic resetting models developed before the beginning of this thesis considered the resetting as an external agent taking the walker to the initial position instantaneously. This is far from what one can observe in real systems, where resetting often has a cost (temporal, energetic-wise...) and its characteristics may also depend on the state of the system. If

resetting models the return of an animal to the nest, for instance, the far the animal moves away, the longer it will take to return. Also, the homecoming will be more expansive energy-wise. As another example, in the restart of a stochastic algorithm, the process is neither instantaneous and it has a temporal cost to be considered in the running time of the method. Thus, considering these effects of resetting is important to characterize certain type of processes.

The *second objective* is related to the capacity of resetting to generate a NESS and also render optimal first passage times for random walks. This is:

O2. *Study the properties of resetting acting on stochastic processes and, in particular, on random walks (e.g. existence and shape of the stationary state, optimal first passage time,...). The properties may vary in terms of the particularities of the process and the resetting mechanism.*

At the beginning of this thesis, the vast majority of works on the topic considered Markovian resetting, i.e. with exponentially distributed reset times. They show that a NESS is reached in such cases. This raises the question of when and under which condition this property holds. One may consider, for instance, resets at times drawn from non-exponential distributions or include more complex elements to the model, as done in the compendium of articles summarized in the following chapter. Similarly, the capacity of resetting to render optimal first passage times is another property of interest for the community that deserves to be studied from a more general perspective.

Chapter 2

Results

In this chapter the most important results from the four articles in the compendium are summarized. The crucial points are introduced as a guide to follow the manuscripts, as well as to connect the results between them, giving a wider picture of its overall contribution to the field of stochastic resetting. The full texts of the published works are included in the appendices of the thesis.

The four articles summarized in this chapter are a sequence of models, each of which introducing novel elements to the previous. On this basis, the chapter is organized in four sections, corresponding to the four articles, respectively. In Section 2.1, the results from [60] (Appendix A) are presented, where a general model of stochastic motion with resets is introduced. Then, in Section 2.2 an inactive period after each reset is introduced to the model. This is studied in [61] (Appendix B). Section 2.3 corresponds to the results from [62] (Appendix C), where a non-instantaneous resetting mechanism is introduced and its effects to the overall dynamics are analysed. All these models are built on the basis of renewal equations and are focused on studying both the spatial dynamics of the motion and its first arrival (or passage) to a certain position. In [63] (Appendix D), two novel magnitudes to describe stochastic motion with resetting are considered, being the conditioned forward and the backward times. The results therein are summarized in Section 2.4.

A note on notation. *The results here presented proceed from articles elaborated at different moments. Hence, the notation used in each of them was chosen in terms of the particularities of the work. In this chapter, the notation will be unified to ease the reading and to facilitate a unified comprehension of the results. Thus, it may slightly differ from the notation used in the articles included in the appendix.*

2.1 First model

The main objective of the first work (see Appendix A or reference [60]) is to develop a general framework to study stochastic motion under resets. For this purpose, we employ renewal equations to find the *general propagator* $\rho(x, t)$ for a random walk under resetting in terms of the propagator $P(x, t)$ for the resetting-free random walk and the *reset time* PDF $\varphi_R(t)$. In particular, one finds that

$$\hat{\rho}(x, s) = \frac{\mathcal{L}_s[\varphi_R^*(t)P(x, t)]}{1 - \hat{\varphi}_R(s)}, \quad (2.1)$$

in the Laplace space for the time variable (see Eq. (2.2) in the article). From this, the MSD can be readily computed to be

$$\langle \hat{x}^2(s) \rangle = \frac{\mathcal{L}_s[\varphi_R^*(t)\langle \hat{x}^2(t) \rangle_m]}{1 - \hat{\varphi}_R(s)}. \quad (2.2)$$

Similarly, one can find the general survival probability of the walker not reaching a particular position x to be

$$\hat{\sigma}_x(s) = \frac{\mathcal{L}_s[\varphi_R^*(t)Q_x(t)]}{1 - \mathcal{L}_s[\varphi_R(t)Q_x(t)]}, \quad (2.3)$$

also in the Laplace space for the time variable (see Eq. (2.10) in the article). Here, $Q_x(t)$ is the survival probability of the dynamics without resetting. And the mean first arrival time can be obtained using Eq. (1.21):

$$\langle t \rangle_x = \frac{\int_0^\infty \varphi_R^*(t)Q_x(t)dt}{1 - \int_0^\infty \varphi_R(t)Q_x(t)dt}. \quad (2.4)$$

The generality of this formulation permits the analysis of many different systems. For instance, one can recover the results from [37] by choosing a Gaussian PDF for diffusive motion and exponentially distributed reset times. But it also allows us to generalize these results for other dynamics and resetting mechanisms (see Section III in the article) or studying the effects of resetting on more intricate processes (see Section IV in the article).

The most relevant results for the scope of this thesis are those in Section III of the aforementioned article. There, the existence of a NESS and a finite, optimal MFPT are analysed for different types of stochastic motion and resetting mechanisms. More specifically, sub-diffusive motion, diffusion and

Levy flights are considered, and the reset time PDF is chosen to be a Mittag-Leffler distribution, i.e.

$$\varphi_R(t) = \frac{t^{\gamma_R-1}}{\tau_R^{\gamma_R}} E_{\gamma_R, \gamma_R} \left[- \left(\frac{t}{\tau_R} \right)^{\gamma_R} \right]. \quad (2.5)$$

The choice of this distribution may at first glance seem arbitrary but it allows us to recover exponential PDFs for $\gamma_R = 1$, i.e.

$$\varphi_R(t) = \frac{1}{\tau_R} e^{-\frac{t}{\tau_R}}, \quad (2.6)$$

and also study power-law reset time PDFs such that $\varphi_R(t) \sim t^{-1-\gamma_R}$ for $\gamma_R < 1$. In the following, the results on the transport properties and the first passage of the overall process are summarized.

2.1.1 Transport properties

In the article we focus on isotropic random walks ($\langle x(t) \rangle_m = 0$) with $\langle x^2(t) \rangle_m \sim t^p$, where the subindex m means *motion*. This is, we consider all the processes without a preferential direction, from sub-diffusion $p < 1$ to diffusion $p = 1$, super-diffusion $1 < p < 2$ or Lévy flights $p = \infty$. With this, from Eq. (2.2) and Eq. (2.5) we find that the global MSD behaves as

$$\langle x^2(t) \rangle \sim \begin{cases} t^p, & \text{for } 0 < \gamma_R < 1 \\ t^0, & \text{for } \gamma_R = 1 \end{cases} \quad (2.7)$$

Thus, all types of motion reach a stationary value for exponential resetting ($\gamma_R = 1$), which generalizes the results in [37] and other works. Otherwise, when the resetting time is distributed according to a power-law Mittag-Leffler PDF ($\gamma_R < 1$), the MSD of the outcoming process scales as the MSD of the underlying dynamics. In this case the resetting only modifies the MSD by a multiplicative factor.

When a NESS is reached ($\gamma_R = 1$), the stationary PDF can be readily found from Eq. (2.1). In the benchmark of the article, this corresponds to the Markovian choice of the reset time PDF in Eq. (2.6). When the underlying motion is sub-diffusive, the stationary PDF reads

$$\rho_{ss}(x) = \frac{1}{\sqrt{4D\tau_R^\gamma}} e^{-\frac{|x|}{\sqrt{D\tau_R^\gamma}}}, \quad (2.8)$$

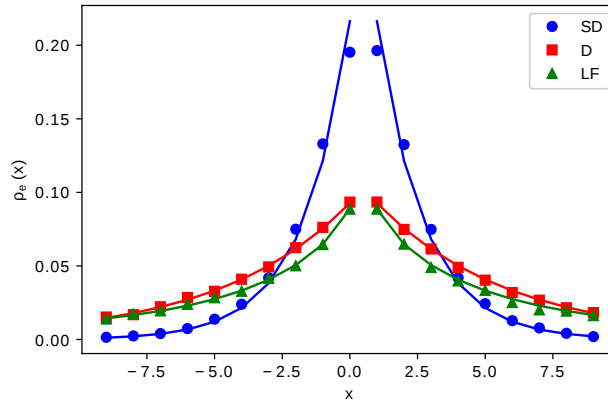


FIGURE 2.1: Stationary PDF of the overall process for sub-diffusive motion (SD), diffusion (D) and Lévy flights (LF). The dots, squares and triangles correspond to the numerical simulations, and the solid curves to the analytical expressions from Eqs. (2.8) and (2.9). Further details on the simulations can be found in the article.

where $\gamma \leq 1$ is the sub-diffusive exponent, with $\gamma = 1$ corresponding to diffusion (see Eq. (1.23) with $r = 1/\tau_R$). Otherwise, for an underlying Lévy motion, the stationary PDF can be found to be

$$\rho_{ss}(x) = 2 \int_0^{+\infty} \frac{\cos(kx)}{1 + \tau_R D k^\alpha} dk \sim \frac{1}{|x|^{1+\alpha}}, \text{ as } |x| \rightarrow \infty \quad (2.9)$$

with α the Lévy exponent ($\alpha \rightarrow 2$ corresponding to the diffusive limit). In the article, these two expressions are compared to numerical simulations of the process showing a good agreement (see Figure 2.1).

2.1.2 First passage time

To study the first passage of the walker to a given position x we consider a general form for the survival probability of the underlying process (i.e. for the process without resetting) of the form

$$Q_x(t) \sim t^{-q}, \quad q > 0, \quad (2.10)$$

for long t . This is, without resetting, the probability of not having reached the target scales as Eq. (2.10). The choice includes the survival probability for sub-diffusion when $q = \gamma/2$ with $\gamma < 1$ (see [7]), diffusion when $q = 1/2$ and Lévy flights when $q = 1 - 1/\alpha$ with $1 < \alpha < 2$ (see [64]). When this process is restarted at times given by Eq. (2.5), the survival probability can

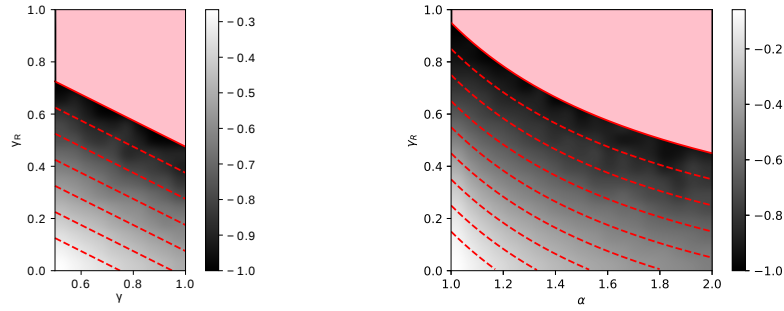


FIGURE 2.2: The tail exponent β of the survival probability $\sigma_x(t) \sim t^\beta$ of the overall process is shown for sub-diffusive motion (panel A) and Lévy flight (panel B), both restarted at times given by a Mittag-Leffler PDF with decay exponent γ_R . The solid curves are the limit between finite (flat pink region) and infinite (gradient) MFPT (MFAT for Lévy flights) in both plots. In panel A, it corresponds to $\gamma_R + \gamma/2 = 1$, while in panel B its equation reads $\gamma_R - 1/\alpha = 0$. Further details on the simulation may be found in the article.

be found to decay as

$$\sigma_x(t) \sim t^{-q-\gamma_R}, \text{ if } q + \gamma_R \leq 1. \quad (2.11)$$

Now, whenever $\gamma_R + q \leq 1$ the MFPT (MFAT for Lévy flights) diverges (see Section 1.1.2). Otherwise, if $q + \gamma_R > 1$, the MFPT in Eq. (2.4) is finite. In Figure 2.2 numerical simulations of the survival time are shown to be in good agreement with this results.

Interestingly, the MFPT can be finite even when the reset time PDF decays as a power law with infinite mean (pink region in Figure 2.2). For the sake of simplicity, let us consider the particular case of diffusion, corresponding to $\gamma = 1$ in panel A and $\alpha = 2$ in panel B. In such a case, the MFPT is finite when the reset time PDF decays as

$$\varphi_R(t) \sim t^{-1-\gamma_R}, \text{ with } 1/2 < \gamma_R < 1.$$

This is, the overall MFPT may be finite even when the mean reset time diverges. Recall that the MFPT of diffusion without resetting also diverges and its survival probability decays as

$$Q_x(t) \sim t^{-1/2},$$

corresponding to a PDF decaying as $t^{-3/2}$. Thus, an infinite mean reset time is capable of rendering a finite MFPT.

2.1.3 Summary

From renewal equations, a simple and versatile model to study stochastic processes with resets is formulated. It is employed to study sub- and super-diffusive motion and different resetting time PDFs. In recent years, other authors have applied the very same ideas to analyse different types of processes [52, 65, 66].

The results from the article show that, on one hand, the scaling of the MSD with time is unaltered when the resets come from a PDF with all diverging moments ($\gamma_R < 1$ in Eq. (2.5)). On the other hand, the MSD reaches a stationary value when all the moments of the reset time PDF are finite ($\gamma_R = 1$ in Eq. (2.5)). This raises the question of whether there is a smooth transition between the two cases or not. In [65] a Pareto-type distribution has been considered, which can have none, one, two, or any amount of finite moments in terms of its tail exponent. There, the authors show that the transition between non-altered scaling of the MSD and reaching a stationary value is soft and progressive. In particular, this soft transition happens in the region where the first moment of the reset time PDF is finite and the second diverges.

In [60] the decay exponent of the reset time PDF is shown to be particularly relevant for the properties of the first passage time of diffusion. While for $\gamma_R < 1/2$ the MFPT diverges, it is finite when $\gamma_R > 1/2$. The change in the properties of diffusion with scale-free resetting at $\gamma_R = 1/2$ will be seen to be non-exclusive of the MFPT in the articles to come.

2.2 Second model

In the second paper (see Appendix B or reference [61]), a novel element is incorporated to the model. It consists on a residence period after the resets during which the walker remains immobile. The motivation behind this model lies in that when a process is restarted, it usually requires a recovery period before starting anew. One may think of the time a random walk needs to travel to the reset position or the time an algorithm requires to start again.

Similarly to the previous model, we make use of renewal equations to get the statistics of the overall process. Here, we build a two-state model (one for the motion and one for the resting period), to get the general propagator

$$\hat{\rho}(x, s) = \frac{\hat{\phi}_S^*(s)\hat{\phi}_R(s)\delta(x) + \mathcal{L}_s[\varphi_R^*(t)P(x, t)]}{1 - \hat{\phi}_R(s)\hat{\phi}_S(s)}, \quad (2.12)$$

in the Laplace space for the time variable. In the equation, the Laplace transform of $\varphi_S(t)$ appears, which is the *residence time* PDF (i.e. the PDF of the time that the walker remains immobile after a reset). Note that this result reduces to the one in Eq. (2.1) when the residence period is chosen to be null, i.e. $\varphi_S(t) = \delta(t)$, corresponding to $\hat{\varphi}_S(s) = 1$ and $\hat{\varphi}_S^*(s) = 0$ in Eq. (2.12).

The survival probability of the motion with a target at a given position x can be computed to give

$$\hat{\sigma}_x(s) = \frac{\mathcal{L}_s[\varphi_R^*(t)Q_x(t)] + \mathcal{L}_s[\varphi_R^*(t)Q_x(t)]\hat{\varphi}_S^*(s)}{1 - \mathcal{L}_s[\varphi_R(t)Q_x(t)]\hat{\varphi}_S(s)} \quad (2.13)$$

and, when existing, the MFPT reads

$$\langle t \rangle_x = \frac{I_1 + \tau_s I_2}{1 - I_2}, \quad (2.14)$$

where

$$I_1 = \int_0^\infty \varphi_R^*(t)Q_x(t)dt, \quad (2.15)$$

$$I_2 = \int_0^\infty \varphi_R(t)Q_x(t)dt \quad (2.16)$$

and $\tau_s = \int_0^\infty t\varphi_S(t)dt$ is the mean residence time. Again, these results reduce to the ones from the previous model when the residence time is null ($\hat{\varphi}_S(s) = 1$ in Eq. (2.13) and $\tau_s = 0$ in Eq. (2.14)).

The new scenario is analysed similar to the model without residence period. Both the reset time and the residence time PDFs are chosen to be of the form in Eq. (2.5) for the reasons above mentioned. Then, the transport properties are studied in Sections III and IV from [61], while the first arrival properties are shown in Section V therein. In the following, the main results in the article are summarized.

2.2.1 Transport properties

When considering the collective transport of the dynamics, the residence period can be thought as a dynamic trap at the reset position. Whenever a particle resets its position, it is forced to stay immobile during a certain time.

Therefore, this new mechanism will reduce the transport capacity of the previously studied system. More specifically, if the MSD of the underlying motion scales as $\langle x^2(t) \rangle_m \sim t^p$, the MSD taking into account resets and the residence period scales as

$$\langle x^2(t) \rangle \sim t^a \quad (2.17)$$

with

$$a = \begin{cases} \gamma_S - 1, & \text{for } \gamma_R = 1 \\ p + \gamma_S - \gamma_R, & \text{for } \gamma_R < 1, \gamma_S < \gamma_R \\ p, & \text{for } \gamma_R < 1, \gamma_S \geq \gamma_R, \end{cases}$$

depending on the relation between the parameters γ_S and γ_R , being the tail exponents of the residence and the reset time PDFs respectively. Considering the residence period gives rise to a rich variety of transport regimes. There are three possible scenarios:

- When the reset time PDF is short-tailed ($\gamma_R = 1$), the motion may either collapse ($\langle x^2(t) \rangle \rightarrow 0$ for $\gamma_S < 1$), which is the case of a long-tailed residence time PDF, or tend to a stationary value ($\langle x^2(t) \rangle \rightarrow t^0$ for $\gamma_S = 1$). In the latter, the PDF in the NESS can be found to be

$$\rho_{ss}(x) = \frac{\tau_S}{\tau_R + \tau_S} \delta(x) + \frac{\tau_R}{\tau_R + \tau_S} \frac{e^{-\frac{|x|}{\sqrt{D\tau_R^\gamma}}}}{\sqrt{4D\tau_R^\gamma}} \quad (2.18)$$

for sub-diffusion (diffusion for $\gamma = 1$), and

$$\rho_{ss}(x) = \frac{\tau_S}{\tau_R + \tau_S} \delta(x) + \frac{\tau_R}{\tau_R + \tau_S} \int_0^{+\infty} \frac{\cos(kx)}{1 + \tau_R D_\alpha k^\alpha} dk \sim \frac{1}{|x|^{1+\alpha}}, \quad (2.19)$$

as $|x| \rightarrow \infty$, for Lévy flights (diffusion when $\alpha \rightarrow 2$). Notably, the shape of both the PDFs is the same as for a null residence period (see Eq. (2.8) and Eq. (2.9) and compare to the second term of the corresponding PDFs with residence period), weighted by the portion of time spent in the exploring state $\tau_R/(\tau_R + \tau_S)$. The rest of the time $\tau_S/(\tau_R + \tau_S)$ is spent at the origin in the residence state, i.e. the PDF of the walker is $\delta(x)$ (first term in Eq. (2.18) and Eq. (2.19)).

- When the reset time PDF is long-tailed ($\gamma_R < 1$) and the tail of the residence time PDF is even longer ($\gamma_S < \gamma_R$), the transport regime of the walker is modified. In Figure 2.3 all the cases are summarized in terms

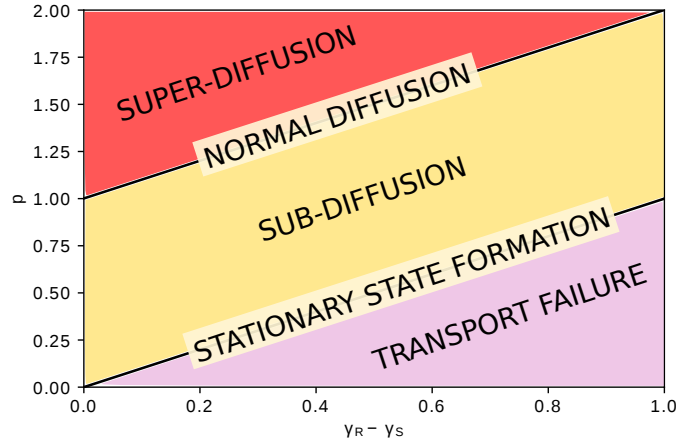


FIGURE 2.3: Summary of the transport regimes for an underlying motion with $\langle x^2(t) \rangle_m \sim t^p$ and reset and residence time distributions given by Eq. (2.5) with γ_R and γ_S respectively.

of p and the difference between the tail exponents $\gamma_R - \gamma_S$. This difference is relevant because it measures the asymptotics of the time spent by the walker in each of the two states. If it stays in the residence state longer than in the exploring state ($\gamma_R > \gamma_S$), the transport capacity of the system is diminished. For instance, an underlying super-diffusive process may become diffusive or even sub-diffusive when the reset-and-residence mechanism applies. Also, a sub-diffusive process may end up reaching a stationary state and more notably, if the residence period is long enough, the walkers may end up being trapped at the reset position (transport failure in Figure 2.3).

- When the reset time PDF is long-tailed ($\gamma_R < 1$) and the tail of the residence time PDF is shorter ($\gamma_S \geq \gamma_R$), the transport regime of the walker does not change. This is, when the time spent in the exploring regime is asymptotically longer than in the residence regime, the first prevails and the scenario is similar to the previous model (see Eq. (2.2)).

2.2.2 First passage time

The first passage properties of the walker under resets and the succeeding residence period was also studied in [61] in terms of the underlying motion and the characteristics of resetting. As in the previous model, we consider a general decay for the survival probability of the walker, i.e.

$$Q_x(t) \sim t^{-q}, \quad q > 0$$

	$\gamma_S = 1$	$\gamma_S < 1$
$\gamma_R + q > \gamma_S$	Finite MFPT	$\sigma_x(t) \sim t^{-(1-\gamma_S)}$
$\gamma_R + q \leq \gamma_S$	$\sigma_x(t) \sim t^{-(1-\gamma_R-q)}$	$\sigma_x(t) \sim t^{-(1-\gamma_R-q)}$

TABLE 2.1: Summary of the different cases for the asymptotic behaviour of the overall survival probability $\sigma_x(t)$. When it decays more rapidly than $\sigma_x(t) \sim t^{-1}$, the MFPT is finite (top-left case in the Table).

for long t . Then, the overall survival probability behaves differently depending on the reset and the residence time PDFs with parameters γ_R and γ_S respectively. In Table 2.1 all the casuistics in terms of the tail exponents are summarized.

- When the residence time PDF is long-tailed ($\gamma_S < 1$), the MFPT always diverges because the time the walker stays immobile after a reset is infinite (in average). However, the decay of the survival probability in this case may be determined either by the residence exponent γ_S or the motion exponent $\gamma_R + q$ (see previous article) depending on which of them is smaller. Then, when the residence time PDF is more important than the exploration time ($\gamma_S < \gamma_R + q$), the first is the one determining the decay of the overall survival probability and $\sigma_x(t) \sim t^{-(1-\gamma_S)}$. Otherwise, when the residence time is asymptotically shorter than the exploration time ($\gamma_S \geq \gamma_R + q$), the latter governs the overall process and $\sigma_x(t) \sim t^{-(1-\gamma_R-q)}$.
- Otherwise, when the residence time is exponential ($\gamma_R = 1$), the behaviour of the MFAT in this scenario is equivalent to the one studied in [60] (see Section 2.1.2). The difference lies in a finite additive factor accounting for the time the walker stays at the origin, which does not affect the asymptotic behaviour. Thus, the MFAT is finite whenever $\gamma_R + q \geq \gamma_R = 1$ and diverges for $\gamma_R + q < \gamma_S = 1$. In the latter case, the survival probability decays as $\sigma_x(t) \sim t^{-(1-\gamma_R-q)}$.

As done for the previous model, the general exponent q have a particular expression for every type of motion. The details on the sub-diffusive and diffusive cases and the Levy flights can be found in the article from Appendix B.

2.2.3 Summary

Using renewal equations to describe stochastic processes under resets permits an easy and straightforward introduction of novel elements to the model. The residence period that has been included in this article may allow resetting models to describe more diverse scenarios. The residence period barely affects the dynamics of the process at short times. When it reaches a steady state, the model with a residence period only differs from the previous in that a portion of the particles accumulate at the origin. Nevertheless, at longer times, the residence period may significantly affect the dynamics. Both the existence of the MFPT and the transport regime depend on the asymptotic relation between the residence and the reset time PDFs.

It is particularly interesting how the scaling of the MSD of the overall process may be smoothly modified by the combination of resets and the posterior residence period. Thus, a proper choice of the reset and the residence time PDFs could be used to tune the transport regime of a given process.

2.3 Third model

In the previous article, a recovery time after is included after the resets and before the stochastic process starts again. The model presented therein may serve in certain scenarios, but it considers the reset time and the residence period as independent random variables. This may be unreal in some cases. Think of the simple example of a diffusive walker with instantaneous resetting as studied in [37] and in the first article of this thesis. If we aim to consider the non-instantaneous nature of resetting in this case, the time needed by the walker to start again (i.e. the time it needs to return to the resetting position) would depend on its position. If the reset comes when the walker is near the resetting position, the reset will be faster than when far positions are reached. Thus, the time before starting again is correlated with the stochastic process and the reset time itself. In the third article of the thesis (see Appendix C or reference [62]) the transport and stationary properties of these dynamics are studied.

In the paper, a two-state model is introduced, similar to the one in [61]. The first state is called to be an *exploring state* described by a propagator $P(x, t)$ and lasting at a stochastic time given by a reset time PDF $\varphi_R(t)$. The second state or *returning state* consists on a ballistic motion with velocity v towards the origin. At the origin, the walker starts the exploring phase once

again. A renewal equation formalism allows us to find the global propagator of the process in the Laplace space for time to be

$$\hat{\rho}(x, s) = \frac{\Pi^*(x, s) + \frac{1}{v} e^{\frac{|x|}{v}s} \int_{|x|}^{+\infty} dz e^{-\frac{|z|}{v}s} \Pi(z, s)}{1 - \int_{-\infty}^{+\infty} dz e^{-\frac{|z|}{v}s} \Pi(z, s)}, \quad (2.20)$$

where

$$\Pi(x, s) = \mathcal{L}_s[\varphi_R(t)P(x, t)] \quad (2.21)$$

and

$$\Pi^*(x, s) = \mathcal{L}_s[\varphi_R^*(t)P(x, t)]. \quad (2.22)$$

Similarly, in the long t limit (small s), the MSD of the walker with resets can be expressed in terms of the moments of the dynamics without resetting $\langle |x|^n \rangle_P$ as

$$\langle \hat{x}^2(s) \rangle \simeq \frac{\mathcal{L}_s[\varphi_R^*(t)\langle x^2(t) \rangle_P] + \frac{1}{3v} \mathcal{L}_s[\varphi_R(t)\langle |x|^3(t) \rangle_P]}{1 - \hat{\varphi}_R(s) + \frac{s}{v} \mathcal{L}_s[\varphi_R^*(t)\langle |x|(t) \rangle_P]}. \quad (2.23)$$

In the infinite v limit, the expression for instantaneous resetting can be recovered (see Eq. (2.2)). Note that the absolute odd moments of the dynamics without resetting are important to describe the MSD with non-instantaneous resetting.

2.3.1 Markovian resetting

When the reset time PDF is exponential as in Eq. (2.6), the PDF from Eq. (2.20) reaches a stationary being

$$\rho_{ss}(x) = \frac{\hat{P}(x, s = 1/\tau_R) + \frac{1}{v\tau_R} \int_{|x|}^{+\infty} dz \hat{P}(z, s = 1/\tau_R)}{\tau_R + \frac{1}{v\tau_R} \langle |\hat{x}|(s = 1/\tau_R) \rangle_P}, \quad (2.24)$$

where the Laplace transform of $P(x, t)$ appears and also its absolute first moment $\langle |\hat{x}|(t) \rangle_P$. This expression has been derived in the context of a random walk with non-instantaneous returns, but it may also describe other stochastic processes with non-instantaneous resets. It is interesting to consider the stationary state when the free motion is diffusive. From Eq. (2.24), it reads

$$\rho_{ss}(x) = \frac{1}{\sqrt{4D\tau_R}} e^{-|x|/\sqrt{D\tau_R}}. \quad (2.25)$$

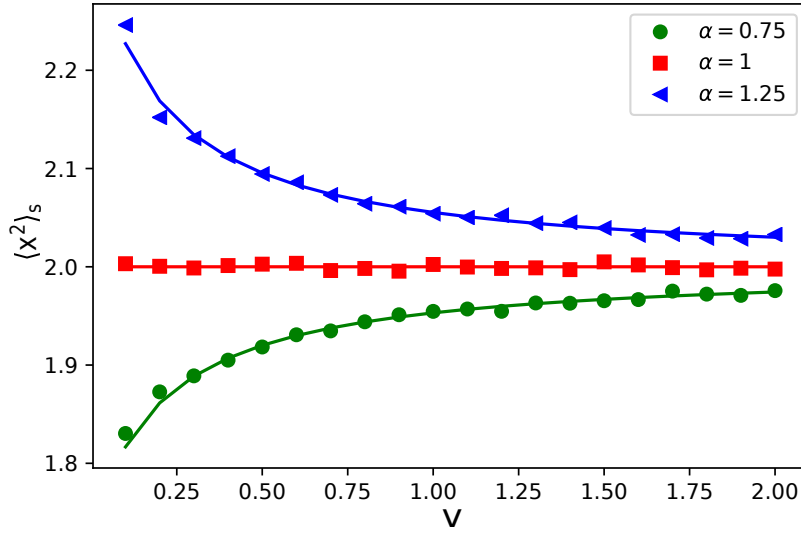


FIGURE 2.4: Stationary MSD for different fractional Brownian motion processes (see the article in Appendix C for further details) with Markovian resetting in terms of the return velocity v . Depending on the moments of the underlying motion, the MSD may increase, decrease or be independent with the returning velocity.

This is, the NESS is independent of the returning velocity and its PDF is the same as for instantaneous resets (see Eq. (2.9) for $\gamma_R = 1$ or reference [37]).

As for the stationary MSD, a general expression can be found in terms of the moments of the free motion:

$$\langle x^2 \rangle_{ss} = \frac{\langle \hat{x}^2(s = 1/\tau_R) \rangle_P + \frac{r}{3v} \langle |\hat{x}^3|(s = 1/\tau_R) \rangle_P}{\tau_R + \frac{1}{v\tau_R} \langle |\hat{x}|(s = 1/\tau_R) \rangle_P}. \quad (2.26)$$

Again, it reduces to the instantaneous resetting case when $v \rightarrow +\infty$. What is interesting here is that the stationary MSD may increase or decrease with the return velocity depending on the moments of the free motion. Let us define the ratio

$$\kappa = \frac{3}{\tau_R} \frac{\langle |\hat{x}|(s = 1/\tau_R) \rangle_P \langle \hat{x}^2(s = 1/\tau_R) \rangle_P}{\langle |\hat{x}^3|(s = 1/\tau_R) \rangle_P}. \quad (2.27)$$

Then, if $\kappa > 1$, the stationary MSD decreases with v , while when $\kappa < 1$ it increases with the returning velocity. In the limiting case $\kappa = 1$ the stationary MSD is independent of the returning velocity (e.g. when the free motion is diffusive). In Figure 2.4 we show this feature for a fractional brownian motion which allows us to switch between the different regimes for κ .

2.3.2 Pareto resetting

In the previous articles we used Mittag-Leffler PDFs to study long tailed distributions. Nevertheless, this choice is limited to decays such that $\varphi_R(t) \sim 1/t^{1+\gamma_R}$, with $\gamma_R < 1$, being the $\gamma_R = 1$ case an exponential PDF (see Section 2.1). In the current article scale-free resets are modeled by a Pareto PDF, i.e.

$$\varphi_R(t) = \frac{\gamma_R/\tau_R}{(1+t/\tau_R)^{1+\gamma_R}}. \quad (2.28)$$

This allows us to study an unrestricted range of decay exponents. Note that this definition is slightly different from the one in the article (see Eq. (2.29) therein), where $r = 1/\tau_R$ is used instead of τ_R . The aim of this choice is to keep consistency with the notation used in the previous articles. Regarding the exponent, it can take any real positive value ($\gamma_R > 0$), including the $0 < \gamma_R < 1$ region already considered with the Mittag-Leffler PDF above. With this, reset times with finite mean but diverging second moment ($1 < \gamma_R < 2$) can be studied too, and similarly for higher moments of the reset time PDF.

In the following, only diffusion will be considered for simplicity. From Eq. (2.20), one can see that a NESS is never attained when $\gamma < 1$. Recall that in such a case, a NESS is neither attained for instantaneous resetting (see Section 2.1). Contrarily, when $\gamma_R > 1$, the dynamics do reach a NESS with stationary PDF

$$\begin{aligned} \rho_{ss}(x) = & \frac{(\gamma_R - 1)/\sqrt{4\pi}}{\sqrt{D\tau_R} + \frac{D}{v} \frac{\Gamma(\gamma_R - \frac{1}{2})}{\Gamma(\gamma_R - 1)}} \left[\Gamma\left(\gamma_R - \frac{1}{2}\right) U\left(\gamma_R - \frac{1}{2}, \frac{1}{2}, \frac{x^2}{4D\tau_R}\right) \right. \\ & \left. + \frac{|x|}{2v\tau_R} \Gamma\left(\gamma_R + \frac{1}{2}\right) U\left(\gamma_R + \frac{1}{2}, \frac{3}{2}, \frac{x^2}{4D\tau_R}\right) \right], \end{aligned} \quad (2.29)$$

where $U(a, b, z)$ is the *Tricomi confluent hypergeometric function*. Asymptotically, it decays as

$$\rho_{ss}(x) \sim \frac{1}{|x|^{2\gamma_R - 1}}.$$

This is, as we increase γ_R , the even moments of the stationary PDF progressively become finite (all the odd moments are null due to the symmetry of the process). For instance, the MSD diverges when $\gamma_R < 2$, and it converges for $\gamma_R > 2$. Similarly, the fourth moment diverges when $\gamma_R < 3$ and converges otherwise, and so on and so forth.

The divergence of the MSD can be studied in more detail in terms of γ_R . From Eq. (2.23), one can find that, in the long t limit,

$$\langle x^2(t) \rangle \sim t^a \quad (2.30)$$

with

$$a = \begin{cases} 1, & \text{for } 0 < \gamma_R \leq 1 \\ 2 - \gamma_R, & \text{for } 1 < \gamma_R \leq 2 \\ 0, & \text{for } 2 < \gamma_R \end{cases}$$

Therefore, diffusion with scale-free, non-instantaneous resetting may still have a diffusive behaviour whenever the first moment of the reset time PDF diverges ($\gamma_R \leq 1$). This result is equivalent to the one found in [60] for instantaneous resetting. Nevertheless, if the tail decays more rapidly ($1 < \gamma_R \leq 2$), the transport regime becomes sub-diffusive and the exponent progressively decrease as $\gamma_R \rightarrow 2$. This is also equivalent to the instantaneous resetting scenario [65]. Finally, when $\gamma_R > 2$, the MSD attains a stationary.

2.3.3 Return time PDF

A natural question to ask about walkers with non-instantaneous resetting is how much time does it spend to return to the origin. Intuitively, it should depend on the type of motion: the faster it moves away from the origin, the longer it will take to return. Also, the longer the reset time is, the far the walker will be able to reach; therefore, the return time will be longer. Thus, the return time should depend on both the motion and the resetting.

In [62], an expression for the PDF of the *returning time* $\varphi_r(t)$ is found in terms of the free motion and the reset time PDFs:

$$\varphi_r(t) = 2v \int_0^\infty dt' P(vt, t') \varphi_R(t'). \quad (2.31)$$

And the n -th moment reads:

$$\langle t_r^n \rangle = \frac{1}{v^n} \int_0^{+\infty} dt \varphi_R(t) \langle |x(t)|^n \rangle_P. \quad (2.32)$$

This is, there is a one-to-one correspondence between the n -th moment of the return time PDF and the n -th moment of the motion PDF.

For diffusion with Markovian resetting, one can easily derive the return time PDF to be

$$\varphi_r(t) = \frac{v}{\sqrt{D\tau_R}} e^{-\frac{v}{\sqrt{D\tau_R}} t}. \quad (2.33)$$

This is, the return time PDF is also exponential (as the reset time PDF) and one can define a return rate to be

$$r_r = \frac{v}{\sqrt{D\tau_R}}, \quad (2.34)$$

which depends on the reset time PDF via the reset rate $r = 1/\tau_R$, on the diffusion via its constant D and also on the return velocity v .

If instead of diffusion with Markovian resets we consider scale-free resetting with a Pareto reset time PDF, the return time PDF becomes a bit more intricate:

$$\varphi_r(t) = \frac{v\gamma_R}{\sqrt{\pi D\tau_R}} \Gamma\left(\gamma_R + \frac{1}{2}\right) U\left(\gamma_R + \frac{1}{2}, \frac{1}{2}; \frac{v^2}{4D\tau_R} t^2\right) \sim \frac{1}{t^{2\gamma_R+1}} \quad (2.35)$$

The n -th moment of the PDF can be also computed from Eq. (2.32) (also from Eq.(2.35)) to give

$$\langle t_r^n \rangle = \frac{\Gamma(1+n)\Gamma(1+\frac{n}{2})\Gamma(\gamma_R - \frac{n}{2})}{\sqrt{\pi}\Gamma(\gamma_R)} \left(\frac{\sqrt{4D\tau_R}}{v}\right)^n, \quad (2.36)$$

only for $\gamma_R < n/2$. Otherwise, it is infinite. Thus, depending on the tail exponent of the Pareto PDF γ_R , the n -th moment may diverge or have a finite value. If

$$\gamma_R > \frac{n}{2}, \quad (2.37)$$

then the n -th moment of the return time PDF converges. In other words, all the moments such that $n < 2\gamma_R$ exist, while they diverge for $n \geq 2\gamma_R$. In particular, regarding the mean of the return time, it exists whenever $\gamma_R > 1/2$; again, for scale-free resetting, $\gamma_R = 1/2$ becomes relevant when describing the statistical properties of the process.

2.3.4 Summary

Renewal equations permits an easy introduction of a finite velocity resetting mechanism to diffusion. In the case that the reset time is Markovian, the stationary distribution is independent of the return velocity and equal to the stationary state found in [37] for instantaneous resetting. Contrarily, when the reset time PDF is scale-free, a stationary state is only reached when the first moment of the reset time exists ($\gamma_R < 1$). When considering the MSD of the position of the walker, it scales linearly with time in such a case. For $1 < \gamma_R < 2$ a sub-diffusive behaviour with exponent smoothly decreasing

linearly with γ_R until $\gamma_R \geq 2$, where a stationary MSD is reached. This result is equivalent to the asymptotic behaviour of diffusion with instantaneous resetting [65].

The return time PDF is also analysed in the article. The distribution is exponential when the reset time PDF is exponential too, while for Pareto reset time PDFs it takes the form of a Tricomi confluent hypergeometric function. In the latter case, the mean return time is finite only when $\gamma_R > 1/2$. This happens as well for the first passage time of diffusion with instantaneous resets (see Section 2.1.2).

2.4 Conditioned backward and forward times

In the last work of the thesis (see Appendix D or reference [63]) we recover the scenario from the first model: a random walk with instantaneous resetting. More in particular, the random walk is considered to be diffusive for the sake of simplicity, though the results displayed in the following may be extrapolated to other types of stochastic processes.

The main objective of this paper is to take advantage of the intrinsic relation between renewal processes and resetting to bring novel tools to analyse the processes under resets. In the three models presented above (and in the vast majority of the stochastic resetting literature [54]), the MSD and the first completion of the process are the main objects of study. Here, the *conditioned backward and forward times* are introduced as additional elements to explore the dynamics of the system.

Similar to the well-known backward and forward times from renewal theory (see [67] and Chapter 7 in [68] for details), the conditioned backward B and forward F times respectively correspond to the times since the last and until the next reset *given that* the position of the walker $x(t)$ is known at the current time. This is, from a present observation of the process, one can estimate when the time of the closest resets.

In terms of the propagator $\rho(x, t)$ and $Q(t)$ defined in Eq. (1.10) (i.e. the probability of the last event happening at time t), the long time limit of the conditioned backward time PDF can be written as:

$$f(B|x, t) \simeq \frac{Q(t)}{\rho(x, t)} \varphi_R^*(B) P(x, B), \quad (2.38)$$

where $P(x, t)$ is, in this case, the Gaussian PDF of a diffusive process and

$\varphi_R^*(t)$ the survival probability of the reset time PDF. Similarly, the conditioned forward time PDF reads, in the long time limit:

$$f(F|x, t) \simeq \frac{\int_0^t dt' Q(t-t') \varphi_R(t'+F) P(x, t')}{\rho(x, t)}. \quad (2.39)$$

Especially interesting is when the conditioned backward or forward time PDFs reach a stationary. Then, we can define

$$f(B|x) \equiv \lim_{t \rightarrow \infty} f(B|x, t) \quad (2.40)$$

and

$$f(F|x) \equiv \lim_{t \rightarrow \infty} f(F|x, t), \quad (2.41)$$

respectively. In such a case, whenever the process is measured after a long time, only the position of the walker (or state, in general) is needed to get information about the last and the next reset. Note that, for instance, the time dependence of the conditioned backward time comes from $Q(t)/\rho(x, t)$ only. Therefore, if this ratio reaches a stationary value (i.e. $\lim_{t \rightarrow \infty} Q(t)/\rho(x, t)$ is finite and non-zero), then a stationary conditioned backward time PDF exists. Remarkably, these expressions are general for any stochastic process with resets, though in the article we put the focus on diffusion. In the following, the results for a diffusive random walker with exponential and Pareto reset time PDFs are exposed.

2.4.1 Markovian resetting

When the resetting is Markovian, it is well-known that the propagator reaches the NESS in Eq. (1.23). Also,

$$\lim_{t \rightarrow \infty} Q(t) = \frac{1}{\langle t \rangle_{\varphi_R}} = \frac{1}{\tau_R} \quad (2.42)$$

is time independent. Thus, from Eq. (2.38), the conditioned backward time PDF does not depend on time neither and it behaves as

$$f(B|x) \sim \frac{e^{-\frac{B}{\tau_R}} - \frac{x^2}{4DB}}{\sqrt{B}}. \quad (2.43)$$

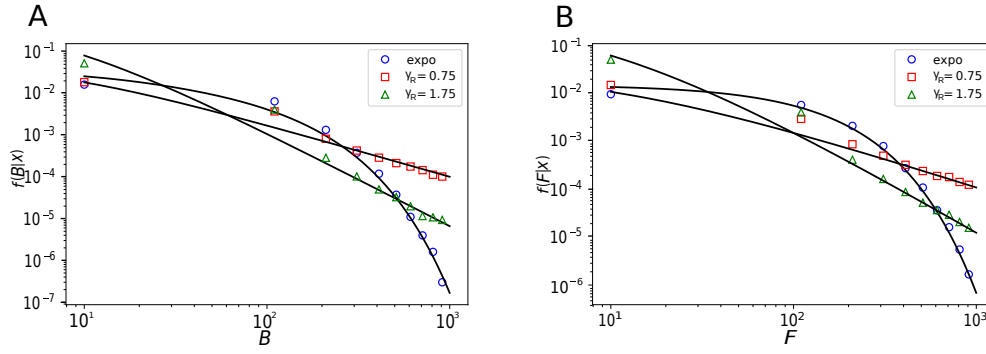


FIGURE 2.5: Stationary conditioned backward (*panel A*) and forward (*panel B*) time distribution for diffusion and exponential resetting with $\tau_R = 20$ (circles) and under Pareto resetting with $\tau_R = 5$ and two different values of the decay exponent: $\gamma_R = 0.75$ (squares) and $\gamma_R = 1.75$ (triangles). The solid lines have been drawn from the behaviours in Eq. (2.43) and Eq. (2.46) for the exponential and Pareto cases of panel A, respectively. In panel B, Eq. (2.44) and Eq. (2.47) have been plotted, respectively.

Similarly, the conditioned forward time PDF can be found to be

$$f(F|x) \simeq \frac{1}{\tau_R} e^{-\frac{F}{\tau_R}}. \quad (2.44)$$

Note that, while in the article from Appendix D the exponential PDF is defined in terms of the rate r , here we use the mean τ_R to parameterize it. They are related through $r = 1/\tau_R$.

Therefore, at long times, if the current position is known, the statistics of the backward and the forward times can be readily obtained. The conditioned forward time PDF, for instance, is exponential and independent on the position of the walker, i.e. the probability of an upcoming reset is always the same. This is due to the Markovianity of the resetting process. Otherwise, the conditioned backward time PDF does depend on the current position of the walker. In Figure 2.5 a good agreement with simulations of the process is shown.

2.4.2 Pareto resetting with $\gamma_R > 1$

If, instead of resetting at times given by an exponential PDF, the reset time PDF is a Pareto distribution of the form in Eq. (2.28), the dynamics of the walker become different. In such a case, the long-time behaviour extremely depends on the tail exponent γ_R and, in particular, on whether the first moment of the reset time PDF exists or not.

Let us start by the case where the first moment of $\varphi_R(t)$ exists, i.e. $\gamma_R > 1$. In such a case, the dynamics reach a stationary state given by

$$\rho_s(x) = \frac{\gamma_R - 1}{4\pi D\tau_R} \Gamma\left(\gamma_R - \frac{1}{2}\right) U\left(\gamma_R - \frac{1}{2}, \frac{1}{2}, \frac{x^2}{4D\tau_R}\right). \quad (2.45)$$

As for the exponential reset time PDF, $\lim_{t \rightarrow \infty} Q(t) = 1/\langle t \rangle_{\varphi_R}$, which is finite for $\gamma_R > 1$. Therefore, in this case Eq. (2.38) tends to an asymptotic PDF which behaves as

$$f(B|x) \sim \frac{e^{-\frac{x^2}{4DB}}}{\sqrt{B}(1 + B/\tau_R)^{\gamma_R}}. \quad (2.46)$$

And from Eq. (2.39), the conditioned forward time PDF also reaches a stationary form which depends on F via

$$f(F|x) \sim \frac{U\left(\gamma_R + \frac{1}{2}, \frac{1}{2}, \frac{x^2}{4D(\tau_R + F)}\right)}{(1 + F/\tau_R)^{\gamma_R + \frac{1}{2}}}. \quad (2.47)$$

Again, for long enough measurement times, information about the backward and the forward times can be obtained from the current position only. In this case the PDFs become more intricate, but statistical information (e.g. mean, variance or higher moments) can still be obtained from these expressions. The simulations for this scenario are also displayed in Figure 2.5.

2.4.3 Pareto resetting with $0 < \gamma_R < 1$

When the first moment of the reset time PDF diverges ($\gamma_R < 1$) the scenario becomes more intricate. A stationary state is not reached in this case and the long time limit of the dynamics is not universal for all values of γ_R . This is, when $t \gg T$ and also $t \gg x^2/D$,

$$\rho(x, t) \simeq \begin{cases} \frac{\Gamma(\frac{1}{2} - \gamma_R)}{2\pi\Gamma(1 - \gamma_R)} \frac{1}{\sqrt{Dt}} & \text{if } 0 < \gamma_R < \frac{1}{2} \\ \frac{\sin(\pi\gamma_R)\Gamma(2\gamma_R - 1)}{\pi\Gamma(\gamma_R)(Dt)^{1 - \gamma_R}} \frac{1}{|x|^{2\gamma_R - 1}}, & \text{if } \frac{1}{2} < \gamma_R < 1, \end{cases} \quad (2.48)$$

which behave differently for $\gamma_R < 1/2$ than for $\gamma_R > 1/2$. Once again, a transition between two distinct behaviours is found at $\gamma_R = 1/2$, which can be observed in numerical simulations too (see Figure 2.6)

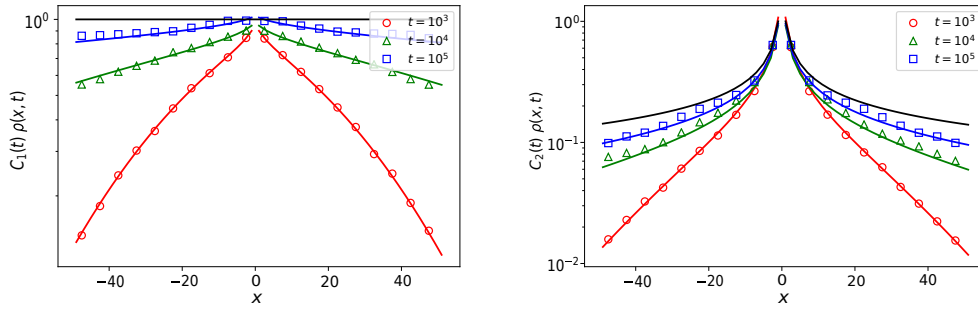


FIGURE 2.6: Panel A: Propagator of diffusion with Pareto resetting ($\gamma_R = 0.25$) for the simulation of $N = 10^5$ trajectories at different measurement times t . The multiplicative factor in the y-axis is $C_1(t) = \frac{2\pi\Gamma(1-\gamma_R)}{\Gamma(1/2-\gamma_R)}\sqrt{Dt}$. As the time increases, the renormalized propagator tends to be flat as found in Eq. (2.48). **Panel B:** Propagator of diffusion with Pareto resetting ($\gamma_R = 0.75$) for the simulation of $N = 10^5$ trajectories at different measurement times t . The multiplicative factor in the y-axis is $C_2(t) = \frac{\pi\Gamma(\gamma_R)(Dt)^{1-\gamma_R}}{\sin(\pi\gamma_R)\Gamma(2\gamma_R-1)}$. As time increases, the propagator approaches this scaling limit. In both panel A and panel B, the diffusion constant is $D = 0.5$ and $T = 1$ in the Pareto reset distribution. The dots, the triangles and the squares correspond to the propagator obtained from the simulations. The solid black curves correspond to the asymptotic behaviour found in Eq. (2.48). Both panels have been plotted in Log-Lin axis.

In the long t limit,

$$Q(t) \simeq \frac{\tau_R^{-\gamma_R}}{\Gamma(1-\gamma_R)\Gamma(\gamma_R)t^{1-\gamma_R}}, \quad t \gg \tau_R, \quad (2.49)$$

and, with this, one can analyse the asymptotic behaviour of the conditioned forward and the backward times in Eq. (2.38) and Eq. (2.39). Let us start by the first. While the dependence on B is the same as in Eq. (2.46), the ratio between $Q(t)$ and the propagator when $t \gg x^2/D$ is

$$\frac{Q(t)}{\rho(x, t)} \simeq \begin{cases} \frac{2\pi}{\Gamma(\gamma_R)\Gamma(\frac{1}{2}-\gamma_R)} \frac{\sqrt{D}}{T^{\gamma_R}t^{\frac{1}{2}-\gamma_R}} & \text{if } 0 < \gamma_R < \frac{1}{2} \\ \frac{\Gamma(\gamma_R)}{\Gamma(2\gamma_R-1)} \frac{|x|^{2\gamma_R-1}}{D^{1-\gamma_R}T^{\gamma_R}}, & \text{if } \frac{1}{2} < \gamma_R < 1, \end{cases} \quad (2.50)$$

which is time independent only for $\gamma_R > 1/2$. Consequently, a stationary conditioned backward time PDF is reached only in this case (see Figure 2.5

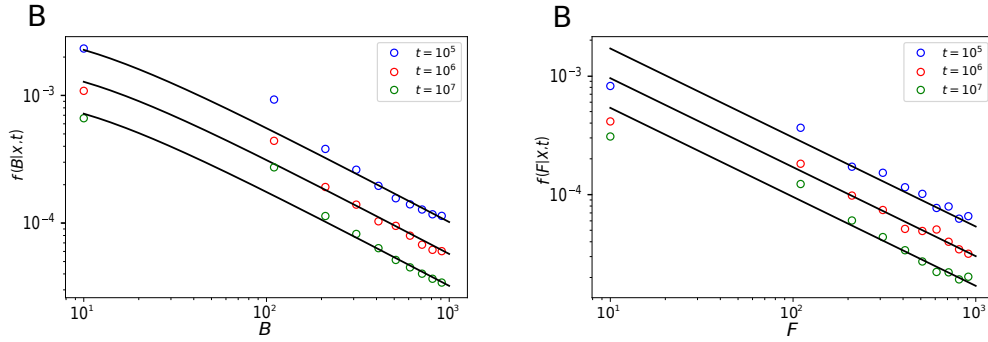


FIGURE 2.7: *Conditioned backward (A) and forward (B) time PDF for diffusion and Pareto resetting with $\tau_R = 5$ and $\gamma_R = 0.25$. Three different measurement times have been plotted, showing that $f(B|x,t)$ and $f(F|x,t)$ do not reach a stationary shape. Both the panels A and B have been obtained averaging $N = 10^6$ different trajectories with diffusion constant $D = 0.1$.*

for numerical simulations of the process). Furthermore, the conditioned forward time PDF can be found to decay as

$$f(F|x,t) \sim \begin{cases} \frac{t^{\gamma_R - \frac{1}{2}}}{F^{\frac{1}{2} + \gamma_R}}, & \text{for } 0 < \gamma_R < \frac{1}{2} \\ \frac{\tau_R^{\gamma_R - \frac{1}{2}}}{F^{\frac{1}{2} + \gamma_R}}, & \text{for } \frac{1}{2} < \gamma_R < 1 \end{cases} \quad (2.51)$$

with F . Similar to the backward time, there is a transition at $\gamma_R = 1/2$ such that below this value, the conditioned forward time PDF does not reach a stationary shape, while it does when $\gamma_R > 1/2$. This has also been corroborated via numerical simulations. In Figure 2.5 the case $\gamma_R = 3/4$ is shown to reach a stationary distribution, while in Figure 2.7 the case $\gamma_R = 1/4$ is shown to be time-dependent.

2.4.4 Summary

From the concepts of backward and forward time of renewal theory, one can define the corresponding times under the condition that the current position of the walker or, in general, the current state of the stochastic process are known. Provided that the dynamics started a long time ago, it is sometimes possible to obtain the PDF of the backward and the forward times conditioned to the position of the walker at the present time. This may be of interest for those cases where the time since the process started is unknown, but the current state of the system can be easily measured.

In this work we again find a transition in the properties of the system for $\gamma_R = 1/2$. Firstly, the propagator of the walker with Pareto reset time PDF with $\gamma_R < 1/2$ differs significantly from the propagator when $\gamma_R > 1/2$ (see Figure 2.6). Secondly, this distinct behaviour provokes that the properties of the conditioned forward and backward times also change at $\gamma_R = 1/2$.

Chapter 3

Conclusions

In this thesis, the resetting of random walks has been studied from a renewal perspective, developing three different models with increasing complexity and proposing novel tools to gain knowledge about the walkers. The conclusions of each work composing the thesis may be found in the corresponding articles. Here, in order to conclude the thesis as a unity, we review the objectives proposed in Section 1.4, giving an overview of our contribution to the field of stochastic resetting.

Modelling stochastic resetting by means of renewal equations present several advantages respecting to the use of the diffusion equation with resets (see **O1** in Section 1.4). In the model from the fourth article (see Appendix D), the temporal dynamics of resetting are treated independently of the spatial dynamics of the walker. This dissociation is important because the temporal dynamics of resetting can be described as a renewal process, which have been thoroughly studied in the literature (see, for instance, Chapter 7 in [68]). During the last years, in fact, many authors have been employing renewal theory to model stochastic processes under restarts [52, 65, 66].

More importantly, from renewal equations one can build a general framework for stochastic processes under resets (see **O1'** in Section 1.4). This permits us considering many types of walkers and reset time distributions in a simple and straightforward manner (see Section 2.1). Furthermore, novel elements can be intuitively introduced to the model, making it more complex and malleable to describe practical scenarios (see Section 2.2 and Section 2.3). This point leads us to the last objective.

Using renewal equations to model stochastic motion under resetting has allowed us to widen the knowledge about this class of processes (see **O2** in Section 1.4). Do resetting always generate a NESS? If not, under which circumstances does stationarity arise? Does it always render optimal MFPTs? These questions are considered in all the models described in the previous

section. In the first model, for instance, the existence of a NESS and an optimal MFPT is studied for a general class of dynamics. The very same properties have been also analysed for more intricate models, as the ones in the second and the third articles. Notably, for long-tailed reset time PDFs such that $\varphi_R(t) \sim 1/t^{1+\gamma_R}$, the decay exponent $\gamma_R = 1/2$ becomes particularly relevant on the description of the system. There are several properties of the system that change drastically when moving from below ($\gamma_R < 1/2$) to above ($\gamma_R > 1/2$) this change-point.

Finally, the framework herein employed allows us to define the conditioned forward and backward times in the article from Section 2.4. Studying these magnitudes contribute to the description of stochastic processes with resetting, taking advantage of its connection with renewal theory.

3.1 Open questions and further work

To finish, let us highlight some lines of research that may be of interest for the community, following from the results presented on this thesis. Resetting has been lately considered on many different stochastic processes other than movement [52, 69, 70]. The list of systems that may be described by stochastic resetting is endless: computer algorithms, investing strategies, human behaviour, chemical reactions, etc.

Besides the novel elements introduced in this thesis, another interesting mechanism to further consideration is resetting triggered by the dynamics of the process itself. This is, instead of being random, resetting could be self-triggered when a given condition is fulfilled (e.g. finding food in the case of animal foraging or getting stuck in a local minimum on a stochastic algorithm). In this same direction, resetting models should be employed to describe natural processes in more detail. At this point, the vast majority of the works devoted to the topic (including ours) focus on studying the properties of well-known, academic stochastic processes under resets. Nevertheless, apart from the work in [71], the experimental applications of these models are yet to be considered.

Furthermore, there are some open questions yet to be investigated. What is the reason behind the drastic change of behaviour at $\gamma_R = 1/2$ for diffusion with long-tailed reset time PDFs? Do the results from this thesis hold for other type of reset time PDFs? Are there other reset-based mechanisms able to tune the transport regime of diffusion? These and many other questions may widen our knowledge of stochastic processes under resets.

Bibliography

- [1] Elliott W Montroll and George H Weiss. “Random walks on lattices. II”. In: *Journal of Mathematical Physics* 6.2 (1965), pp. 167–181.
- [2] J. Klafter and I. M. Sokolov. *First Steps in Random Walks: From Tools to Applications*. Oxford University Press, Aug. 2011. ISBN: 9780199234868.
- [3] Vicenç Méndez, Daniel Campos, and Frederic Bartumeus. *Stochastic foundations in movement ecology*. Springer, 2016.
- [4] Erik Sparre Andersen. “On the fluctuations of sums of random variables II”. In: *Mathematica Scandinavica* 2 (1954), pp. 195–223.
- [5] M Khantha and V Balakrishnan. “First passage time distributions for finite one-dimensional random walks”. In: *Pramana* 21.2 (1983), pp. 111–122.
- [6] S Condamin et al. “First-passage times in complex scale-invariant media”. In: *Nature* 450.7166 (2007), pp. 77–80.
- [7] Govindan Rangarajan and Mingzhou Ding. “First passage time problem for biased continuous-time random walks”. In: *Fractals* 8.02 (2000), pp. 139–145.
- [8] V Balakrishnan and M Khantha. “First passage time and escape time distributions for continuous time random walks”. In: *Pramana* 21.3 (1983), pp. 187–200.
- [9] Samuel Karlin and James McGregor. “The Classification of Birth and Death Processes”. In: *Transactions of the American Mathematical Society* 86.2 (1957), pp. 366–400. (Visited on 06/06/2022).
- [10] “Introduction to the Mathematics of Population, Nathan Keyfitz, Addison-Wesley Publishing Co., London, 1968, pp. 450”. In: *The Australian and New Zealand Journal of Sociology* 5.2 (1969), pp. 162–162.
- [11] Norman Kaplan, Aidan Sudbury, and Trygve S Nilsen. “A branching process with disasters”. In: *Journal of Applied Probability* 12.1 (1975), pp. 47–59.

- [12] AG Pakes, AC Trajstman, and PJ Brockwell. "A stochastic model for a replicating population subjected to mass emigration due to population pressure". In: *Mathematical Biosciences* 45.1-2 (1979), pp. 137–157.
- [13] Peter J Brockwell, J Gani, and Sidney I Resnick. "Birth, immigration and catastrophe processes". In: *Advances in Applied Probability* 14.4 (1982), pp. 709–731.
- [14] Peter J Brockwell. "The extinction time of a general birth and death process with catastrophes". In: *Journal of Applied Probability* 23.4 (1986), pp. 851–858.
- [15] DNP Murthy. "A model for population extinction". In: *Applied Mathematical Modelling* 5.4 (1981), pp. 227–230.
- [16] Floyd B Hanson and Henry C Tuckwell. "Logistic growth with random density independent disasters". In: *Theoretical Population Biology* 19.1 (1981), pp. 1–18.
- [17] AC Trajstman. "A bounded growth population subjected to emigrations due to population pressure". In: *Journal of Applied Probability* 18.3 (1981), pp. 571–582.
- [18] EG Kyriakidis and Andris Abakuks. "Optimal pest control through catastrophes". In: *Journal of applied probability* 26.4 (1989), pp. 873–879.
- [19] EG Kyriakidis. "Stationary probabilities for a simple immigration-birth-death process under the influence of total catastrophes". In: *Statistics & Probability Letters* 20.3 (1994), pp. 239–240.
- [20] Randall J Swift. "Transient probabilities for a simple birth-death-immigration process under the influence of total catastrophes". In: *International Journal of Mathematics and Mathematical Sciences* 25.10 (2001), pp. 689–692.
- [21] EG Kyriakidis. "Transient solution for a simple immigration birth–death catastrophe process". In: *Probability in the Engineering and Informational Sciences* 18.2 (2004), pp. 233–236.
- [22] David Stirzaker. "Letters to the Editor-Disasters". In: *Mathematical Scientist* 26.1 (2001), p. 59.
- [23] Xiuli Chao and Yuxi Zheng. "Transient analysis of immigration birth–death processes with total catastrophes". In: *Probability in the Engineering and Informational Sciences* 17.1 (2003), pp. 83–106.

- [24] Antonis Economou and Demetrios Fakinos. "A continuous-time Markov chain under the influence of a regulating point process and applications in stochastic models with catastrophes". In: *European Journal of Operational Research* 149.3 (2003), pp. 625–640.
- [25] Antonis Economou and Demetris Fakinos. "Alternative approaches for the transient analysis of Markov chains with catastrophes". In: *Journal of Statistical Theory and Practice* 2.2 (2008), pp. 183–197.
- [26] B Krishna Kumar and D Arivudainambi. "Transient solution of an M/M/1 queue with catastrophes". In: *Computers & Mathematics with applications* 40.10-11 (2000), pp. 1233–1240.
- [27] Antonio Di Crescenzo et al. "On the M/M/1 queue with catastrophes and its continuous approximation". In: *Queueing Systems* 43.4 (2003), pp. 329–347.
- [28] N Metropolis. "The beginning". In: *Los Alamos Science* 15 (1987), pp. 125–130.
- [29] Jaroslaw Sobieszczanski-Sobieski, Alan Morris, and Michel Van Tooren. *Multidisciplinary design optimization supported by knowledge based engineering*. John Wiley & Sons, 2015.
- [30] Michael Luby, Alistair Sinclair, and David Zuckerman. "Optimal speedup of Las Vegas algorithms". In: *Information Processing Letters* 47.4 (1993), pp. 173–180.
- [31] Helmut Alt et al. "A method for obtaining randomized algorithms with small tail probabilities". In: *Algorithmica* 16.4 (1996), pp. 543–547.
- [32] Eric Horvitz et al. "A Bayesian Approach to Tackling Hard Computational Problems (Preliminary Report)". In: *Electronic Notes in Discrete Mathematics* 9 (2001), pp. 376–391.
- [33] Henry Kautz et al. "Dynamic restart policies". In: *Aaai/iaai* 97 (2002), pp. 674–681.
- [34] Bernardo A Huberman, Rajan M Lukose, and Tad Hogg. "An economics approach to hard computational problems". In: *Science* 275.5296 (1997), pp. 51–54.
- [35] Jinbo Huang. "The Effect of Restarts on the Efficiency of Clause Learning." In: 7 (2007), pp. 2318–2323.
- [36] Susanna C Manrubia and Damián H Zanette. "Stochastic multiplicative processes with reset events". In: *Physical Review E* 59.5 (1999), p. 4945.

- [37] Martin R Evans and Satya N Majumdar. "Diffusion with stochastic resetting". In: *Physical Review Letters* 106.16 (2011), p. 160601.
- [38] Miquel Montero and Javier Villarroel. "Monotonic continuous-time random walks with drift and stochastic reset events". In: *Physical Review E* 87.1 (2013), p. 012116.
- [39] Vicenç Méndez and Daniel Campos. "Characterization of stationary states in random walks with stochastic resetting". In: *Physical Review E* 93.2 (2016), p. 022106.
- [40] Miquel Montero and Javier Villarroel. "Directed random walk with random restarts: The Sisyphus random walk". In: *Phys. Rev. E* 94 (2016), p. 032132.
- [41] Miquel Montero, Axel Masó-Puigdellosas, and Javier Villarroel. "Continuous-time random walks with reset events". In: *The European Physical Journal B* 90.9 (2017), p. 176.
- [42] V. P. Shkilev. "Continuous-time random walk under time-dependent resetting". In: *Physical Review E* 96.1 (2017), p. 012126.
- [43] Martin R Evans and Satya N Majumdar. "Diffusion with resetting in arbitrary spatial dimension". In: *Journal of Physics A: Mathematical and Theoretical* 47.28 (2014), p. 285001.
- [44] Xavier Durang, Malte Henkel, and Hyunggyu Park. "The statistical mechanics of the coagulation–diffusion process with a stochastic reset". In: *Journal of Physics A: Mathematical and Theoretical* 47.4 (2014), p. 045002.
- [45] Arnab Pal. "Diffusion in a potential landscape with stochastic resetting". In: *Physical Review E* 91.1 (2015), p. 012113.
- [46] Christos Christou and Andreas Schadschneider. "Diffusion with resetting in bounded domains". In: *Journal of Physics A: Mathematical and Theoretical* 48.28 (2015), p. 285003.
- [47] Arnab Pal, Anupam Kundu, and Martin R Evans. "Diffusion under time-dependent resetting". In: *Journal of Physics A: Mathematical and Theoretical* 49.22 (2016), p. 225001.
- [48] Apoorva Nagar and Shamik Gupta. "Diffusion with stochastic resetting at power-law times". In: *Physical Review E* 93.6 (2016), p. 060102.

- [49] Martin R Evans and Satya N Majumdar. “Diffusion with optimal resetting”. In: *Journal of Physics A: Mathematical and Theoretical* 44.43 (2011), p. 435001.
- [50] Shlomi Reuveni, Michael Urbakh, and Joseph Klafter. “Role of substrate unbinding in Michaelis–Menten enzymatic reactions”. In: *Proceedings of the National Academy of Sciences* 111.12 (2014), pp. 4391–4396.
- [51] Daniel Campos and Vicenç Méndez. “Phase transitions in optimal search times: How random walkers should combine resetting and flight scales”. In: *Physical Review E* 92.6 (2015), p. 062115.
- [52] Sergey Belan. “Restart Could Optimize the Probability of Success in a Bernoulli Trial”. In: *Phys. Rev. Lett.* 120 (8 2018), p. 080601.
- [53] Arnab Pal and Shlomi Reuveni. “First passage under restart”. In: *Physical Review Letters* 118.3 (2017), p. 030603.
- [54] Martin R Evans, Satya N Majumdar, and Grégory Schehr. In: 53.19 (2020), p. 193001.
- [55] Satya N Majumdar, Sanjib Sabhapandit, and Grégory Schehr. “Random walk with random resetting to the maximum position”. In: *Physical Review E* 92.5 (2015), p. 052126.
- [56] Martin R Evans and Satya N Majumdar. “Effects of refractory period on stochastic resetting”. In: *Journal of Physics A: Mathematical and Theoretical* 52.1 (2018), 01LT01.
- [57] Javier Villarroel and Miquel Montero. “Continuous-time ballistic process with random resets”. In: *Journal of Statistical Mechanics: Theory and Experiment* 2018.12 (2018), p. 123204.
- [58] Shlomi Reuveni. “Optimal Stochastic Restart Renders Fluctuations in First Passage Times Universal”. In: *Phys. Rev. Lett.* 116 (2016), p. 170601.
- [59] A. Checkin and I. M. Sokolov. “Random Search with Resetting: A Unified Renewal Approach”. In: *Phys. Rev. Lett.* 121 (2018), p. 050601.
- [60] Axel Masó-Puigdellosas, Daniel Campos, and Vicenç Méndez. “Transport properties and first-arrival statistics of random motion with stochastic reset times”. In: *Phys. Rev. E* 99 (2019), p. 012141.
- [61] Axel Masó-Puigdellosas, Daniel Campos, and Vicenç Méndez. “Stochastic movement subject to a reset-and-residence mechanism: transport properties and first arrival statistics”. In: *Journal of Statistical Mechanics: Theory and Experiment* 2019.3 (2019), p. 033201.

- [62] Axel Masó-Puigdellosas, Daniel Campos, and Vicenç Méndez. “Anomalous Diffusion in Random-Walks With Memory-Induced Relocations”. In: *Frontiers in Physics* 7 (2019), p. 112.
- [63] Axel Masó-Puigdellosas, Daniel Campos, and Vicenç Méndez. “Conditioned backward and forward times of diffusion with stochastic resetting: A renewal theory approach”. In: *Phys. Rev. E* 106 (2022), p. 034126.
- [64] Aleksei V Chechkin et al. “First passage and arrival time densities for Lévy flights and the failure of the method of images”. In: *Journal of Physics A: Mathematical and General* 36.41 (2003), p. L537.
- [65] Anna S. Bodrova, Aleksei V. Chechkin, and Igor M. Sokolov. “Scaled Brownian motion with renewal resetting”. In: *Phys. Rev. E* 100 (2019), p. 012120.
- [66] Jaume Masoliver. “Telegraphic processes with stochastic resetting”. In: *Phys. Rev. E* 99 (1 2019), p. 012121.
- [67] D.R. Cox. *Renewal Theory*. Methuen’s monographs on applied probability and statistics. Methuen; New York, Wiley, 1962.
- [68] Sheldon M Ross. *Introduction to probability models*. Academic press, 2014.
- [69] Urna Basu, Anupam Kundu, and Arnab Pal. “Symmetric exclusion process under stochastic resetting”. In: *Phys. Rev. E* 100 (3 2019), p. 032136.
- [70] Matteo Magoni, Satya N. Majumdar, and Grégory Schehr. “Ising model with stochastic resetting”. In: *Phys. Rev. Research* 2 (3 2020), p. 033182.
- [71] Ofir Tal-Friedman et al. “Experimental Realization of Diffusion with Stochastic Resetting”. In: *The Journal of Physical Chemistry Letters* 11 (2020), pp. 7350–7355.

Appendix A

First Article

Transport properties and first arrival statistics of random motion with stochastic reset times

Axel Masó-Puigdellosas, Daniel Campos and Vicenç Méndez

Grup de Física Estadística. Departament de Física, Universitat Autònoma de Barcelona, 08193 Bellaterra, Spain

This paper has been published in *Phys. Rev. E* **99**, 012141

Transport properties and first-arrival statistics of random motion with stochastic reset times

Axel Masó-Puigdellosas, Daniel Campos, and Vicenç Méndez

Grup de Física Estadística, Departament de Física, Facultat de Ciències, Edifici Cc. Universitat Autònoma de Barcelona, 08193 Bellaterra (Barcelona), Spain

(Received 3 October 2018; published 28 January 2019)

Stochastic resets have lately emerged as a mechanism able to generate finite equilibrium mean-square displacement (MSD) when they are applied to diffusive motion. Furthermore, walkers with an infinite mean first-arrival time (MFAT) to a given position x may reach it in a finite time when they reset their position. In this work we study these emerging phenomena from a unified perspective. On one hand, we study the existence of a finite equilibrium MSD when resets are applied to random motion with $\langle x^2(t) \rangle_m \sim t^p$ for $0 < p \leq 2$. For exponentially distributed reset times, a compact formula is derived for the equilibrium MSD of the overall process in terms of the mean reset time and the motion MSD. On the other hand, we also test the robustness of the finiteness of the MFAT for different motion dynamics which are subject to stochastic resets. Finally, we study a biased Brownian oscillator with resets with the general formulas derived in this work, finding its equilibrium first moment and MSD and its MFAT to the minimum of the harmonic potential.

DOI: [10.1103/PhysRevE.99.012141](https://doi.org/10.1103/PhysRevE.99.012141)**I. INTRODUCTION**

The strategies employed by animals when they seek food are complex and strongly dependent on the species. A better understanding of their fundamental aspects would be crucial to control some critical situations as the appearance of invading species in a certain region or to prevent weak species to extinct, for instance.

In recent decades, a lot of effort has been put into the description of the territorial motion of animals [1]. Among others, random-walk models as correlated random walks and Lévy walks [2,3] or Lévy flights [4] are commonly used. Nevertheless, in the vast majority of these approaches, only the foraging stage of the territorial dynamics is described (i.e., the motion patterns while they are collecting), leaving aside the fact that some species return to their nest after reaching their target.

Having in mind that limitation, Evans and Majumdar [5] studied the properties of a macroscopic model consisting on a diffusive process subject to resets with constant rate (mesoscopically equivalent to consider exponentially distributed reset times), which introduces this back-to-the-nest stage. For this process, the mean first-passage time (MFPT) is finite and the mean-square displacement (MSD) reaches an equilibrium value. The latter result allows us to define the home range of a given species being a quantitative measure of the region that animals occupy around its nest.

From then on, multiple works have been published generalizing this seminal paper [6–18], by introducing for instance absorbing states [7] or generalizing it to d -dimensional diffusion [10]. Some works have also been devoted to the study of Lévy flights when they are subject to constant rate resets [19,20] and others have focused on the analysis of first passage processes subject to general resets [21–23]. Also, stochastic resets have been studied as a new element within the continuous-time random-walk (CTRW) formulation [24–28].

Despite the amount of works devoted to this topic, the existence of an equilibrium MSD and the finiteness of the mean first-arrival time (MFAT) found in Ref. [5] for diffusive processes with exponential resets have not been explicitly tested in general. In this work we address this issue by analyzing these properties for a general motion propagator with resets from a mesoscopic perspective. From all the existing papers, in Ref. [29] Eule and Metzger perform a similar study to ours but using Langevin dynamics to describe the movement. Our work differs from that one in the fact that we start from a general motion propagator $P(x, t)$, which allows us to derive an elegant and treatable expression for the first moment and the MSD of the overall process in terms of the motion first moment and MSD respectively [see Eq. (4)]. Moreover, the formalism herein employed eases the inclusion of processes which are not trivial to model in the Langevin picture as Lévy flights or Lévy walks.

This paper is organized as follows. In Sec. II A we find an expression for the propagator of the overall process in the Laplace-position space and a general formula for the MSD of the overall process in terms of the motion MSD; the first-arrival properties of the system are studied in Sec. II B. In Sec. III we apply the general results to three types of movement (subdiffusive, diffusive, and Lévy), and in Sec. IV we apply the formalism to study the transport properties and the first arrival of a biased Brownian oscillator. Finally, we conclude the work in Sec. V.

II. GENERAL FORMULATION

In this section we use a renewal formalism to study both the transport properties of a random motion and its first-arrival statistics. Concretely, we derive formulas for the global properties of the system in terms of the type of random motion and the reset distribution. We focus in three measures which are of special interest in the study of movement processes: the first moment, the MSD and the MFAT.

A. Transport properties

Let us consider a general motion propagator $P(x, t)$ starting at $x = 0$ and $t = 0$ which is randomly interrupted and starts anew at times given by a reset-time distribution $\varphi_R(t)$. When one of these resets happens, the motion instantaneously recommences from $x = 0$ according to $P(x, t)$ and so on and so forth. Then, the propagator of the overall process, which we call $\rho(x, t)$, is an iteration of multiple repetitions of $P(x, t)$ and the running time of each is determined by $\varphi_R(t)$.

We start by building a mesoscopic balance equation for $\rho(x, t)$. For simplicity, we assume that the overall process starts at the origin. Then, the following integral equation is fulfilled:

$$\rho(x, t) = \varphi_R^*(t)P(x, t) + \int_0^t \varphi_R(t')\rho(x, t-t')dt', \quad (1)$$

where $\varphi_R^*(t) = \int_t^\infty \varphi_R(t')dt'$ is the probability of the first reset happening after t . The first term in the right-hand side accounts for the cases where no reset has occurred until t and, therefore, the overall process is described by the motion propagator. The second term accounts for the cases where at least one reset has occurred before t and the first one has been at time $t' < t$, in which case the system is described by the overall propagator with a delay t' . Notably, we have introduced $\rho(x, t-t')$ as the propagator of the process starting at $x = 0$ at time t' [formally, it should be $\rho(x, t; 0, t')$]. This can be done independently of the form of $P(x, t)$ as long as the first realization of the process does not affect the following ones. When this is so, the scenario at t' is equivalent to a system starting at $t_0 = 0$ and having a time $t-t'$ to reach x .

Taking Eq. (1) to the Laplace space for the time variable, we can isolate the propagator of the overall process to be

$$\hat{\rho}(x, s) = \frac{\mathcal{L}[\varphi_R^*(t)P(x, t)]}{1 - \hat{\varphi}_R(s)}, \quad (2)$$

where $\mathcal{L}[f(t)] = \hat{f}(s) = \int_0^\infty e^{-st} f(t)dt$ denotes the Laplace transform. We can now obtain a general equation for the first moment of the overall process multiplying by x at both sides of Eq. (2) and integrating over x . Doing so, one gets

$$\langle \hat{x}(s) \rangle = \frac{\mathcal{L}[\varphi_R^*(t)\langle x(t) \rangle_m]}{1 - \hat{\varphi}_R(s)}, \quad (3)$$

where $\langle x(t) \rangle_m$ is the time-dependent first moment of the motion process. Nevertheless, usually this process is symmetric and its first moment is zero. In these cases, the second moment or MSD becomes the most relevant magnitude to describe the transport of the system. From Eq. (2), instead of multiplying by x , if we do so by x^2 and integrate over x we get

$$\langle \hat{x}^2(s) \rangle = \frac{\mathcal{L}[\varphi_R^*(t)\langle x^2(t) \rangle_m]}{1 - \hat{\varphi}_R(s)}, \quad (4)$$

where $\langle x^2(t) \rangle_m$ is the motion MSD. The importance of this equation lies in the fact that, if we know the motion MSD and the reset-time probability density function (PDF) separately, we can introduce them into Eq. (4) and directly obtain the transport information about the overall process.

The renewal formulation used herein differs from the method most commonly used in the bibliography to study random-walk processes with resets, consisting on introducing

a reset term *ad hoc* to the master equation of the process (see Ref. [5], for instance). Contrarily, it resembles the techniques employed in Ref. [20] to study Lévy flights with exponentially distributed resets or in Ref. [23] to study from a general perspective the first passage problem with resets. In these works, processes described by a known propagator or completion time distribution which are subject to resets are studied using a renewal approach.

1. Exponentially distributed reset times

Let us study the particular case where reset times are exponentially distributed [$\varphi_R(t) = \frac{1}{\tau_m} e^{-t/\tau_m}$], keeping the movement as general as before. In this scenario, the real space-time propagator of the overall process in Eq. (2) can be found by applying the inverse Laplace transform to be

$$\rho_e(x, t) = e^{-\frac{t}{\tau_m}} P(x, t) + \frac{1}{\tau_m} \int_0^t e^{-\frac{t-t'}{\tau_m}} P(x, t') dt'. \quad (5)$$

Under the condition that the Laplace transform of $P(x, t)$ exists at $s = \frac{1}{\tau_m}$, an equilibrium is reached and the distribution there can be generally written as

$$\rho_e(x) = \frac{\hat{P}(x, \frac{1}{\tau_m})}{\tau_m}. \quad (6)$$

The required condition for the equilibrium distribution to exist includes a wide range of processes from the most studied in the bibliography: Brownian motion, Lévy flights, etc. Similarly, an expression for the equilibrium first moment of the overall process in terms of the motion first moment can be derived from Eq. (3) reading

$$\langle x \rangle_e(\infty) = \frac{\langle \hat{x}(\frac{1}{\tau_m}) \rangle_m}{\tau_m}, \quad (7)$$

and for the MSD we have

$$\langle x^2 \rangle_e(\infty) = \frac{\langle \hat{x}^2(\frac{1}{\tau_m}) \rangle_m}{\tau_m}. \quad (8)$$

Equation (8) introduces an extra condition on the type of motion for it to define a finite area around the origin: the Laplace transform of its MSD must be finite at $s = \frac{1}{\tau_m}$. For instance, despite Lévy flights reaching an equilibrium state when they are subject to constant rate resets, since its MSD diverges so does the MSD of the overall process.

Multiple processes can be found in the bibliography with a MSD which is Laplace transformable and, therefore, reach an equilibrium MSD when exponential resets are applied to them. Some of these processes are Lévy walks, ballistic, or even turbulent motion [30]. Notably, Eq. (6) is also applicable to movement in more than one dimension when it is rotational invariant. In this case, the movement can be described by a one-dimensional propagator $P(r, t)$ where r is the radial distance from the origin. Therefore, any process without a preferred direction as correlated random walks and Lévy walks in the plane [2] or self-avoiding random walks for arbitrary spatial dimension [31] are significant processes which form a finite-size area when they are subject to exponential resets.

B. First arrival

The second remarkable result from Ref. [5] is the existence of a finite MFPT when diffusive motion is subject to constant rate resets. Since then, several works have been published focused on the first completion time with resets [21–23] but none of them have put the focus on the generality of these results with respect to the properties of the random motion. During the writing of this paper we have realized that a deep analysis of the first passage for search processes has been recently done in Ref. [32]. Nevertheless, besides our general qualitative analysis being similar to the one performed there, we study in detail cases of particular interest in a movement ecology context as subdiffusive motion, Lévy flights, or random walks in potential landscapes. Moreover, we perform numerical simulations of the process to check our analytical results.

In this work we use the MFAT as a measure of the time taken by the process to arrive to a given position, instead of crossing it as is considered in the MFPT. This is motivated by the fact that for Lévy flights the MFPT has an ambiguous interpretation due to the possibility of extremely long jumps in infinitely small time steps. Contrarily, the MFAT can be clearly interpreted and its properties have been deeply studied in Ref. [33].

Before focusing on practical cases, let us start with the general renewal formulation. We build a renewal equation for the survival probability of the overall process $\sigma_x(t)$ in terms of the survival probability of the motion $Q_x(t)$ and the reset-time PDF $\varphi_R(t)$, similar to the equation for the propagator in the previous section:

$$\sigma_x(t) = \varphi_R^*(t)Q_x(t) + \int_0^t \varphi_R(t')Q_x(t')\sigma_x(t-t')dt'. \quad (9)$$

Here, the first term on the right-hand side corresponds to the probability of not having reached x , nor a reset has occurred in the period $t \in (0, t]$. The second term is the probability of not having reached x when at least one reset has happened at time t . In the latter, we account for the probability $Q_x(t')$ of not having reached x in the first trip, which ends at a random time t' , and the probability of not reaching x at any other time after the first reset $\sigma_x(t-t')$; and these two conditions are averaged over all possible first reset times t' . Applying the Laplace transform and isolating the overall survival probability we obtain

$$\hat{\sigma}_x(s) = \frac{\mathcal{L}[\varphi_R^*(t)Q_x(t)]}{1 - \mathcal{L}[\varphi_R(t)Q_x(t)]}. \quad (10)$$

This equation, which has been recently derived by similar means in Ref. [32], is the cornerstone from which the existence of the MFAT is studied. If in the asymptotic limit the survival probability behaves as

$$\sigma_x(t) \sim t^{-\beta}, \quad (11)$$

then for $\beta > 1$ the MFAT is finite, while for $\beta \leq 1$ it diverges. Since we have the expression of the survival probability in the Laplace space, it is convenient to rewrite these conditions for $\hat{\sigma}_x(s)$ instead. Let us consider the following situations:

(i) When $\beta > 1$, the Laplace transform of the survival probability tends to a constant value for small s . The MFAT

is finite and can be found as

$$T_F = \int_0^\infty tq_x(t)dt = \lim_{s \rightarrow 0} \hat{\sigma}_x(s), \quad (12)$$

where $q_x(t) = -\frac{\partial \sigma_x(t)}{\partial t}$ is the first-arrival time distribution of the overall process. Concretely, the MFAT can be found in terms of the distributions defined above as

$$T_F = \frac{\int_0^\infty \varphi_R^*(t)Q_x(t)dt}{1 - \int_0^\infty \varphi_R(t)Q_x(t)dt}. \quad (13)$$

(ii) When $\beta = 1$, the Laplace transform of the survival probability tends to infinity for small s . Therefore, in this case, the MFAT is infinite since

$$\lim_{s \rightarrow 0} \hat{\sigma}_x(s) = \infty,$$

so

$$T_F = \infty.$$

(iii) When $\beta < 1$, the Laplace transform of the survival probability diverges as $\hat{\sigma}_x(s) \sim s^{\beta-1}$ for small s . The MFAT is infinite and the survival probability decays as $\sigma_x(t) \sim t^{-\beta}$ with time.

Notably, when the reset times are exponentially distributed [$\varphi_R(t) = \frac{1}{\tau_m}e^{-\frac{t}{\tau_m}}$], the MFAT of the overall process is always finite for motion survival probabilities which are Laplace-transformable. Concretely, in this particular case Eq. (13) reduces to

$$T_F = \frac{\tau_m \hat{Q}_x\left(\frac{1}{\tau_m}\right)}{\tau_m - \hat{Q}_x\left(\frac{1}{\tau_m}\right)}. \quad (14)$$

III. FREE MOTION

To get a deeper intuition about the results in the previous section, let us take generic expressions for both the reset-time distribution and the motion propagator. In the first place we study well-known processes which do not have environmental constraints (potential landscapes, barriers, etc.).

A. Transport properties

Let us start by studying the transport properties of the overall process for a symmetric motion, i.e.,

$$\langle x(t) \rangle_m = 0, \quad (15)$$

with a MSD scaling as

$$\langle x^2(t) \rangle_m \sim t^p, \quad (16)$$

with $0 < p \leq 2$. This choice includes subdiffusive motion for $p < 1$, diffusive motion for $p = 1$ and superdiffusive motion with for $p > 1$. Also, we take the reset-time distributions to be

$$\varphi_R(t) = \frac{t^{\gamma_R-1}}{\tau_m^{\gamma_R}} E_{\gamma_R, \gamma_R} \left[-\left(\frac{t}{\tau_m}\right)^{\gamma_R} \right], \quad (17)$$

with $0 < \gamma_R \leq 1$, where

$$E_{\alpha, \beta}(z) = \sum_{n=0}^{\infty} \frac{(-z)^n}{\Gamma(\alpha n + \beta)}$$

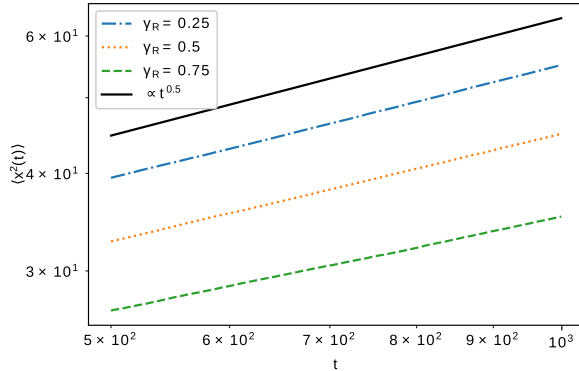


FIG. 1. The asymptotic behavior of the MSD of the overall process for subdiffusive motion with $p = 0.5$ is shown in a log-log plot. Three different exponents $\gamma_R < 1$ for the reset-time distribution are considered and all of them are seen to scale as the solid black guide line of slope 0.5. Therefore, the reset exponent γ_R only affects multiplicatively to the transport regime.

is the generalized Mittag-Leffler function with constant parameters α and β . This allows us to recover the exponential distribution for $\gamma_R = 1$ and we can also study power law behaviors of the type $\varphi_R(t) \sim t^{-1-\gamma_R}$ for $\gamma_R < 1$. For this distribution, the survival probability $\varphi_R^*(t) = \int_t^\infty \varphi(t') dt'$ reads

$$\varphi_R^*(t) = E_{\gamma_R, 1} \left[- \left(\frac{t}{\tau_m} \right)^{\gamma_R} \right]. \quad (18)$$

For a wide study about the properties of the Mittag-Leffler function we refer the reader to [34]. In this case, since the first moment is zero, the MSD becomes the most significant moment of the process. From Eq. (8) one can see that MSD of the overall process has two possible behaviors for large t (see Appendix 1 for details):

$$\langle x^2(t) \rangle \sim \begin{cases} t^p, & \text{for } \gamma_R < 1 \\ t^0, & \text{for } \gamma_R = 1 \end{cases}. \quad (19)$$

Therefore, for power-law reset-time PDFs with any exponent $\gamma_R < 1$, the MSD of the overall process scales as the motion MSD, so that a long-tailed reset PDF does not modify the transport regime. To illustrate this, in Fig. 1 we show simulations of the asymptotic behavior of the overall MSD for subdiffusive motion with long-tailed resets. There we see that, as can be seen from Eq. (19), long-tailed resets only affect the transport multiplicatively but not modify the regime.

When the motion is a Lévy flight, the MSD diverges for all t , i.e.,

$$\langle x^2(t) \rangle_m = \infty, \quad t > 0.$$

Hence, from Eq. (4), the MSD of the overall process also diverges for any reset-time PDF except for the pointless case $\varphi_R(t) = \delta(t)$.

Regarding exponential reset-time distributions case ($\gamma_R = 1$), an equilibrium state is reached and we can in principle compute an equilibrium distribution. We start by considering a subdiffusive propagator (see Eq. (A2) in Ref. [35]) which,

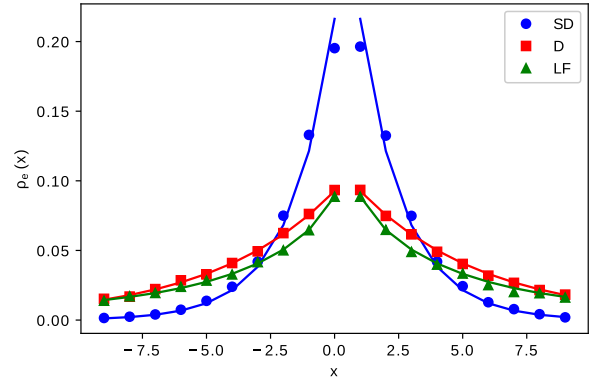


FIG. 2. Equilibrium distribution of the overall process with subdiffusive (SD) with $\gamma = 0.5$, diffusive (D) and Lévy flight (LF) with $\alpha = 1.5$ motion propagator, all with $D = 0.1$, and exponential reset times with $\tau_m = 10$. Each stochastic simulation is compared to the corresponding analytical expressions Eqs. (21) and (23) (solid lines).

in the Fourier-Laplace space, reads

$$\hat{P}(k, s) = \frac{1}{s + Ds^{1-\gamma}k^2}, \quad (20)$$

with D the (sub-)diffusion constant. This propagator describes subdiffusive movement for $\gamma < 1$ and diffusive movement for $\gamma = 1$. Then, the equilibrium distribution given by Eq. (6) becomes a symmetric exponential distribution

$$\rho_e(x) = \frac{1}{\sqrt{4D\tau_m^\gamma}} e^{-\frac{|x|}{\sqrt{D\tau_m^\gamma}}}, \quad (21)$$

where for $\gamma = 1$ we recover the equilibrium distribution found in Ref. [5]. If instead of a subdiffusive propagator we consider a superdiffusive motion and, in particular, the propagator for a Lévy flight in the Fourier-Laplace space,

$$\hat{P}(k, s) = \frac{1}{s + D|k|^\alpha}, \quad (22)$$

with $\alpha < 2$ and D a constant, the equilibrium distribution of the overall process becomes

$$\rho_e(x) = 2 \int_0^\infty \frac{\cos(kx)}{1 + \tau_m D k^\alpha} dk. \quad (23)$$

In Fig. 2 we compare both analytical results in Eqs. (21) and (23) with numerical Monte Carlo simulations of the process. The agreement is seen to be excellent.

B. First arrival

Let us now study the MFAT for a general motion survival probability decaying as

$$Q_x(t) \sim t^{-q}, \quad q > 0 \quad (24)$$

for long t and the same reset-time distribution defined in Eq. (17). Under these assumptions, the asymptotic behavior of the overall survival probability is (see Appendix 2 for details)

$$\sigma_x(t) \sim t^{-\gamma_R - q}, \quad \text{if } \gamma_R + q \leq 1, \quad (25)$$

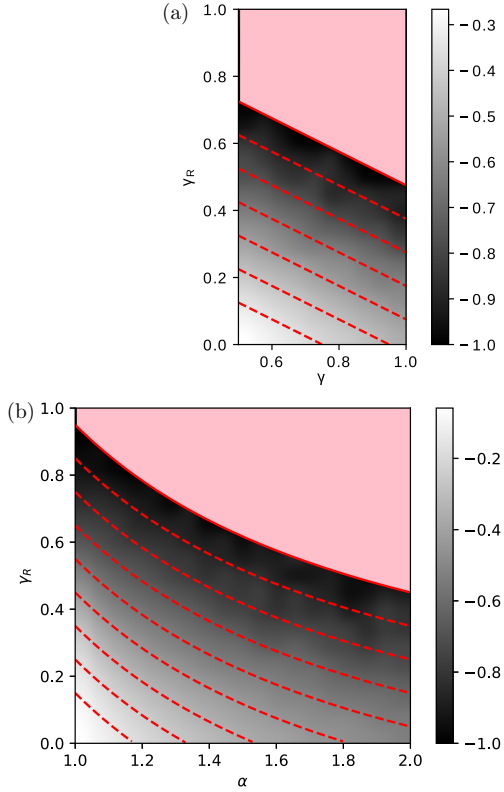


FIG. 3. The tail exponent β of the survival probability $\sigma_x(t) \sim t^\beta$ of the overall process at $x = 0.5$ is shown for subdiffusive motion with exponent γ in (a) and Lévy flight motion with exponent α in (b), both subject to resets at times given by a Mittag-Leffler distribution with tail parameter γ_R and $\tau_m = 10$. The values of β have been computed for $\gamma_R \in \{0.05, 0.1 \dots 0.9, 0.95\}$, and $\gamma \in \{0.5, 0.55 \dots 0.9, 0.95\}$ in (a) and $\alpha \in \{1.05, 1.1 \dots 1.9, 1.95\}$ in (b). Gaussian interpolation has been applied to smooth the simulated results. In each plot, the solid red curve [$\gamma_R + \frac{\gamma}{2} = 1$ in (a) and $\gamma_R - \frac{1}{\alpha} = 0$ in (b)] corresponds to the limit between finite (flat pink region) and infinite (gradient) MFAT. The dashed curves are the analytical level curves for $\beta = 0.9, 0.8 \dots$ from top to bottom. The black regions observed just below the limiting curves are due to the discretization of the parameter space.

as has been recently found in Ref. [32] by similar means. This implies that, in this case, $T_F = \infty$. However, when $\gamma_R + q > 1$ the MFAT is finite and can be expressed as

$$T_F(x) = \frac{\int_0^\infty E_{\gamma_R, 1} \left[-\left(\frac{t}{\tau_m}\right)^{\gamma_R} \right] Q_x(t) dt}{1 - \int_0^\infty \frac{t^{\gamma_R-1}}{\tau_m^{\gamma_R}} E_{\gamma_R, \gamma_R} \left[-\left(\frac{t}{\tau_m}\right)^{\gamma_R} \right] Q_x(t) dt}. \quad (26)$$

The two regions where the MFAT is finite and infinite for a subdiffusive [Fig. 3(a)] and a Lévy flight motion process [Fig. 3(b)] are shown in Fig. 3. Let us study these two cases separately. As shown in Ref. [36], for a subdiffusive motion, the survival probability in the long-time limit decays as

$$Q_x(t) \sim t^{-\frac{\gamma}{2}}, \quad (27)$$

with $0 < \gamma < 1$. For $\gamma = 1$ we recover the survival probability of a diffusion process. Here we can identify $q = \frac{\gamma}{2}$ and from Eq. (25) the survival probability of the overall process decays as

$$\sigma_x(t) \sim t^{-\gamma_R - \frac{\gamma}{2}}, \quad (28)$$

when $\gamma_R + \frac{\gamma}{2} \leq 1$ and the MFAT is infinite in this region of exponents. Contrarily, the MFAT is finite when $\gamma_R + \frac{\gamma}{2} > 1$. This result has been compared with stochastic simulations of the process [Fig. 3(a)], where the limiting curve $\gamma_R = 1 - \frac{\gamma}{2}$ and the tail exponent for the overall survival probability are in clear agreement with the analytical results.

We have also studied the survival probability when the underlying motion is governed by Lévy flights propagator. In this case, the survival probability decays as

$$Q_x(t) \sim t^{\frac{1}{\alpha}-1}, \quad (29)$$

with $1 < \alpha < 2$, as shown in Ref. [33]. Here we can also recover the diffusive behavior for $\alpha = 2$. Identifying $q = 1 - \frac{1}{\alpha}$, the overall survival probability reads

$$\sigma_x(t) \sim t^{\frac{1}{\alpha} - \gamma_R - 1} \quad (30)$$

in the asymptotic limit and for $\gamma_R - \frac{1}{\alpha} \leq 0$. In this case the MFAT is infinite while for $\gamma_R - \frac{1}{\alpha} > 0$ it is finite. In Fig. 3(b) we present the results to see that these two regions are also found in a stochastic simulation of the overall process.

Unlike the existence of an equilibrium MSD, the finiteness of the MFAT is not drastically broken when the reset-time distribution changes from short to long-tailed. A remarkable property that we can see in Fig. 3 is that both the reset-time distribution and the motion first-arrival time distribution can have an infinite mean value and still the mean value of the overall process is finite. This property has been explicitly tested by computing the simulated MFAT for parameters in the white region in Fig. 3 for both the subdiffusive and the Lévy flight case, and also for the diffusive limiting case. The simulated MFAT is compared to the one obtained from numerical integration of Eq. (13) and the results are shown to be in agreement (Fig. 4).

IV. BROWNIAN MOTION IN A BIASED HARMONIC POTENTIAL

In this section we study the transport and the first-arrival statistics of a Brownian particle starting at $x = 0$ with a white, Gaussian noise with diffusion constant D . It moves inside a biased harmonic potential $V(x) = \frac{1}{2}k(x - x_0)^2$ and it has a drift γ . Unlike the cases studied in the previous section, here the movement has an intrinsic bias towards the point x_0 . This, in an ecological context, can be seen as the knowledge the animal have about the optimal patches to find food.

When this system is constrained by constant rate resets (i.e., exponentially distributed reset times), an equilibrium distribution is attained as shown in Ref. [12] by introducing resets to the Fokker-Plank equation of the system. Instead, with the general formalism derived in Sec. II, we can first study the system without resets and introduce the results to the formulas derived above. Then, we start from the Langevin equation for the Brownian particle in an harmonic

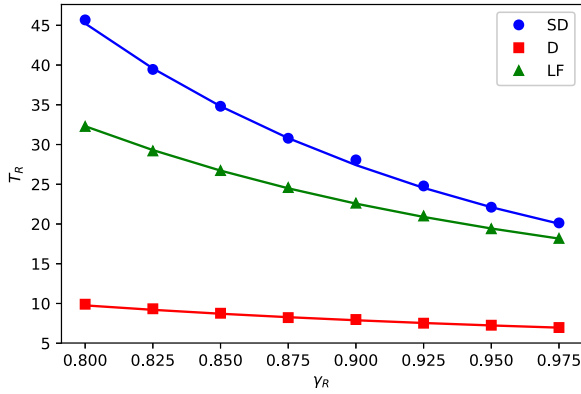


FIG. 4. The simulated MFAT for three representative cases of subdiffusion (SD) with $\gamma = 0.5$, diffusion (D) with $\gamma = 1$ and a Lévy Flight with $\alpha = 1.5$, all with $D = 0.1$, are compared to the analytical results obtained from Eq. (13) (solid curves) for different reset distribution tail exponents γ_R and $\tau_m = 10$. Concretely, the MFAT is computed at a distance $x = 0.5$ from the origin.

potential [37]:

$$\frac{dx}{dt} = -\frac{D}{\gamma} \frac{\partial V(x)}{\partial x} + \sqrt{2D}\eta(t), \quad (31)$$

where the over-damped limit has been implicitly taken and $\eta(t)$ is a Gaussian noise so that $\langle \eta(t) \rangle = 0$ and $\langle \eta(t)\eta(t') \rangle = \delta(t - t')$ (i.e., a white noise). For a biased harmonic potential it becomes

$$\frac{dx}{dt} = -DF(x - x_0) + \sqrt{2D}\eta(t), \quad (32)$$

where $F = k/\gamma$ has been defined. From this equation, the first moment and the MSD of the particle can be derived (see Ref. [38] for specific methods and tools) to be

$$\langle x(t) \rangle_m = x_0(1 - e^{-DFt}) \quad (33)$$

and

$$\begin{aligned} \langle x^2(t) \rangle_m &= \left(\frac{1}{F} + x_0^2 \right) (1 - e^{-2DFt}) \\ &\quad - 2x_0^2 e^{-DFt} (1 - e^{-DFt}), \end{aligned} \quad (34)$$

respectively. Introducing these expressions to the main equations for the moments of the process [Eqs. (3) and (4)] we can obtain the Laplace space dynamics of the mean

$$\langle \hat{x}(s) \rangle = x_0 \left[\frac{1}{s} - \frac{\hat{\varphi}_R^*(s + DF)}{1 - \hat{\varphi}_R(s)} \right] \quad (35)$$

and the MSD

$$\begin{aligned} \langle \hat{x}^2(s) \rangle &= \left(\frac{1}{F} + x_0^2 \right) \left[\frac{1}{s} - \frac{\hat{\varphi}_R^*(s + 2DF)}{1 - \hat{\varphi}_R(s)} \right] \\ &\quad - 2x_0^2 \frac{\hat{\varphi}_R^*(s + DF) - \hat{\varphi}_R^*(s + 2DF)}{1 - \hat{\varphi}_R(s)}, \end{aligned} \quad (36)$$

in terms of the reset-time PDF. For small s , the terms with $1 - \hat{\varphi}_R(s)$ in the denominator can be neglected with respect to the term $\frac{1}{s}$ when the distribution $\varphi_R(t)$ is long tailed. This is because in the $s \rightarrow 0$ limit, the numerator of these terms

remains finite while the denominator $1 - \hat{\varphi}_R(s) \sim s^{\gamma_R}$, with $\gamma_R < 1$. Therefore, for long-tailed reset-time distributions, the first is the dominant term. However, for exponentially distributed resets we have that

$$\frac{\hat{\varphi}_R^*(s + 2DF)}{1 - \hat{\varphi}_R(s)} = \frac{1}{s} \frac{1}{1 + 2DF\tau_m} + \mathcal{O}(s^0)$$

and, equivalently,

$$\frac{\hat{\varphi}_R^*(s + DF)}{1 - \hat{\varphi}_R(s)} = \frac{1}{s} \frac{1}{1 + DF\tau_m} + \mathcal{O}(s^0).$$

Therefore, the equilibrium first moment and MSD of the overall process can be seen to be

$$\langle x(\infty) \rangle_e = x_0 \left(1 - \kappa_{\gamma_R} \frac{1}{1 + DF\tau_m} \right) \quad (37)$$

and

$$\begin{aligned} \langle x^2(\infty) \rangle_e &= \left(\frac{1}{F} + x_0^2 \right) \left(1 - \kappa_{\gamma_R} \frac{1}{1 + 2DF\tau_m} \right) \\ &\quad - \kappa_{\gamma_R} 2x_0^2 \frac{DF\tau_m}{(1 + DF\tau_m)(1 + 2DF\tau_m)}, \end{aligned} \quad (38)$$

respectively, with $\kappa_{\gamma_R} = 1$ for $\gamma_R = 1$ and $\kappa_{\gamma_R} = 0$ for $\gamma_R < 1$. Then, when the reset distribution is long-tailed, both the equilibrium mean and MSD are equal to the ones for the process without resets. However, when resets are exponentially distributed, the values of the equilibrium mean and MSD are diminished by the factors preceded by κ_{γ_R} in the equations right above. This difference has been tested for the MSD by means of a stochastic simulation of the Langevin equation (Fig. 5). As happens for the transport properties of the free processes studied in Sec. III, for this type of movement we also find that long-tailed reset distributions do not affect the significant features of the MSD (and also the mean in this case), while reset times which are distributed exponentially do affect actively the long-time behavior of the overall process.

Let us now study its MFAT for this system. The first-arrival distribution $q_{x_0}(t)$ at the minimum of the potential for this motion process has been found to be [37]

$$q_{x_0}(t) = \frac{2De^{-DFt}|x_0|}{\sqrt{2\pi\sigma_t^3}} \exp \left\{ -\frac{(x_0 e^{-DFt})^2}{2\sigma_t} \right\}, \quad (39)$$

from which the survival probability can be found as

$$Q_{x_0}(t) = \int_t^\infty q_{x_0}(t') dt', \quad (40)$$

with $\sigma_t = (1 - e^{-DFt})/F$. In the asymptotic limit, the first-arrival distribution decays as $q_{x_0}(t) \sim e^{-DFt}$ and so does the survival probability $Q_{x_0}(t) \sim e^{-DFt}$ since the decay is exponential. A direct consequence of this is that the global survival probability also has a short tail. This can be seen by looking at Eq. (10): When the asymptotic limit of $Q_{x_0}(t)$ is exponential, the expression of the global survival probability in the Laplace space tends to a finite value for small s , which is in fact the first-arrival time of the global process (see Appendix 3 for further details).

In Fig. 5 we compare the analytical result predicted by Eq. (13), taking the survival probability in Eq. (39) instead of the ones studied in Sec. III, with Monte Carlo simulations

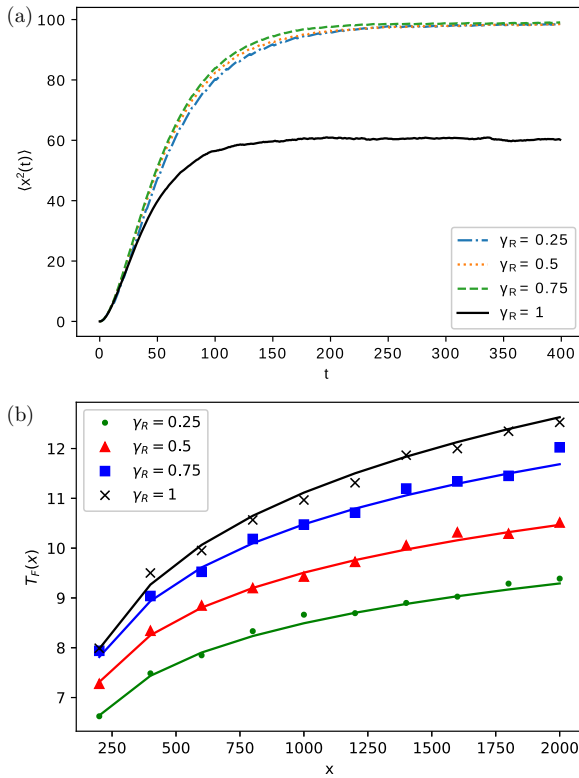


FIG. 5. In (a) we show the MSD as a function of time for a simulation of a Brownian motion ($D = 0.25$) with an harmonic force $F = 1$ with equilibrium point at $x_0 = 10$ subject to resets with $\tau_m = 10$ and different γ_R parameters. For all three $\gamma_R < 1$ the MSD tends to the same value, which is larger than the equilibrium MSD for $\gamma_R = 1$. In (b) the simulated MFAT for $F = 1$, $D = 1$, and $\tau_m = 10$ is compared to the analytical result for Mittag-Leffler reset distributions with different γ_R (solid curves).

of the Langevin equation in Eq. (32). They are seen to be in perfect agreement. Here, unlike for the free motion processes, resets always penalize the arrival to the target.

V. CONCLUSIONS

In this work we have derived an expression for the first moment, the MSD and the MFAT of stochastic motion with resets from a unified, renewal formulation. Concretely, we find them in terms of a general resetting mechanism and the type of stochastic motion. This opens the analysis of resets acting on a vast range of stochastic motion processes without the need of building a particular model for each case.

The existence of an equilibrium MSD and a finite MFAT has been tested for a wide class of stochastic processes subject to random resets. The first turns to be extremely sensitive with respect to the reset-time distribution. On one hand, when the reset-time distribution is long-tailed, the transport regime of the overall process is qualitatively equivalent to the regime of the motion [see Eq. (19) for free motion and Eqs. (37) and (38) for the biased harmonic Brownian oscillator]. On the other

hand, for exponential distributions of reset times, qualitative changes are observed regarding the transport of the overall process. Concretely, we have found that for a free motion process with MSD scaling as $\langle x^2(t) \rangle_m \sim t^p$, an equilibrium state with finite MSD is reached. For the Brownian oscillator, both the equilibrium mean and MSD are modified by the resetting mechanism. Therefore, while exponentially distributed resets actively affect the long-time behavior of both processes, when long-tailed reset-time distributions with infinite mean are chosen, the asymptotics of the motion process are not modified.

Regarding the first-arrival time, we have seen that the difference between long-tailed and exponentially distributed reset times is not as marked as for the transport properties. In fact, the transition between them is seen to be soft [compare Figs. 5(a) and 5(b), for instance]. Interestingly, for the free motion process case, we find that a motion process with an infinite MFAT, when it is restarted at times given by a long-tailed PDF (i.e., with infinite mean), may have a finite MFAT (see Fig. 4)

ACKNOWLEDGMENTS

This research has been supported by the Ministerio de Economía y Competitividad through Grant No. CGL2016-78156-C2-2-R.

APPENDIX: ASYMPTOTIC ANALYSIS

In this Appendix we derive the results in Eqs. (19) and (25) about the asymptotic behavior of the MSD Eq. (A1) and the survival probability Eq. (A2), respectively, for a motion process with resets. Concretely, we compute them for motion MSD as in Eq. (16) and the survival probability as in Eq. (24). Also, in Eq. (A3) we compute the MFAT for an exponentially decaying motion survival probability.

1. Mean-square displacement of a free process with resets

We start by rewriting the general expression for the MSD in Eq. (4) as

$$\langle \hat{x}(s) \rangle = \frac{T_1(s)}{T_2(s)}, \quad (\text{A1})$$

with $T_1(s) = \mathcal{L}[\varphi_R^*(t) \langle x^2(t) \rangle^P]$ and $T_2(s) = 1 - \hat{\varphi}_R(s)$. To study the long t limit of the MSD, in the Laplace space we must study the small s limit. Let us start by $T_2(s)$. In the Laplace space, the Mittag-Leffler distribution can be seen [34] to be

$$\hat{\varphi}_R(s) = \frac{1}{1 + (\tau_m s)^{\gamma_R}}, \quad (\text{A2})$$

from which

$$T_2(s) = 1 - \frac{1}{1 + (\tau_m s)^{\gamma_R}} = \frac{(\tau_m s)^{\gamma_R}}{1 + (\tau_m s)^{\gamma_R}} \sim s^{\gamma_R} \quad (\text{A3})$$

in the small s limit. Let us proceed now with $T_1(s)$. In the long t limit, the Mittag-Leffler survival probability in Eq. (18) can be seen [34] to behave as

$$\varphi_R^*(t) \sim \begin{cases} t^{-\gamma_R}, & \text{for } \gamma_R < 1 \\ e^{-t/\tau_m}, & \text{for } \gamma_R = 1 \end{cases} \quad (\text{A4})$$

Then, with Eq. (16) it follows that

$$T_1(s) \sim \begin{cases} \mathcal{L}[t^{p-\gamma_R}] \sim s^{\gamma_R-1-p}, & \text{for } \gamma_R < 1 \\ \mathcal{L}[t^p e^{-t/\tau_m}] \sim s^0, & \text{for } \gamma_R = 1. \end{cases} \quad (\text{A5})$$

Putting the elements together,

$$\langle \hat{x}(s) \rangle \sim \begin{cases} s^{-1-p}, & \text{for } \gamma_R < 1 \\ s^{-1}, & \text{for } \gamma_R = 1. \end{cases} \quad (\text{A6})$$

Finally, applying the inverse Laplace transform one finds

$$\langle x(t) \rangle \sim \begin{cases} t^p, & \text{for } \gamma_R < 1 \\ t^0, & \text{for } \gamma_R = 1. \end{cases} \quad (\text{A7})$$

2. Survival probability of a free process with resets

We proceed similarly to the MSD case. Here we start from Eq. (25) and we rewrite it as

$$\hat{\sigma}_x(s) = \frac{T_1'(s)}{1 - T_2'(s)}, \quad (\text{A8})$$

with $T_1'(s) = \mathcal{L}[\varphi_R^*(t)Q_x(t)]$ and $T_2'(s) = \mathcal{L}[\varphi_R(t)Q_x(t)]$. Let us start for the latter. As in the previous case, we study the small s limit, where we have that

$$T_2'(0) = \int_0^\infty \varphi_R(t)Q_x(t)dt < \int_0^\infty \varphi_R(t)dt = 1. \quad (\text{A9})$$

In the second step we have used that the survival probability $Q_x(t) < 1$, $\forall t > 0$, and in the last step the normalization of $\varphi_R(t)$ is used. Then, the denominator of Eq. (A8) is strictly positive when $s \rightarrow 0$, which implies that the decaying of $\hat{\sigma}_x(s)$ when $s \rightarrow 0$ is exclusively determined by the decaying of the numerator $T_1'(s)$, i.e.,

$$\hat{\sigma}_x(s) \sim \frac{T_1'(s)}{1 - T_2'(0)} \sim T_1'(s) \quad (\text{A10})$$

for small s . Applying the inverse Laplace transform to this expression one gets the equivalent relation

$$\sigma_x(t) \sim \mathcal{L}^{-1}[T_1'(s)] = \varphi_R^*(t)Q_x(t) \quad (\text{A11})$$

for long t . If the survival probability of the motion process decays as $Q_x(t) \sim t^{-q}$, $q > 0$, as assumed in the main text, and $\varphi_R^*(t)$ is again the Mittag-Leffler survival probability,

which decays as in Eq. (A4), we have that

$$\sigma_x(t) \sim t^{-\gamma_R-q} \quad (\text{A12})$$

asymptotically. On one hand, if $\gamma_R + q \leq 1$, then the mean first-arrival time is infinite. On the other hand, if $\gamma_R + q > 1$, which includes exponentially distributed reset times for $\gamma_R = 1$, then the mean first-arrival time is finite and can be found as

$$T_F(x) = \hat{\sigma}_x(0) = \frac{\int_0^\infty \varphi_R^*(t)Q_x(t)dt}{1 - \int_0^\infty \varphi_R(t)Q_x(t)dt}. \quad (\text{A13})$$

Finally, taking a Mittag-Leffler reset-time distribution, one recovers the result in Eq. (13) of the main text.

3. MFAT for exponential motion survival probability

Here we show that when the motion survival probability is of the form $Q_x(t) = e^{-r(x)t}$, the overall process MFAT is always finite. In this particular case and from Eq. (10), the overall survival probability in the Laplace space can be written as

$$\hat{\sigma}_x(s) = \frac{\mathcal{L}[\varphi_R^*(t)e^{-r(x)t}]}{1 - \mathcal{L}[\varphi_R(t)e^{-r(x)t}]} = \frac{\hat{\varphi}_R^*[s + r(x)]}{1 - \hat{\varphi}_R[s + r(x)]}. \quad (\text{A14})$$

Taking the limit $s \rightarrow 0$ one can get the MFAT:

$$T_F = \lim_{s \rightarrow 0} \hat{\sigma}_x(s) = \frac{\hat{\varphi}_R^*[r(x)]}{1 - \hat{\varphi}_R[r(x)]}. \quad (\text{A15})$$

The Laplace transform of the survival probability can be expressed as

$$\hat{\varphi}_R^*(s) = \mathcal{L}\left[\int_t^\infty \varphi_R(t')dt'\right] = \frac{1 - \hat{\varphi}_R(s)}{s},$$

thus,

$$T_F = \frac{1}{r(x)}, \quad (\text{A16})$$

which is of course finite for all $r(x)$ and independent of $\varphi_R(t)$. In fact, this result is obvious because the completion rate of a process with $Q_x(t) = e^{-r(x)t}$ is constant in time and, therefore, resetting it does not modify its completion time. Regarding the motion survival probability of the process in Sec. IV, since the finiteness of the MFAT is determined by the long t behavior of the survival probability, when only the asymptotic decay is exponential, the mean first-arrival time is also finite.

- [1] A. Okubo and S. A. Levin, *Diffusion and Ecological Problems: Modern Perspectives*, Vol. 14 (Springer Science & Business Media, Berlin, 2002).
- [2] F. Bartumeus, M. G. E. da Luz, G. Viswanathan, and J. Catalan, *Ecology* **86**, 3078 (2005).
- [3] V. Méndez, D. Campos, and F. Bartumeus, *Stochastic Foundations in Movement Ecology* (Springer-Verlag, Berlin/Heidelberg, 2014).
- [4] A. M. Reynolds and C. J. Rhodes, *Ecology* **90**, 877 (2009).
- [5] M. R. Evans and S. N. Majumdar, *Phys. Rev. Lett.* **106**, 160601 (2011).
- [6] M. R. Evans and S. N. Majumdar, *J. Phys. A: Math. Theor.* **44**, 435001 (2011).

- [7] J. Whitehouse, M. R. Evans, and S. N. Majumdar, *Phys. Rev. E* **87**, 022118 (2013).
- [8] M. R. Evans, S. N. Majumdar, and K. Mallick, *J. Phys. A: Math. Theor.* **46**, 185001 (2013).
- [9] S. Gupta, S. N. Majumdar, and G. Schehr, *Phys. Rev. Lett.* **112**, 220601 (2014).
- [10] M. R. Evans and S. N. Majumdar, *J. Phys. A: Math. Theor.* **47**, 285001 (2014).
- [11] X. Durang, M. Henkel, and H. Park, *J. Phys. A: Math. Theor.* **47**, 045002 (2014).
- [12] A. Pal, *Phys. Rev. E* **91**, 012113 (2015).
- [13] S. N. Majumdar, S. Sabhapandit, and G. Schehr, *Phys. Rev. E* **92**, 052126 (2015).

- [14] C. Christou and A. Schadschneider, *J. Phys. A: Math. Theor.* **48**, 285003 (2015).
- [15] A. Pal, A. Kundu, and M. R. Evans, *J. Phys. A: Math. Theor.* **49**, 225001 (2016).
- [16] A. Nagar and S. Gupta, *Phys. Rev. E* **93**, 060102 (2016).
- [17] R. Falcao and M. R. Evans, *J. Stat. Mech.: Theory Exp.* (2017) 023204.
- [18] D. Boyer, M. R. Evans, and S. N. Majumdar, *J. Stat. Mech.: Theory Exp.* (2017) 023208.
- [19] Ł. Kuśmierz, S. N. Majumdar, S. Sabhapandit, and G. Schehr, *Phys. Rev. Lett.* **113**, 220602 (2014).
- [20] Ł. Kuśmierz and E. Gudowska-Nowak, *Phys. Rev. E* **92**, 052127 (2015).
- [21] T. Rotbart, S. Reuveni, and M. Urbakh, *Phys. Rev. E* **92**, 060101 (2015).
- [22] S. Reuveni, *Phys. Rev. Lett.* **116**, 170601 (2016).
- [23] A. Pal and S. Reuveni, *Phys. Rev. Lett.* **118**, 030603 (2017).
- [24] M. Montero and J. Villarroel, *Phys. Rev. E* **87**, 012116 (2013).
- [25] D. Campos and V. Méndez, *Phys. Rev. E* **92**, 062115 (2015).
- [26] V. Méndez and D. Campos, *Phys. Rev. E* **93**, 022106 (2016).
- [27] M. Montero, A. Masó-Puigdellosas, and J. Villarroel, *Eur. Phys. J. B* **90**, 176 (2017).
- [28] V. P. Shkilev, *Phys. Rev. E* **96**, 012126 (2017).
- [29] S. Eule and J. J. Metzger, *New J. Phys.* **18**, 033006 (2016).
- [30] J. Klafter, A. Blumen, and M. F. Shlesinger, *Phys. Rev. A* **35**, 3081 (1987).
- [31] H. Duminil-Copin and A. Hammond, *Commun. Math. Phys.* **324**, 401 (2013).
- [32] A. Chechkin and I. M. Sokolov, *Phys. Rev. Lett.* **121**, 050601 (2018).
- [33] A. V. Chechkin, R. Metzler, V. Y. Gonchar, J. Klafter, and L. V. Tanatarov, *J. Phys. A: Math. Gen.* **36**, L537 (2003).
- [34] A. M. Mathai and H. J. Haubold, *Special Functions for Applied Scientists* (Springer-Verlag, New York, 2008).
- [35] R. Metzler and J. Klafter, *Phys. Rep.* **339**, 1 (2000).
- [36] G. Rangarajan and M. Ding, *Phys. Lett. A* **273**, 322 (2000).
- [37] Z. Hu, L. Cheng, and B. J. Berne, *J. Chem. Phys.* **133**, 034105 (2010).
- [38] C. Gardiner, *Stochastic Methods*, Vol. 13 (Springer-Verlag, Berlin/Heidelberg, 2009).

Appendix B

Second Article

Stochastic movement subject to a reset-and-residence mechanism: transport properties and first arrival statistics

Axel Masó-Puigdellosas, Daniel Campos and Vicenç Méndez

*Grup de Física Estadística. Departament de Física, Universitat Autònoma de
Barcelona, 08193 Bellaterra, Spain*

This paper has been published in *J. Stat. Mech.* (2019) 033201

Journal of Statistical Mechanics:
Theory and Experiment



PAPER: CLASSICAL STATISTICAL MECHANICS, EQUILIBRIUM AND NON-EQUILIBRIUM

Stochastic movement subject to a reset-and-residence mechanism: transport properties and first arrival statistics

Recent citations

- [First passage under stochastic resetting in an interval](#)
Arnab Pal and V. V. Prasad

To cite this article: Axel Masó-Puigdellosas *et al* *J. Stat. Mech.* (2019) 033201

View the [article online](#) for updates and enhancements.



IOP | ebooks™

Bringing you innovative digital publishing with leading voices to create your essential collection of books in STEM research.

Start exploring the collection - download the first chapter of every title for free.

PAPER: Classical statistical mechanics, equilibrium and non-equilibrium

Stochastic movement subject to a reset-and-residence mechanism: transport properties and first arrival statistics

Axel Masó-Puigdellosas¹, Daniel Campos and Vicenç Méndez

Grup de Física Estadística, Facultat de Ciències, Departament de Física,
Edifici Cc, Universitat Autònoma de Barcelona, 08193 Bellaterra
(Barcelona), Spain
E-mail: axel.maso@uab.cat

Received 31 October 2018

Accepted for publication 28 January 2019

Published 4 March 2019

Online at stacks.iop.org/JSTAT/2019/033201
<https://doi.org/10.1088/1742-5468/ab02f3>



CrossMark

Abstract. In this work, we consider stochastic movement with random resets to the origin followed by a random residence time before the motion starts again. First, we study the transport properties of the walker, i.e. we derive an expression for the mean square displacement of the overall process and study its dependence on the statistical properties of the resets and the residence times probability density functions (PDFs) and the type of movement. From this general formula, we see that the inclusion of the residence after the resets is able to induce super-diffusive to sub-diffusive (or diffusive) regimes and it can also make a sub-diffusive walker reach a constant mean square displacement or even collapse. Second, we study how the reset-and-residence mechanism affects the survival probability of different search processes to a given position, showing that the long time behavior of the reset and residence time PDFs determine the existence of the mean first arrival time.

Keywords: stochastic particle dynamics, stochastic processes, stationary states, Brownian motion

¹ Author to whom any correspondence should be addressed.

Contents

1. Introduction	2
2. The process	3
3. Transport regime analysis	5
3.1. Long tail $\varphi_{\text{R}}(t)$ PDF	6
3.2. Exponential $\varphi_{\text{R}}(t)$ PDF	6
4. Stationary state	8
5. Mean first arrival time	10
5.1. Infinite MFAT	12
5.2. Finite MFAT	14
6. Conclusions	15
Acknowledgments	15
References	16

1. Introduction

The territorial dynamics of animals are compound multi-stage processes. When they are seeking for food, their behaviour is completely different than when they are resting or socializing around their nest or just exploring potential areas to migrate. Therefore, a complete model to describe spatial occupation of animals should consider a combination of different states and the overall process would end up determining their region of influence, which is technically called the home range [1].

Among these states, the movement for searching has been the main object of study [2–5] but resting phases [6] or migrations [7] have also been analysed. Also, data-oriented models [8] and macroscopic models based in the Fokker–Planck equation [9, 10] have been employed to study the home range of animals in practical cases. Nevertheless, a mesoscopic multi-stage formulation is still lacking.

The inclusion of resets in diffusive motion [11] is a first step in the formulation of a model able to capture the global dynamics from the multiple internal states of the animals. After that, multiple works have been devoted to study many types of processes with different resetting mechanisms [12–32], some of them focusing on the completion time of the processes [33, 34], or using resets to concatenate different processes [35, 36].

Generally, resets have been treated as an instantaneous action that connects two different realisations of a given process. This, for most of the applications of stochastic search (including movement ecology), is not realistic. Nevertheless, some works have introduced a penalizing period after a reset happens using the Michaelis–Mentens reaction scheme. In particular, search processes with constant rate restarts and finite time overheads were studied in [37, 38] and an equation for the first completion time

Stochastic movement subject to a reset-and-residence mechanism: transport properties and first arrival statistics distribution of a process with constant rate restarts and a general PDF for the time overheads was derived in [39]. Also, in [40] a stochastic process with Poissonian resets followed by a generally distributed quiescent time has been recently studied using a renewal approach.

Following this line, we study the transport properties and the first arrival statistics of a walker which may experience resets after which we introduce a residence (or resting) quiescent period before starting anew. Unlike the previous works, our most interesting results correspond to the particular case where both the reset and the residence time PDFs have a power-law decay. For this case we show that the inclusion of the residence period generates a wide variety of transport regimes. Previous models have already shown this capacity of resting states to modify the transport regime of a process (see for instance [41, 42] or [43] for a successful application).

In an ecological context, the residence period can be interpreted as the time spent by an animal at the nest between two consecutive foraging trips. Furthermore, assuming that the animal ceases to do any task when it decides to return to the nest, the quiescent time could also include the time spent by the animal to go there. This partially solves the unphysical instantaneous nature of resets.

This paper is organised as follows. In section 2 we present the model and we derive an expression for the probability of the walker being at position x at time t . In section 3 we find a formula for the overall mean square displacement (MSD) in terms of the MSD of the movement process and its long-term behaviour is analysed, while in section 4 we study the case where a stationary state is reached. Finally, in section 5 the first arrival statistics of the process are studied and, in the cases where it is finite, a general expression for the mean first arrival time (MFAT) is found. We conclude the work in section 6.

2. The process

Let us introduce the general formulation of the process studied in this paper. In order to describe both the movement process and the resting of the walker in the nest, we define two different states. The first state, $i = 1$, corresponds to the movement stage, while in the second state, $i = 2$, the walker rests at the origin. First, we study the transition probabilities between the two states. Let $\varphi_R(t)$ be the reset time PDF (i.e. the distribution of times the walker spends travelling) and $\varphi_S(t)$ or residence time PDF (i.e. the distribution of times that the walker stays at the origin before moving again). Then, the probability of arriving at state $i = 1, 2$ at time t can be written as

$$j_1(t) = \delta(t) + \int_0^t j_2(t-t')\varphi_S(t')dt' \quad (2.1)$$

$$j_2(t) = \int_0^t j_1(t-t')\varphi_R(t')dt', \quad (2.2)$$

where the $\delta(t)$ in the first equation indicates that the process starts at state $i = 1$. The second term in the first equation and the second equation are the probabilities of

Stochastic movement subject to a reset-and-residence mechanism: transport properties and first arrival statistics

reaching the state i from state i' ; which is the probability of reaching the state i' at any past time $t - t'$ and stay there for a time t' , when the walker switches back to i . Transforming equations (2.1) and (2.2) by Laplace for the time variable we get

$$\hat{j}_1(s) = \frac{1}{1 - \hat{\varphi}_R(s)\hat{\varphi}_S(s)} \quad (2.3)$$

$$\hat{j}_2(s) = \frac{\hat{\varphi}_R(s)}{1 - \hat{\varphi}_R(s)\hat{\varphi}_S(s)} \quad (2.4)$$

where $\mathcal{L}[f(t)] = \hat{f}(s) = \int_0^\infty e^{-st}f(t)dt$ is the laplace transform of $f(t)$. The next step is to introduce the spatial motion in the model. The overall probability that the walker is at point x at time t can be split into two parts $\rho(x, t) = \rho_1(x, t) + \rho_2(x, t)$, where $\rho_i(x, t)$ is the partial probability when it is at state i . For the state $i = 1$ we define the propagator $P(x, t)$ as the time-dependent distribution of the walker position during a single movement stage. On the other hand, we take the position of the the walker to be fixed at $x = 0$ when it is in the resting state ($i = 2$). With these considerations, the time-dependent PDF for each of the states becomes

$$\rho_1(x, t) = \int_0^t dt' j_1(t - t') \varphi_R^*(t') P(x, t'), \quad (2.5)$$

$$\rho_2(x, t) = \delta(x) \int_0^t dt' j_2(t - t') \varphi_S^*(t') \quad (2.6)$$

where $\varphi_{R,S}^*(t) = \int_t^\infty \varphi_{R,S}(t') dt'$. These equations can be read as follows: the position distribution of the walker in each of the states $i = 1, 2$ at time t is the probability of getting there any time before ($j_1(t - t')$ and $j_2(t - t')$, respectively), stay there for the remaining time ($\varphi_R^*(t')$ and $\varphi_S^*(t')$ respectively), with the dynamics of the walker described by the corresponding propagator ($P(x, t')$ and $\delta(x)$, respectively). Transforming by Laplace in time, and substituting the transition probabilities by their explicit expressions given in equations (2.3) and (2.4) we get

$$\hat{\rho}_1(x, s) = \frac{\mathcal{L}[\varphi_R^*(t)P(x, t)]}{1 - \hat{\varphi}_R(s)\hat{\varphi}_S(s)} \quad (2.7)$$

$$\hat{\rho}_2(x, s) = \frac{\hat{\varphi}_S^*(s)\hat{\varphi}_R(s)}{1 - \hat{\varphi}_R(s)\hat{\varphi}_S(s)} \delta(x). \quad (2.8)$$

Hence,

$$\hat{\rho}(x, s) = \frac{\hat{\varphi}_S^*(s)\hat{\varphi}_R(s)\delta(x) + \mathcal{L}[\varphi_R^*(t)P(x, t)]}{1 - \hat{\varphi}_R(s)\hat{\varphi}_S(s)} \quad (2.9)$$

is the PDF of the overall process. In particular, when the time PDF at the origin is taken as $\varphi_S(t) = \delta(t)$, this expression reduces to the case in [44]. Also, if we consider only exponentially distributed resets, this expression reduces to the first result in [40]. There, the case where the reset time and the residence period (refractory period therein)

Stochastic movement subject to a reset-and-residence mechanism: transport properties and first arrival statistics are correlated is also considered and a general propagator for the resulting process is derived.

3. Transport regime analysis

In the previous section we have derived an expression for the probability $\rho(x, t)$ that the walker is at point x at time t . Here we will study the asymptotic behaviour of the MSD. Particularly, we study how the tails of the reset and residence time PDFs modify the transport properties of the overall process, leaving for the next section the study of the cases where the walker reaches a stationary state.

To do so, we start from equation (2.9). If we multiply at both sides by x^2 and integrate over the whole spatial domain we get an equation for the overall MSD in the Laplace space in terms of the time PDFs and the movement MSD:

$$\mathcal{L}[\langle x^2(t) \rangle] = \frac{\mathcal{L}[\varphi_R^*(t)\langle x^2(t) \rangle_m]}{1 - \hat{\varphi}_R(s)\hat{\varphi}_S(s)}. \quad (3.1)$$

Here, the subindex m in $\langle x^2(t) \rangle_m$ indicates that the MSD corresponds to the movement stage, while the expression without subindex $\langle x^2(t) \rangle$ corresponds to the overall process. In order to study more explicitly the MSD we choose a particular expression for the time PDFs:

$$\varphi_R(t) = \frac{t^{\gamma_R-1}}{\tau_m^{\gamma_R}} E_{\gamma_R, \gamma_R} \left[- \left(\frac{t}{\tau_m} \right)^{\gamma_R} \right] \quad (3.2)$$

$$\varphi_S(t) = \frac{t^{\gamma_S-1}}{\tau_s^{\gamma_S}} E_{\gamma_S, \gamma_S} \left[- \left(\frac{t}{\tau_s} \right)^{\gamma_S} \right] \quad (3.3)$$

with

$$E_{\alpha, \beta}(z) = \sum_{n=0}^{\infty} \frac{(-z)^n}{\Gamma(\alpha n + \beta)}, \quad (3.4)$$

being the Mittag-Leffler function, and $0 < \gamma_i \leq 1$ and τ_i (for $i = R, S$) are characteristic parameters. In the large time limit and for $\gamma_i < 1$ we have that $\varphi_i(t) \sim t^{-1-\gamma_i}$. The choice of these PDFs is motivated by the fact that we can recover exponential PDFs for $\gamma_R = 1$ and we can also study power-law behaviours for $\gamma_R < 1$. The first correspond to constant rate events, i.e. at any time there is the same probability of switching from one state to the other. As for the latter, they are a type of PDFs with infinite mean frequently used in the modelling of movement processes. Particularly, sub-diffusion processes are usually modelled by introducing power law tails in the waiting time PDF between two consecutive jumps (see [5]). The difference here is that the resetting mechanism constantly forces the system to wait at the origin, which makes the effect of the long tailed waiting time PDF at the origin much stronger.

Let us also assume that the movement process follows a general MSD which scales as

$$\langle x^2(t) \rangle_m \sim t^p, \quad (3.5)$$

Stochastic movement subject to a reset-and-residence mechanism: transport properties and first arrival statistics

with $0 < p < 2$. Then, the asymptotic behaviour of the overall process MSD can be found by taking the small s limit of equation (3.1) and performing the inverse Laplace transform on the result. Doing so for the whole range of parameters, one finds three different behaviours $\langle x^2(t) \rangle \sim t^a$ depending on the relative values of γ_R and γ_S :

$$a = \begin{cases} \gamma_S - 1, & \gamma_S \leq \gamma_R = 1 \\ p + \gamma_S - \gamma_R, & \gamma_S < \gamma_R < 1 \\ p, & \gamma_S \geq \gamma_R < 1. \end{cases} \quad (3.6)$$

This expression, which groups the main results of this section, shows that the inclusion of the residence at the origin generates a competition between the tails of the PDFs $\varphi_R(t)$ and $\varphi_S(t)$. This produces a rich diversity of transport regimes for the overall process in terms of the exponent of the MSD for the movement process and the reset-and-residence mechanism. In the following we study the different cases of equation (3.6) in detail.

3.1. Long tail $\varphi_R(t)$ PDF

Let us start with the cases for which the reset time PDF has a long tail ($\gamma_R < 1$). In figure 1 the exponent of the MSD at the asymptotic limit, obtained with Monte Carlo simulations, is shown for the whole range $0 < \gamma_S < 1$ and $0 < \gamma_R < 1$, for both a sub-diffusive and a super-diffusive case. There, we can observe the two bottom cases in equation (3.6) separated by the analytical limiting case $\gamma_R = \gamma_S$ (red line). Below the red line, the asymptotic exponent of the MSD does not depend on the values of γ_R and γ_S while above the red line the asymptotic exponent decreases like $\gamma_R - \gamma_S$, as we have found in the second case of equation (3.6).

Interestingly, shape of the regimes in equation (3.6) does not depend on the movement transport regime exponent p . Therefore, the competition is exclusively between the tails of the reset and residence time PDFs. When the tail of $\varphi_R(t)$ decays equally or slower than the tail of $\varphi_S(t)$ ($\gamma_S \geq \gamma_R < 1$), asymptotically there are less walkers resetting their position than leaving the origin, which makes the residence stage negligible. On the other hand, when the tail of $\varphi_S(t)$ decays slower than the tail of $\varphi_R(t)$ ($\gamma_S < \gamma_R < 1$), the residence PDF becomes significant and the overall transport regime is affected by the reset and residence time PDFs. In fact, this change of behaviour is a consequence of the requirement of the walker to have restarted its position for the residence mechanism to be triggered. Therefore, when the reset times are asymptotically longer than the residence times, the asymptotic behaviour of the MSD is as if there was no residence [44]. Otherwise, when the residence times are asymptotically longer, the effect of the particles stacked at the origin becomes qualitatively relevant.

3.2. Exponential $\varphi_R(t)$ PDF

When the reset time PDF $\varphi_R(t)$ is exponential, the asymptotic behaviour of the MSD changes drastically. This case includes both power law and exponential PDFs for $\varphi_S(t)$. In figure 2 we show the simulated MSD for long tailed residence time PDFs and different movement: sub-diffusive and diffusive processes, and super-diffusive Lévy walks. In all three cases, the MSD increases for short times until it reaches a maximum value and

Stochastic movement subject to a reset-and-residence mechanism: transport properties and first arrival statistics

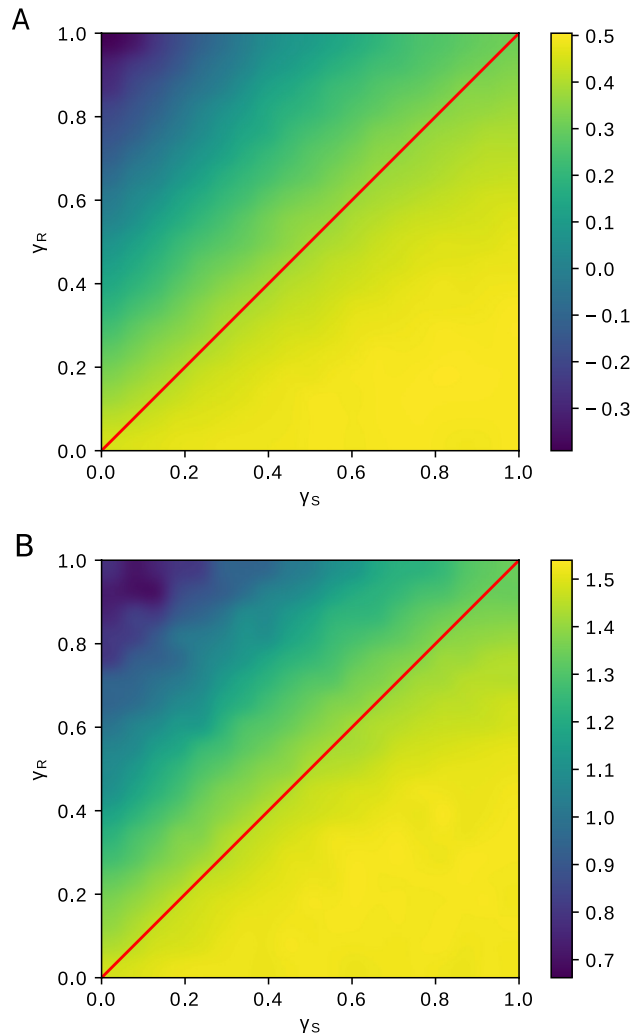


Figure 1. Exponent a of the asymptotic behaviour of the MSD of the overall process $\langle x^2(t) \rangle \sim t^a$ with respect to the long tailed reset and residence time PDFs exponents γ_R and γ_S respectively is shown. The plots correspond to simulations of two different movement processes: a sub-diffusive process with $p = 0.5$ in (A) and a super-diffusive Lévy walk with $p = 1.5$ in (B). For both cases, in the region below the red line ($\gamma_R = \gamma_S$) the exponent is constant and equal to the movement MSD exponent $a = p$ while in the region above the line the exponent diminishes progressively.

starts to decrease as predicted with the first case in equation (3.6). The asymptotic decay depends exclusively on the residence time PDF exponent γ_S and in this regime the movement process only modifies multiplicatively the overall MSD.

To summarize, in figure 3 we present a phase diagram with the possible transport regimes. There we can see that a super-diffusive process ($p > 1$) can be transformed to a sub-diffusive (or diffusive) process when the reset-and-residence mechanism is taken into account. Similarly, a sub-diffusive process ($p < 1$) can derive into a transport

Stochastic movement subject to a reset-and-residence mechanism: transport properties and first arrival statistics

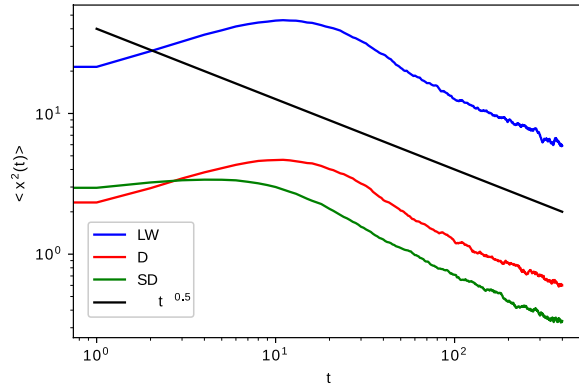


Figure 2. The time evolution of the MSD of a simulation of an overall process with $\gamma_R = 1$ and $\gamma_S = 0.5$ is plotted for a sub-diffusive (SD), a diffusive (D) and a Lévy walk (LW) super-diffusive motion. In all three cases the MSD decreases as $t^{-0.5}$ in the long time limit as predicted by the first case in equation (3.6). See the guide line (black line in the plot) for comparison.

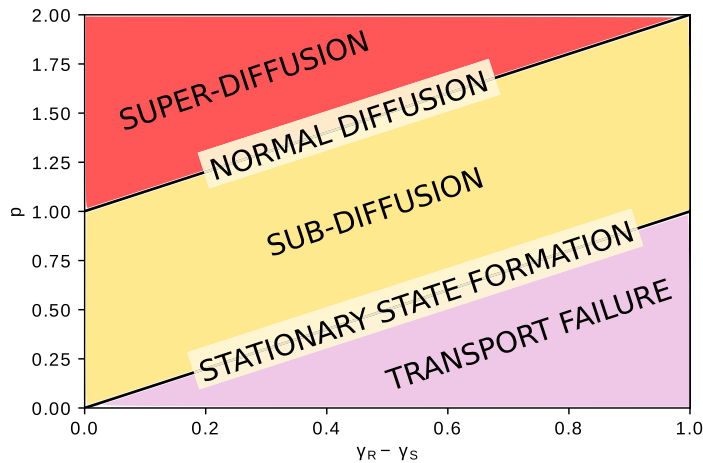


Figure 3. Schematic plot of the different overall transport regimes in terms of the transport regime of the movement process p and the difference between the decaying exponents of the reset and residence time PDFs $\gamma_R - \gamma_S$. In the red region the overall behaviour is super-diffusive. In the yellow region it is sub-diffusive and the pink represents the values for which we have transport failure.

failure regime. Therefore, the reset-and-residence mechanism can be also seen as a tool to slow down the transport regime.

4. Stationary state

In the previous section we have derived in a general manner the transport regime of the overall process and we have also studied how the reset-and-residence mechanism

Stochastic movement subject to a reset-and-residence mechanism: transport properties and first arrival statistics affects the long term behaviour of the system. In this section we study the special case where both the residence and the reset time PDFs are exponential ($\gamma_S = \gamma_R = 1$), so a stationary state is reached. Concretely, we derive a formula for the overall MSD in terms of the MSD of the movement and we find the stationary distribution for some well-known movement processes.

To do so, we start from equation (3.1) and the time PDFs from equations (3.2) and (3.3) with $\gamma_R = 1$ and $\gamma_S = 1$ respectively. With these parameters the Laplace transform of the overall MSD reads

$$\mathcal{L}[\langle x^2(t) \rangle] = \frac{\mathcal{L}[e^{-\frac{t}{\tau_m}} \langle x^2(t) \rangle_m]}{1 - \frac{1}{(1+\tau_m s)(1+\tau_s s)}}. \quad (4.1)$$

In order to find the asymptotic behaviour of the MSD we make use of the final value theorem $\lim_{t \rightarrow \infty} f(t) = \lim_{s \rightarrow 0} s \mathcal{L}[f(t)]$. Doing so, the stationary MSD can be easily found from equation (4.1) giving

$$\langle x^2 \rangle_{\text{st}} = \frac{1}{\tau_m + \tau_s} \int_0^\infty e^{-\frac{t}{\tau_m}} \langle x^2(t) \rangle_m dt. \quad (4.2)$$

For a motion with $\langle x^2(t) \rangle_m = 2Dt^p$ with D , p positive constants, the stationary MSD takes the simple form

$$\langle x^2 \rangle_{\text{st}} = 2D \Gamma(p+1) \frac{\tau_m^{p+1}}{\tau_m + \tau_s}. \quad (4.3)$$

This result has been compared with Monte Carlo simulations in figure 4 for three different types of movement. Let us now calculate the stationary distribution. Doing so it is easy to see that the stationary distribution can be written in terms of the propagator $P(x, t)$ as

$$\rho_{\text{st}}(x) = \frac{\tau_s}{\tau_m + \tau_s} \delta(x) + \frac{\hat{P}(x, s = \frac{1}{\tau_m})}{\tau_m + \tau_s}, \quad (4.4)$$

which has been recently found in [40]. For a propagator of the form

$$P^{\text{SD}}(k, s) = \frac{1}{s + D_\gamma s^{1-\gamma} k^2}$$

in the Fourier–Laplace space, which corresponds to a sub-diffusive process for $\gamma < 1$ and diffusive for $\gamma = 1$, the stationary distribution is

$$\rho_{\text{st}}^{\text{SD}}(x) = \frac{\tau_s}{\tau_m + \tau_s} \delta(x) + \frac{\tau_m}{\tau_m + \tau_s} \frac{e^{-\frac{|x|}{\sqrt{D_\gamma \tau_m}}}}{\sqrt{4D_\gamma \tau_m^\gamma}}. \quad (4.5)$$

If instead of a sub-diffusive (or diffusive) motion we consider a Lévy flight, its propagator is

$$P^{\text{LF}}(k, s) = \frac{1}{s + D_\alpha |k|^\alpha}$$

Stochastic movement subject to a reset-and-residence mechanism: transport properties and first arrival statistics

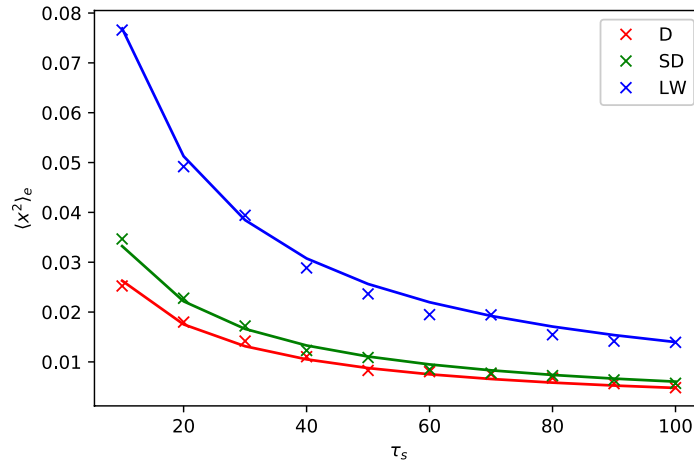


Figure 4. Stationary MSD for a sub-diffusive (SD), a diffusive (D) and a Lévy flight (LF) propagator when they are subject to reset times which are exponential distributed with $\tau_m = 10$ and retained at the origin during a time given by an exponential PDF with different means τ_s . For the propagators we have chosen $p = 0.5$, $D = 1.05 \cdot 10^{-2}$ for the sub-diffusive, $p = 1$, $D = 2.63 \cdot 10^{-3}$ for the diffusive and $p = 1.1$, $D = 6.11 \cdot 10^{-3}$ for the Lévy walk. The crosses correspond to the simulated distributions while the solid curves show the analytical result given in equation (4.3).

in the Fourier–Laplace space, where $\alpha < 2$ and D_α is the corresponding diffusion constant. The stationary distribution reads

$$\rho_{st}^{LF}(x) = \frac{\tau_s}{\tau_m + \tau_s} \delta(x) + 2 \frac{\tau_m}{\tau_m + \tau_s} \int_0^\infty \frac{\cos(kx)}{1 + \tau_m D_\alpha k^\alpha} dk. \quad (4.6)$$

This distribution has divergent second order moment since it decays as $\frac{1}{|x|^{1+\alpha}}$ for large $|x|$. Therefore, despite a stationary state is reached the average region of space covered by the walker around the nest is infinite. Contrarily, for the sub-diffusive and diffusive movement processes we have a finite stationary MSD, the value of which is given by equation (4.3) with properly chosen parameters.

5. Mean first arrival time

In the previous section we have analysed the long-term behaviour of the overall process. Here we perform a first arrival time analysis which is still lacking despite of the previous works including a quiescent period after the resets. It consists on determining the conditions for which the MFAT is finite, taking into account finite and infinite mean PDFs for the reset and residence time PDFs. To do so, we build up a mesoscopic equation for the overall survival probability $\sigma_x(t)$, which is the probability of the walker not having arrived to x at time t . Let us separate the overall survival probability into three temporal non-overlapping processes. If the walker starts at the origin but is moving (i.e. at the state $i = 1$), the three contributions to the overall survival probability are:

Stochastic movement subject to a reset-and-residence mechanism: transport properties and first arrival statistics

- (i) The walker has not yet restarted at time t . This happens with probability $\varphi_R^*(t)$ and in this case the overall survival probability is the same as the motion survival probability $Q_x(t)$.
- (ii) The walker has restarted its position once at time $t' < t$, during which it has not arrived to x , and during the period (t', t) it has not left the origin. The first happens with probability $\varphi_R(t')Q_x(t')$, the second with probability $\varphi_S^*(t - t')$ with $0 \leq t' \leq t$.
- (iii) The walker has restarted its position at least once at time $t' < t$ and it has not reached x before t' , which happens with probability $\varphi_R(t')Q_x(t')$ as in the previous case. However, here the walker leaves the origin after a time $t'' < t - t'$ and in this case the walker is exactly at the initial scenario but instead of having a time t , we have to subtract the time of the first non-triggering journey ($t \rightarrow t - t' - t''$). This happens with probability $\varphi_S(t'')\sigma_x(t - t' - t'')$ given that the first reset was at time t' . These scenarios must be taken into account for all $t'' < t - t'$ and $t' < t$.

Putting the three contributions together we get:

$$\begin{aligned} \sigma_x(t) = & \varphi_R^*(t)Q_x(t) + \int_0^t \varphi_R(t')Q_x(t')\varphi_S^*(t - t')dt' \\ & + \int_0^t \varphi_R(t')Q_x(t')dt' \int_0^{t-t'} \varphi_S(t'')\sigma_x(t - t' - t'')dt'', \end{aligned} \tag{5.1}$$

where $Q_x(t)$ is the survival probability of the movement process and the first, second and third terms in the rhs correspond to cases (i), (ii) and (iii), respectively. Applying the Laplace transform to equation (5.1) we get

$$\hat{\sigma}_x(s) = \frac{\mathcal{L}[\varphi_R^*(t)Q_x(t)] + \mathcal{L}[\varphi_R(t)Q_x(t)]\hat{\varphi}_S^*(s)}{1 - \mathcal{L}[\varphi_R(t)Q_x(t)]\hat{\varphi}_S(s)}, \tag{5.2}$$

which has been also found as a particular case in [40] by assuming non-correlated reset and residence time PDFs on their general result. This equation is completely general so it is valid for any survival probability of the movement process $Q_x(t)$ and any reset and residence time PDFs $\varphi_R(t)$ and $\varphi_S(t)$, respectively. Here we focus on studying the asymptotic behaviour of the overall survival probability for $Q_x(t) \sim t^{-q}$ with $0 < q < 1$. This choice encompasses some processes associated with animal foraging as shown in the particular examples below. For $\varphi_R(t)$ and $\varphi_S(t)$ we consider again expressions (3.2) and (3.3), respectively.

The existence of a MFAT can be determined by taking the limit $s \rightarrow 0$ in equation (5.2) ($T_F = \lim_{s \rightarrow 0} \hat{\sigma}(s)$). In this limit, corresponding to the long t limit, the dominant term in the numerator of equation (5.2) depends on the tail exponents of the PDFs $\varphi_R(t)$ and $\varphi_S(t)$. Concretely, we can distinguish three different cases:

- (a) $\gamma_S \geq \gamma_R + q$. At long times, the first term in the numerator of equation (5.2) dominates over the second (or they are equal in the limiting case). The MFAT is infinite since the survival probability decays as

Stochastic movement subject to a reset-and-residence mechanism: transport properties and first arrival statistics

$$\sigma_x(t) \sim t^{\gamma_R+q-1}. \quad (5.3)$$

- (b) $\gamma_S < \gamma_R + q$, $\gamma_S < 1$. At long times, the second term in the numerator of equation (5.2) is the dominant term. Here, the MFAT is infinite again, with a survival probability decaying as

$$\sigma_x(t) \sim t^{\gamma_S-1}. \quad (5.4)$$

- (c) $\gamma_S < \gamma_R + q$, $\gamma_S = 1$. In this scenario, the MFAT is finite and it can be written as

$$T_F = \frac{I_1 + \tau_s I_2}{1 - I_2}, \quad (5.5)$$

with

$$I_1 = \int_0^\infty E_{\gamma_R,1} \left[- \left(\frac{t}{\tau_m} \right)^{\gamma_R} \right] Q_x(t) dt \quad (5.6)$$

and

$$I_2 = \int_0^\infty \frac{t^{\gamma_R-1}}{\tau_m^{\gamma_R}} E_{\gamma_R,\gamma_R} \left[- \left(\frac{t}{\tau_m} \right)^{\gamma_R} \right] Q_x(t) dt, \quad (5.7)$$

where we have made use of equations (3.2) and (3.3).

From this we see that, when studying the overall survival probability, the reset time PDF couples to the survival probability of the movement process and is the joint tail the one which competes with the residence time PDF. Therefore, the type of movement has a direct effect on which distribution determines the tail exponent of the overall survival probability. To illustrate this, we next study these general results for some particular cases.

5.1. Infinite MFAT

Let us leave the case (c) in the previous Section apart for the moment. From cases (a) and (b) we see that there are two different regions in the state space where the governing tail differs, limited by the plane $\gamma_S = \gamma_R + q$. In the following we test this for two different movement processes: a sub-diffusive random walk (figure 5(A)) and a Lévy flight (figure 5(B)).

The survival probability of a sub-diffusive jump process has been studied in [45], where it was found to be

$$Q_x^{\text{SD}}(t) = \frac{x}{\sqrt{Dt}^\gamma} \sum_{k=0}^{\infty} \frac{\left(-\frac{x}{\sqrt{Dt}^\gamma} \right)^k}{(k+1)! \Gamma\left(1 - \frac{\gamma}{2} - k\frac{\gamma}{2}\right)} \quad (5.8)$$

with $0 < \gamma < 1$. This, in the large time limit decays as

Stochastic movement subject to a reset-and-residence mechanism: transport properties and first arrival statistics

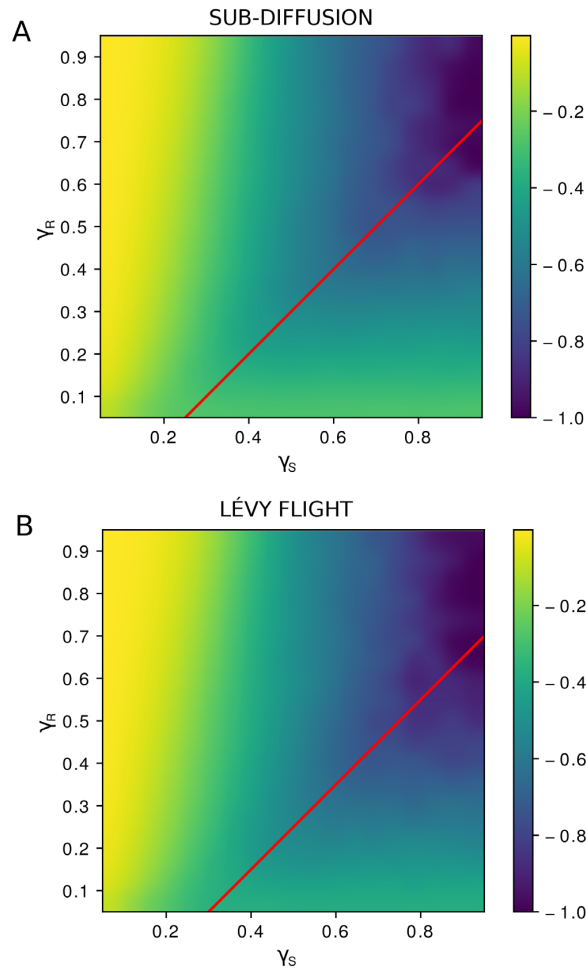


Figure 5. Exponent b of the asymptotic behaviour of the survival probability of the overall process $\sigma_x(t) \sim t^{-b}$ with long tailed reset and residence time PDFs is shown. Their exponents are γ_R and γ_S and the plots are for simulations of two different movement processes: a sub-diffusive process with $\gamma = 0.5$ in (A) and a super-diffusive Lévy walk with $\alpha = 1.5$ in (B). For both cases, in the region above the red line ($\gamma_S = \gamma_R + q$ with $q = 0.25$ in (A) and $q = 0.33$ in (B)) b only changes horizontally with γ_S while below the line b only varies vertically with γ_R . These are the results predicted by the cases (a) and (b) in the main text respectively.

$$Q_x^{\text{SD}} \sim t^{-\frac{\gamma}{2}}. \tag{5.9}$$

For $\gamma = 1$, we can recover the well-known decay for the survival probability of a diffusive process. From the asymptotic expression we can identify $q = \frac{\gamma}{2}$ and, therefore, in this case the limiting plane is $\gamma_S = \gamma_R + \frac{\gamma}{2}$, which is illustrated as a red line in figure 5(A) for the particular case $\gamma = 0.5$. There we can see that, below the line, the tail exponent of the overall survival probability increases upwards and remains constant in the horizontal direction, which means that it depends on the reset tail only.

Stochastic movement subject to a reset-and-residence mechanism: transport properties and first arrival statistics

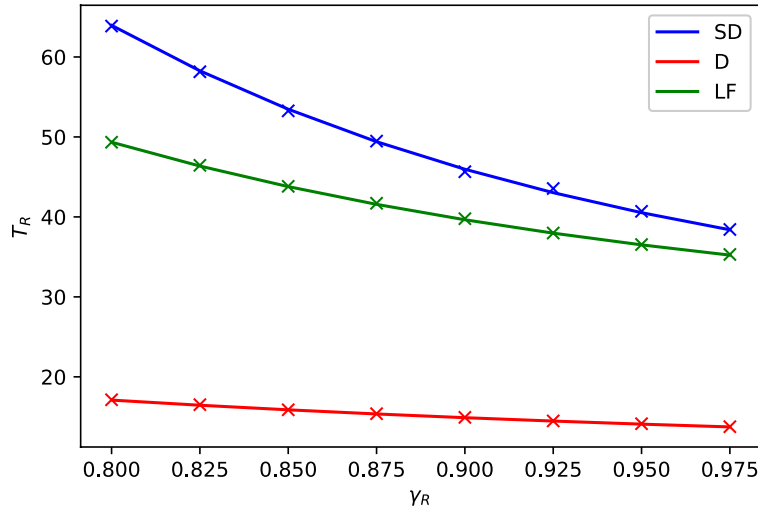


Figure 6. The simulated MFAT (crosses) with an exponential residence time PDF with mean $\tau_s = 10$ and for three representative cases of subdiffusion (SD) with $\gamma = 0.5$, diffusion (D) with $\gamma = 1$ and a Lévy flight with $\alpha = 1.5$, all with $D = 0.1$. We compare our simulations to the analytical result in equation (3.4) (solid curves) for different reset time PDF tail exponents γ_R and $\tau_m = 10$. Concretely, the MFAT is computed at a distance $x = 0.5$ from the origin.

Contrarily, above the red line the decaying exponent of the overall survival probability increases from left to right and remains constant in the vertical direction. Therefore, in this case, it only depends on the residence tail, which is in agreement with cases (a) and (b) above. This general behaviour becomes less clear near the red lines, where the tail competition is evenner. This can be amended by running considerably longer simulations.

Regarding the Lévy flight process, an expression for the Laplace transform of the first arrival survival probability was derived in [46]:

$$\hat{Q}_x^{\text{LF}}(s) = \frac{\alpha D^{1/\alpha} \sin(\pi/\alpha)}{\pi s^{1/\alpha}} \int_0^\infty \frac{1 - \cos(kx)}{s + Dk^\alpha} dk. \quad (5.10)$$

This scales asymptotically as

$$Q_x^{\text{LF}}(t) \sim t^{\frac{1}{\alpha}-1}. \quad (5.11)$$

Here $1 < \alpha < 2$, being $\alpha = 2$ the diffusive limit. In this case, the limiting surface is $\gamma_S = \gamma_R + \frac{1}{\alpha}$, which has been plotted for the particular value $\alpha = 1.5$ in figure 5(B) as a red straight line. As for the previous example, the line separates two different regions in which the dominant exponent is γ_S above the red line and γ_R below.

5.2. Finite MFAT

From the three different cases from equation (5.2), the (c) scenario is the only one where the MFAT is finite. In this case, equation (5.5) gives us its value for different movement survival probabilities. As for the previous situations, we consider the two cases where

Stochastic movement subject to a reset-and-residence mechanism: transport properties and first arrival statistics

the motion is sub-diffusive and a Lévy flight, the survival probabilities of which are in equations (5.8) and (5.10) respectively. In figure 6 we show the simulated MFAT for a sub-diffusive, a diffusive (as a limit of the first) and a Lévy flight process in the (c) scenario. The simulations are compared with the result obtained by numerically integrating equation (5.5) for the different cases.

6. Conclusions

We have studied how a stochastic residence period at the resetting position affects the overall dynamics of a random walker. More specifically, we have employed a renewal approach to derive analytical expressions for the MSD and the survival probability (or MFAT when it is finite), which have been validated with Monte Carlo simulations of different processes such as diffusion, Lévy walks or Lévy flights.

For the MSD we have found that, on one hand, for long tailed reset and residence time PDFs the MSD of the overall process depends strongly on the relation between the tail exponents of both PDFs (γ_R for resets and γ_S for residence times). Concretely, for $\gamma_R \geq \gamma_S$ the overall MSD exponent is the same as the one for the movement process while for $\gamma_R < \gamma_S$ the exponent of the movement process is diminished by a factor $\gamma_R - \gamma_S$. On the other hand, for exponentially distributed reset times, if the residence time PDF is long tailed the overall process collapses to the origin while for an exponential residence time PDF a stationary MSD is reached (see equation (4.2)).

Regarding the decaying exponent of the survival probability when both time PDFs are long tailed, we have seen that the tail of the residence time PDF competes with both the tail of the movement process survival probability and the tail of the reset time PDF. In this case the MFAT is always infinite. Contrarily, when the residence time PDF is exponential, a finite MFAT may be found but only when $q + \gamma_R > 1$ with q and γ_R being the tail exponents of the survival probability of the movement process and the reset time PDF respectively.

We note that, in the context of movement ecology, resets are a natural mechanism to concatenate different trials of a particular behaviour of the animals. In this work we have tried to include explicitly the period that they spend in the nest separating excursions for feeding, mating or any other basic functions. The next step towards a complete model could be the introduction of multiple search strategies with different movement patterns to be chosen during the resting period, similarly to what has been done in [35, 36] for instance. Also, regarding the interpretation of the quiescent time as the time needed by the animal to return to the nest, a further step to be addressed in future works would be the introduction of a process driving the individual gradually towards the nest instead of leaving it in a motionless state.

Acknowledgments

This research has been supported by the Spanish government through Grant No. CGL2016-78156-C2-2-R.

Stochastic movement subject to a reset-and-residence mechanism: transport properties and first arrival statistics

References

- [1] Burt W 1943 *J. Mammal.* **24** 346
- [2] Viswanathan G M, da Luz M G E, Raposo E P and Stanley H E 2011 *The Physics of Foraging: an Introduction to Random Searches and Biological Encounters* (Cambridge: Cambridge University Press)
- [3] Okubo A and Levin S A 2002 *Diffusion and Ecological Problems: Modern Perspectives* vol 14 (Berlin: Springer)
- [4] Bartumeus F, da Luz M G E, Viswanathan G and Catalan J 2005 *Ecology* **86** 3078
- [5] Méndez V, Campos D and Bartumeus F 2014 *Stochastic Foundations in Movement Ecology* (Berlin: Springer)
- [6] Hillen T 2003 *Eur. J. Appl. Math.* **14** 613636
- [7] Bauer S and Klaassen M 2013 *J. Animal Ecol.* **82** 498
- [8] Worton B 1987 *Ecol. Modelling* **38** 277
- [9] Giuggioli L, Abramson G, Kenkre A V M, Suzan G, Marc E and Yates T L 2005 *Bull. Math. Biol.* **67** 1135
- [10] Giuggioli L, Abramson G, Kenkre V M, Parmenter R and Yates T L 2006 *J. Theor. Biol.* **240** 126
- [11] Evans M R and Majumdar S N 2011 *Phys. Rev. Lett.* **106** 160601
- [12] Evans M R and Majumdar S N 2011 *J. Phys. A: Math. Theor.* **44** 435001
- [13] Whitehouse J, Evans M R and Majumdar S N 2013 *Phys. Rev. E* **87** 022118
- [14] Montero M and Villarroel J 2013 *Phys. Rev. E* **87** 012116
- [15] Evans M R, Majumdar S N and Mallick K 2013 *J. Phys. A: Math. Theor.* **46** 185001
- [16] Gupta S, Majumdar S N and Schehr G 2014 *Phys. Rev. Lett.* **112** 220601
- [17] Evans M R and Majumdar S N 2014 *J. Phys. A: Math. Theor.* **47** 285001
- [18] Durang X, Henkel M and Park H 2014 *J. Phys. A: Math. Theor.* **47** 045002
- [19] Kuśmierz Ł, Majumdar S N, Sabhapandit S and Schehr G 2014 *Phys. Rev. Lett.* **113** 220602
- [20] Kuśmierz Ł and Gudowska-Nowak E 2015 *Phys. Rev. E* **92** 052127
- [21] Pal A 2015 *Phys. Rev. E* **91** 012113
- [22] Majumdar S N, Sabhapandit S and Schehr G 2015 *Phys. Rev. E* **92** 052126
- [23] Campos D and Méndez V 2015 *Phys. Rev. E* **92** 062115
- [24] Christou C and Schadschneider A 2015 *J. Phys. A: Math. Theor.* **48** 285003
- [25] Méndez V and Campos D 2016 *Phys. Rev. E* **93** 022106
- [26] Pal A, Kundu A and Evans M R 2016 *J. Phys. A: Math. Theor.* **49** 225001
- [27] Nagar A and Gupta S 2016 *Phys. Rev. E* **93** 060102
- [28] Eule S and Metzger J J 2016 *New J. Phys.* **18** 033006
- [29] Falcao R and Evans M R 2017 *J. Stat. Mech.* **023204**
- [30] Boyer D, Evans M R and Majumdar S N 2017 *J. Stat. Mech.* **023208**
- [31] Shkilev V P 2017 *Phys. Rev. E* **96** 012126
- [32] Belan S 2018 *Phys. Rev. Lett.* **120** 080601
- [33] Pal A and Reuveni S 2017 *Phys. Rev. Lett.* **118** 030603
- [34] Chechkin A and Sokolov I M 2018 *Phys. Rev. Lett.* **121** 050601
- [35] Montero M and Villarroel J 2016 *Phys. Rev. E* **94** 032132
- [36] Montero M, Masó-Puigdellosas A and Villarroel J 2017 *Eur. Phys. J. B* **90** 176
- [37] Reuveni S, Urbakh M and Klafter J 2014 *Proc. Natl Acad. Sci.* **111** 4391
- [38] Rotbart T, Reuveni S and Urbakh M 2015 *Phys. Rev. E* **92** 060101
- [39] Reuveni S 2016 *Phys. Rev. Lett.* **116** 170601
- [40] Evans M R and Majumdar S N 2019 *J. Phys. A: Math. Theor.* **52** 01LT01
- [41] Kumar N, Harbola U and Lindenberg K 2010 *Phys. Rev. E* **82** 021101
- [42] Harbola U, Kumar N and Lindenberg K 2014 *Phys. Rev. E* **90** 022136
- [43] Brockmann D, Hufnagel L and Geisel T 2006 *Nature* **439** 462
- [44] Masó-Puigdellosas A, Campos D and Méndez V 2019 *Phys. Rev. E* **99** 012141
- [45] Rangarajan G and Ding M 2000 *Phys. Lett. A* **273** 322
- [46] Chechkin A V, Metzler R, Gonchar V Y, Klafter J and Tanatarov L V 2003 *J. Phys. A: Math. Gen.* **36** L537

Appendix C

Third Article


Transport properties of random walks under stochastic non-instantaneous resetting

Axel Masó-Puigdellosas, Daniel Campos and Vicenç Méndez

*Grup de Física Estadística. Departament de Física, Universitat Autònoma de
Barcelona, 08193 Bellaterra, Spain*

This paper has been published in *Phys. Rev. E* **100**, 042104

Transport properties of random walks under stochastic noninstantaneous resetting

Axel Masó-Puigdellosas, Daniel Campos, and Vicenç Méndez 

Grup de Física Estadística, Departament de Física, Facultat de Ciències, Edifici Cc, Universitat Autònoma de Barcelona, 08193 Bellaterra (Barcelona), Spain



(Received 20 June 2019; published 4 October 2019)

Random walks with stochastic resetting provides a treatable framework to study interesting features about central-place motion. In this work, we introduce noninstantaneous resetting as a two-state model being a combination of an exploring state where the walker moves randomly according to a propagator and a returning state where the walker performs a ballistic motion with constant velocity towards the origin. We study the emerging transport properties for two types of reset time probability density functions (PDFs): exponential and Pareto. In the first case, we find the stationary distribution and a general expression for the stationary mean-square displacement (MSD) in terms of the propagator. We find that the stationary MSD may increase, decrease or remain constant with the returning velocity. This depends on the moments of the propagator. Regarding the Pareto resetting PDF we also study the stationary distribution and the asymptotic scaling of the MSD for diffusive motion. In this case, we see that the resetting modifies the transport regime, making the overall transport subdiffusive and even reaching a stationary MSD, i.e., a stochastic localization. This phenomena is also observed in diffusion under instantaneous Pareto resetting. We check the main results with stochastic simulations of the process.

DOI: [10.1103/PhysRevE.100.042104](https://doi.org/10.1103/PhysRevE.100.042104)

I. INTRODUCTION

Living organisms and moving particles in general can rarely exhibit free motion independent of environmental or internal constraints. One of these constraints consists of the presence of a privileged location, which is visited with a higher frequency, either for natural or artificial reasons. For instance, in a movement ecology context, the term central-place foraging [1] is often used to describe how animals seek for food near their nest. In other scenarios, such as human visual search [2], a fixed location is also used as a reference point.

From a physical point of view, this topic has been often addressed using stochastic motion models. Historically, the effect from the central point has been modeled via an attracting potential [3]. This allows the authors to analytically study the problem from a treatable perspective. However, these models do not consider the possibility of the walker returning directly to the central point, instead of (or in addition to) feeling an attraction for it. A possible mechanism that could mimic this is the random resetting of its motion to the origin.

It was not until 2011 that a simple model of stochastic motion with a strong bound to a given position was published in the physical literature [4]. There, a diffusive particle is studied when it may occasionally reset its position with a constant probability and the authors find that a nonequilibrium steady state (NESS) is reached and the mean first passage time of the overall process is finite and attains a minimum in terms of the resetting rate. The existence of a NESS has been further studied for different types of motion and resetting mechanisms [5–18], showing that they are not exclusive of diffusion with Markovian resets. Aside from these, other works have

shown that the resetting does not always generate a NESS but transport is also possible when the resetting probability density function (PDF) is long tailed [19–22] or when the resetting process is subordinated to the motion [10,12].

However, the above-cited stochastic resetting models lack some realism as long as resetting is treated as an instantaneous process. Some recent papers include a quiescent period after the resetting [23,24], which could mimic the time required by the walker to return to the origin. But this only serves as a partial solution to the problem since it does not consider the back-to-the-origin movement explicitly. In a slightly different context, this notion of costly resetting has also appeared in some works where search processes with restarts are studied from a Michaelis-Menten reaction scheme perspective [25,26].

In this direction, we propose a two-state model to describe both the exploratory motion and the return to the origin, which we assume to be ballistic. We analyze the main consequences that the application of a noninstantaneous resetting has on the results known for the instantaneous case. Particularly, we derive an expression for the overall propagator to study the transport properties of the overall process for different types of resetting PDFs. We also study the statistics of the returning time in terms of the motion and the resetting PDF.

The paper is organized as follows. In Sec. II, the model is introduced and general expressions for both the overall PDF and the overall MSD are derived. Afterwards, in Sec. II B, the PDF of the time required by a walker to go back to the origin is studied in terms of the propagator and the resetting PDF. In Secs. III and IV we study the particular cases of Markovian and scale-free PDFs, respectively. Finally, we conclude the work in Sec. V.

II. MODEL

We model the dynamics of the walker by considering two different states: an exploring state (state 1) where the motion is described by a general propagator $P(x, t)$ and a returning state (state 2) where the motion is ballistic with velocity v towards the origin defined by $x = 0$. The exploring state ends at a random time according to the resetting time PDF $\varphi_R(t)$, while the returning state ends when the motion reaches the origin. At this time, the process is renewed.

Let us start by introducing the flux of particles between these two states. On one hand, assuming that the motion starts at state 1, the rate of walkers arriving at the exploring state (state 1) is

$$j_1(t) = \delta(t) + \int_{-\infty}^{+\infty} dz \int_0^t dt' j_2(z, t-t') \delta\left(t' - \frac{|z|}{v}\right), \quad (2.1)$$

where the integral term is expressed in terms of the rate of the particle arriving at state 2 at point x at time t , $j_2(x, t)$. This term implements the probability of entering state 2 at position z at any time $t-t' < t$ and subsequently reaching the origin ballistically within time t' [$\delta(t' - |z|/v)$]. The first term on the right-hand side is the initial condition. On the other hand, the rate of walkers arriving at the returning state (state 2) reads

$$j_2(x, t) = \int_0^t j_1(t-t') \varphi_R(t') P(x, t') dt', \quad (2.2)$$

which, unlike for state 1, depends explicitly on the position x (i.e., the rate is not spatially uniform). Here, the probability of arriving at state 2 at position x and time t is the probability of having arrived at state 1 at any past time $t-t'$, times the probability that exploration finished at time t' , given the walker has reached position x . Transforming these two equations by Laplace and isolating for the rates we get the explicit expressions

$$\hat{j}_1(s) = \left[1 - \int_{-\infty}^{+\infty} dz e^{-\frac{|z|}{v}s} \Pi(z, s)\right]^{-1} \quad (2.3)$$

and

$$\hat{j}_2(x, s) = \Pi(x, s) \left[1 - \int_{-\infty}^{+\infty} dz e^{-\frac{|z|}{v}s} \Pi(z, s)\right]^{-1}, \quad (2.4)$$

where we have introduced the notation

$$\Pi(x, s) \equiv \mathcal{L}[\varphi_R(t)P(x, t)], \quad (2.5)$$

and

$$\hat{f}(s) = \mathcal{L}[f(t)] = \int_0^{\infty} e^{-st} f(t) dt$$

is the Laplace transform of $f(t)$.

Let us now introduce the spatial dynamics for each of the states. We write the global propagator as $\rho(x, t) = \rho_1(x, t) + \rho_2(x, t)$, i.e., the overall motion is described by the combination of the propagators in states 1 and 2. Defining the probability that no reset has occurred until time t as $\varphi_R^*(t) = \int_t^{\infty} \varphi_R(t') dt'$, the probability of finding the walker at the

exploring state at point x and time t can be written as

$$\rho_1(x, t) = \int_0^t j_1(t-t') \varphi_R^*(t') P(x, t') dt'. \quad (2.6)$$

Transforming by Laplace and inserting Eq. (2.3), we have

$$\hat{\rho}_1(x, s) = \Pi^*(x, s) \left[1 - \int_{-\infty}^{+\infty} dz e^{-\frac{|z|}{v}s} \Pi(z, s)\right]^{-1}, \quad (2.7)$$

with

$$\Pi^*(x, s) \equiv \mathcal{L}[\varphi_R^*(t)P(x, t)]. \quad (2.8)$$

For the sake of simplicity we will restrict to symmetric random walks, i.e., $P(x, t) = P(-x, t)$. Then, for the returning state (we consider $x > 0$, which is labeled by a plus sign in the following, to later generalize this result for $x < 0$) we have that

$$\hat{\rho}_2^+(x, t) = \int_x^{+\infty} dz \int_0^t dt' j_2(z, t-t') \delta(x-z+vt'). \quad (2.9)$$

This is, to be at position $x > 0$ at time t in the returning state, the motion had to reach this state at a previous time $t-t'$ and position $z > x$ and, during the time t' , the returning ballistic motion must have gone from z to x . Transforming by Laplace, we get

$$\hat{\rho}_2^+(x, s) = \frac{e^{\frac{x}{v}s}}{v} \int_x^{+\infty} dz e^{-\frac{z-x}{v}s} \hat{j}_2(z, s). \quad (2.10)$$

Now, introducing Eq. (2.4) and generalizing it for the negative positions [i.e., $x \rightarrow |x|$ in Eq. (2.10)], we get the general expression for the propagator in the state $i = 2$

$$\hat{\rho}_2(x, s) = \frac{1}{v} e^{\frac{|x|}{v}s} \frac{\int_{|x|}^{+\infty} dz e^{-\frac{|z|-|x|}{v}s} \Pi(z, s)}{1 - \int_{-\infty}^{+\infty} dz e^{-\frac{|z|}{v}s} \Pi(z, s)}. \quad (2.11)$$

Finally, putting both propagators together, the overall propagator $\hat{\rho}(x, s) = \hat{\rho}_1(x, s) + \hat{\rho}_2(x, s)$ turns out to be

$$\hat{\rho}(x, s) = \frac{\Pi^*(x, s) + \frac{1}{v} e^{\frac{|x|}{v}s} \int_{|x|}^{+\infty} dz e^{-\frac{|z|-|x|}{v}s} \Pi(z, s)}{1 - \varphi(s)}, \quad (2.12)$$

where

$$\begin{aligned} \varphi(s) &= \int_{-\infty}^{+\infty} dz e^{-\frac{|z|}{v}s} \Pi(z, s) \\ &= \frac{vs}{\pi} \int_{-\infty}^{+\infty} dk \frac{\Pi(k, s)}{k^2 v^2 + s^2}, \end{aligned} \quad (2.13)$$

with $\Pi(k, s)$ the Fourier-Laplace transform of $\Pi(x, t)$.

Therefore, for a general resetting PDF $\varphi_R(t)$ and propagation $P(x, t)$, one can in principle find the PDF of the overall motion process. In the numerator we have the contributions of the exploring and returning states clearly separated. However, the first term, corresponding to the exploring state, is velocity-dependent since in the denominator v appears explicitly. Therefore, both the exploring and returning states are actively modified by the finiteness of the resetting velocity. Transforming Eq. (2.12) by Fourier one finally gets, after

some calculations,

$$\rho(k, s) = \frac{1}{1 - \varphi(s)} \left[\Pi^*(k, s) + s \frac{\Pi(k, s) - \varphi(s)}{k^2 v^2 + s^2} + \frac{2kv}{k^2 v^2 + s^2} \int_0^\infty dz \sin(kz) \Pi(z, s) \right], \quad (2.14)$$

where

$$\Pi(k, s) = \int_0^\infty e^{-st} \varphi_R(t) P(k, t) dt. \quad (2.15)$$

One can check that $\rho(k=0, s) = 1/s$, so $\rho(x, t)$ is conveniently normalized.

A. MSD

The MSD can be obtained as

$$\langle \hat{x}^2(s) \rangle = - \left[\frac{\partial^2 \rho(k, s)}{\partial k^2} \right]_{k=0}. \quad (2.16)$$

Using Eq. (2.14), after some calculations one obtains

$$\langle \hat{x}^2(s) \rangle = \frac{\mathcal{L}[\varphi_R^*(t) \langle x^2(t) \rangle_P] + \frac{1}{s} \mathcal{L}[\varphi_R(t) \langle x^2(t) \rangle_P] - 2 \frac{v}{s^3} \Phi(s)}{1 - \varphi(s)}, \quad (2.17)$$

where

$$\Phi(s) \equiv s \mathcal{L}[\varphi_R(t) \langle |x(t)| \rangle_P] + v[\varphi(s) - \varphi_R(s)] \quad (2.18)$$

and

$$\begin{aligned} \langle x^2(t) \rangle_P &= \int_{-\infty}^{\infty} x^2 P(x, t) dx, \\ \langle |x|^n(t) \rangle_P &= 2 \int_0^\infty x^n P(x, t) dx, \end{aligned} \quad (2.19)$$

with $n = 1, 2, \dots$. In the large time limit, that is, $s \rightarrow 0$ we can simplify Eq. (2.17) keeping the leading-order terms. One gets, after some algebra

$$\langle \hat{x}^2(s) \rangle \simeq \frac{\mathcal{L}[\varphi_R^*(t) \langle x^2(t) \rangle_P] + \frac{1}{3v} \mathcal{L}[\varphi_R(t) \langle |x|^3(t) \rangle_P]}{1 - \varphi_R(s) + \frac{s}{3v} \mathcal{L}[\varphi_R(t) \langle |x(t)| \rangle_P]}. \quad (2.20)$$

Therefore, a finite returning velocity makes the overall asymptotic MSD depend explicitly on the first and third absolute-value moments of the propagator, in addition to the second moment. Crucially, this dependence disappears when the limit $v \rightarrow \infty$ is taken to recover the equivalent expression for instantaneous resetting [20].

In Secs. III and IV, we explore this and more properties on particular scenarios to analyze in more detail the effect that a finite resetting velocity has at long times, comparing our model to some of the most significant results obtained for instantaneous resets.

B. Returning time PDF

After a resetting event, the random walker is forced to interrupt its motion and go back to the origin with constant velocity v . During the time required to go back to the origin and restart its motion, the walker remains in a state, which hinders the overall propagation. Similar models have been studied in the literature, where the walker is forced to remain

inactive at the origin after resetting [23,24]. Nevertheless, in none of these models the duration of the nonpropagating period is considered to depend explicitly on the motion of the walker, which is a natural correlation to be taken into account.

In Ref. [20], the asymptotic behavior of the overall MSD is studied for a stochastic motion process which resets its position at times distributed according to a resetting PDF, after which remains at the origin during a period determined by a residence time PDF. There, the scaling of the overall MSD is shown to strongly depend on the resetting and the residence time PDFs. In the current model, while the resetting PDF is explicitly introduced, the PDF of the nonpropagating period emerges from the combination of both the resetting time PDF $\varphi_R(t)$ and the stochastic motion performed by the walker, i.e., the propagator $P(x, t)$. Therefore, it is convenient to study the stochastic properties of the returning time for a later analysis of the overall transport properties of the system.

In general, the PDF of the returning time can be written as

$$\varphi_r(t) = \int_{-\infty}^{+\infty} dx \delta\left(t - \frac{|x|}{v}\right) \int_0^\infty dt' P(x, t') \varphi_R(t'), \quad (2.21)$$

which is the probability of the exploratory motion ending at a given position x (t' integral) times the probability of the returning state to last at time t from this position (δ term), averaged over all the possible positions. The integral in x can be performed to give a general expression for the returning time PDF in terms of both the propagator and the resetting PDF:

$$\varphi_r(t) = 2v \int_0^\infty P(vt, t') \varphi_R(t') dt' = 2v \Pi(vt, 0), \quad (2.22)$$

with $\Pi(x, s)$ defined from Eq. (2.5). An equation for the n th moment of the returning time PDF can be also found by multiplying both sides of Eq. (2.22) by t^n and integrating over $t > 0$:

$$\langle t_r^n \rangle = \frac{1}{v^n} \int_0^\infty \varphi_R(t) \langle |x(t)|^n \rangle_P dt. \quad (2.23)$$

It is interesting to observe that the contribution of the motion to the n th moment of the returning time PDF comes exclusively from the n th absolute moment of the motion propagator. In the following we dig into these results for two different types of resetting time PDFs.

1. Markovian resetting

As a first case, we analyze the returning time PDF when the resetting is equally probable at any time. This consists on choosing a reset time PDF of the form

$$\varphi_R(t) = r e^{-rt}. \quad (2.24)$$

The general expressions derived above reduce to

$$\varphi_r(t) = 2vr \hat{P}(vt, r) \quad (2.25)$$

and

$$\langle t_r^n \rangle = \frac{r}{v^n} \langle \hat{x}(r)^n \rangle_P. \quad (2.26)$$

Notably, if the n th moment of the motion has a finite Laplace transform, the n th moment of the returning time PDF converges to a finite value. This includes, for instance, all the

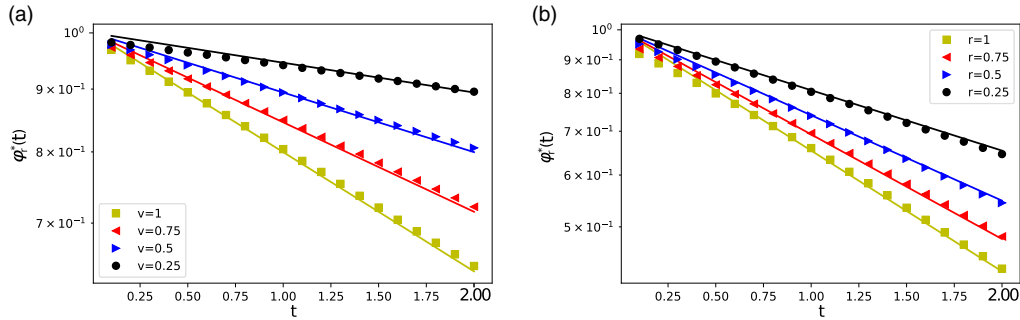


FIG. 1. On the left (a), the returning time survival probability $\varphi_r^*(t) = \int_t^\infty \varphi_r(t') dt' = e^{-v\sqrt{t}}$ for diffusion with $D = 5$ under exponential resetting with $r = 0.25$ is shown for different values of the returning velocity v in a stochastic simulation of the process. On the right (b), the returning time distribution for the same motion is shown with exponential resetting for different r and returning velocity $v = 1$. In both cases, the PDF is represented in a log-linear axis and the exponential behavior can be clearly observed to be in agreement with the corresponding analytical prediction (solid lines).

cases where the moments grow as a power law in time. Between these, let us consider diffusive motion with a Gaussian propagator of the form $P(x, t) = \exp(-x^2/4Dt)/\sqrt{4\pi Dt}$. After some simple calculations, the returning time PDF can be found to be exponential

$$\varphi_r(t) = v\sqrt{\frac{r}{D}} e^{-v\sqrt{\frac{r}{D}t}}. \quad (2.27)$$

This result has been compared to stochastic simulations of the process and it has been seen to be in agreement with them (Fig. 1).

Therefore, for diffusive Gaussian motion, when the resetting PDF is exponential, the duration of the returning state also follows an exponential distribution. In other words, the transition from the returning state to the exploring state is also Markov process and happens at a constant rate, which can be identified to be

$$r_r = v\sqrt{\frac{r}{D}}.$$

Remarkably, the return-to-explore transition rate depends on the explore-to-return rate as a square root. This is, by increasing r , the rate of the return-to-explore transition will be less increased than the rate of the explore-to-return transition. It is also interesting to observe that the returning rate depends linearly with the velocity v . So, aside from the weight factor $\sqrt{r/D}$ related to the propagation ability of the motion, the velocity can be interpreted as the actual transition rate from the returning to the exploring state.

2. Scale-free resetting

Let us now explore the case where the resetting PDF is scale free, meaning that in the long time regime it decays as

$$\varphi_R(t) \sim t^{1+\gamma}, \quad (2.28)$$

with γ a real, positive number. To do so, we employ a particular form of the resetting PDF, being a Pareto distribution of the form

$$\varphi_R(t) = \frac{\gamma r}{(1 + rt)^{1+\gamma}}, \quad (2.29)$$

with $\gamma > 0$. As a difference with the exponential PDF, this choice allows us to study a resetting PDF with diverging moments, having that the m th moment will exist whenever $\gamma > m$. In particular, here we will consider diffusive motion. Introducing the resetting PDF and the propagator to Eq. (2.22), one can formally write

$$\varphi_r(t) = v\gamma\sqrt{\frac{r}{\pi D}} \Gamma\left(\gamma + \frac{1}{2}\right) U\left(\gamma + \frac{1}{2}, \frac{1}{2}; \frac{rv^2}{4D}t^2\right), \quad (2.30)$$

where $U(a, b; z)$ is the Tricomi confluent hypergeometric function or confluent hypergeometric function of the second kind (see Sec. 13 in Ref. [27]). Now, from the long time behavior of the Tricomi function we can obtain the decaying of the returning PDF:

$$\varphi_r(t) \sim t^{-(1+2\gamma)} \text{ as } t \rightarrow \infty. \quad (2.31)$$

Therefore, the returning PDF always decays faster than the resetting PDF [see Eq. (2.28)]. This decaying has been also obtained in stochastic simulations as shown in Fig. 2.

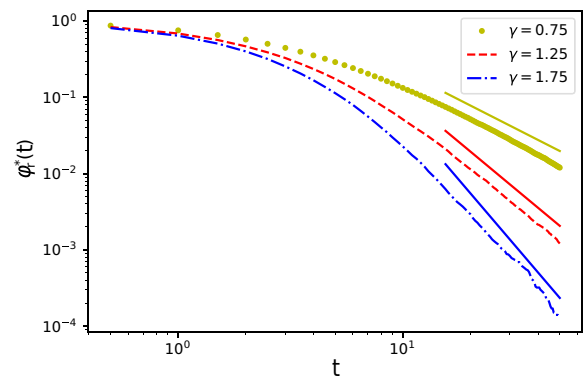


FIG. 2. The returning time survival probability $\varphi_r^*(t) = \int_t^\infty \varphi_r(t') dt' \sim 1/t^{2\gamma}$ is shown for three different simulations with the corresponding γ parameters. A diffusion process with $D = 5$ with resets with $r = 1$ and returning velocity $v = 1$ have been employed. Straight solid lines of slope -2γ have been included as a guide for the eye.

Let us now derive the moments of the returning PDF. To do so, we employ Eq. (2.23) and use the expression for the n th absolute moment of a Gaussian distribution

$$\langle |x(t)|^n \rangle = \Gamma\left(\frac{n+1}{2}\right) \sqrt{\frac{(4D)^n}{\pi}} t^{\frac{n}{2}}. \quad (2.32)$$

This way, one can express the moments of the returning PDF as

$$\langle t_r^n \rangle = 2v\gamma r U\left(\frac{n}{2} + 1, \frac{n}{2} + 1 - \gamma; 0\right). \quad (2.33)$$

Now, the Tricomi confluent hypergeometric function $U(a, b; z)$ at $z=0$ does not converge when $b < 1$. This establishes a condition for the moments of the returning time PDF to exist, being that the n th moment of $\varphi_r(t)$ exist when

$$\gamma > \frac{n}{2}. \quad (2.34)$$

In particular, the returning time will have a finite mean ($n=1$) only if $\gamma > 1/2$. Therefore, for $1/2 < \gamma < 1$, despite the exploration (resetting) time has diverging mean value, the mean returning time to the origin will be finite.

III. MARKOVIAN RESETTING

In this section we analyze the large time behavior of the propagator $\rho(x, t)$ and the MSD $\langle x^2(t) \rangle$ for a random walker under noninstantaneous resettings when the resetting times are drawn from an exponential PDF [Eq. (2.24)]. This has been the most studied case in the literature and various random walks have been tested under this type of resets. For this particular case, one has from Eqs. (2.5) and (2.8) that

$$\Pi(x, s) = r\hat{P}(x, s+r) \quad (3.1)$$

and

$$\Pi^*(x, s) = \hat{P}(x, s+r). \quad (3.2)$$

If $P(x, t)$ has nondiverging moments, in the large time limit (small s), Eq. (2.13) reads

$$\varphi(s) = 1 - sr - \frac{sr}{v} \langle |\hat{x}(s=r)| \rangle_P + O(s^2) \quad (3.3)$$

and the overall propagator reaches the NESS

$$\rho_s(x) = \frac{\hat{P}(x, s=r) + \frac{r}{v} \int_{|x|}^{\infty} \hat{P}(z, s=r) dz}{\frac{1}{r} + \frac{r}{v} \langle |\hat{x}(s=r)| \rangle_P}. \quad (3.4)$$

Here we have made use of Eq. (2.14) and inverted by Fourier. It is interesting to note that this is a general result for any symmetric propagator $P(x, t)$ with finite moments under exponential resetting times.

Despite the tedious calculations employed to reach it, this result is extremely simple to interpret from a physical point of view. We have two different contributions to the PDF at the NESS: the first term in the numerator accounts for the propagation of the stochastic motion, while the second term accounts for the walkers returning to the origin at a finite velocity, after suffering a reset at a position $|z| > |x|$. In fact, taking the limit $v \rightarrow \infty$, corresponding to instantaneous resets, one recovers the result recently found in Ref. [20] for Markovian resetting applied to a general propagator $P(x, t)$.

In Ref. [24], a model with instantaneous resetting followed by a random residence period at the origin was studied. There, it was seen that considering a residence period does not modify the shape of the NESS. In particular, this occurs if one considers the returning time distribution obtained in Eq. (2.25). Contrarily, in Eq. (3.5) one can see that considering a finite returning velocity does modify the shape of the NESS. Therefore, from the model in Ref. [24] with the distribution in Eq. (2.25) one cannot emulate the NESS arising from the noninstantaneous resetting model.

More specifically, for a diffusive random walks the propagator follows a Gaussian distribution, which in the Laplace space takes the form $\hat{P}(x, s) = \sqrt{1/4sD} \exp(-|x|\sqrt{s/D})$. Inserting this result into Eq. (3.5) we obtain

$$\rho_s(x) = \sqrt{\frac{r}{4D}} e^{-|x|\sqrt{r/D}}, \quad (3.5)$$

which is independent of the returning velocity. This is a well-known result already obtained for diffusing particles under Markovian instantaneous resettings [4]. Regarding the MSD, inserting the exponential distribution for the resetting times into Eq. (2.20) one readily finds that the MSD tends, in the $t \rightarrow \infty$ limit, to

$$\langle x^2 \rangle_s = \frac{\langle \hat{x}(s=r)^2 \rangle_P + \frac{r}{3v} \langle |\hat{x}(s=r)|^3 \rangle_P}{\frac{1}{r} + \frac{r}{v} \langle |\hat{x}(s=r)| \rangle_P}. \quad (3.6)$$

Notably, the overall stationary MSD does not depend only on the MSD of the motion $\langle x^2 \rangle_P$ as does when the resetting is instantaneous [4,20] but also on its first and third absolute-value moments.

Let us analyze how the overall MSD depends on the velocity. An extreme (either maximum or minimum) for the MSD in terms of the velocity v does not exist. Nevertheless, depending on the relative values of the three first moments of the motion, the overall MSD may increase, decrease or remain constant with v . General conditions can be indeed established for any propagator under exponential resetting PDF. Thus, we have that the MSD decreases with v if

$$\langle |\hat{x}(s=r)|^3 \rangle_P > 3r \langle |\hat{x}(s=r)| \rangle_P \langle \hat{x}(s=r)^2 \rangle_P, \quad (3.7)$$

and the MSD remains constant with v . It is independent on the velocity if

$$\langle |\hat{x}(s=r)|^3 \rangle_P = 3r \langle |\hat{x}(s=r)| \rangle_P \langle \hat{x}(s=r)^2 \rangle_P. \quad (3.8)$$

In this case, it reduces to the instantaneous resetting value $\langle x^2 \rangle_s = r \langle \hat{x}(s=r)^2 \rangle_P$ [20]. Finally, the MSD increases with v if

$$\langle |\hat{x}(s=r)|^3 \rangle_P < 3r \langle |\hat{x}(s=r)| \rangle_P \langle \hat{x}(s=r)^2 \rangle_P. \quad (3.9)$$

Since $\langle x^2 \rangle_s$ is directly related to the width of the NESS distribution, its shape is affected by the returning velocity v in those cases where $\langle x^2 \rangle_s$ depends on v , that is, when one of the conditions (3.7) or (3.9) is fulfilled. Let us be more specific and consider two cases: the propagators for Brownian motion and for fractional Brownian motion (fBm). In the former case $P(x, t) = [4\pi Dt]^{-1/2} \exp(-x^2/4Dt)$ and the moments involved in Eq. (3.6) are, in the Laplace space,

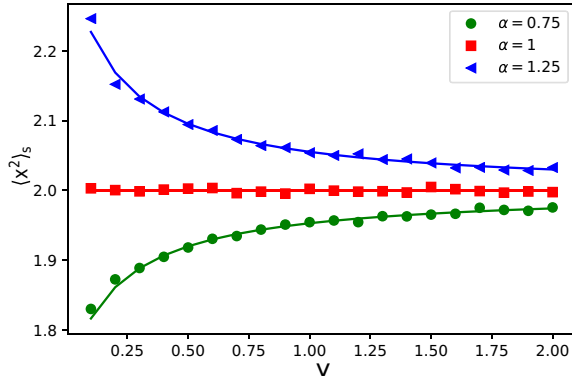


FIG. 3. The results of a stochastic simulation of the stationary MSD for two fractional Brownian motions with $\alpha = 0.75$ and $\alpha = 1.25$, and a normal Brownian motion with $\alpha = 1$ with noninstantaneous resetting ($r = 0.2$) are presented in terms of the returning velocity v . The multiplicative constant has been chosen to be $K = r^\alpha / \Gamma(1 + \alpha)$ in order to have the same instantaneous resetting limit (large v) for all of them. The solid lines are the corresponding analytical predictions from Eq. (3.12).

given by

$$\begin{aligned} \langle \hat{x}(s)^2 \rangle_P &= 2D/s^2 \\ \langle |\hat{x}(s)| \rangle_P &= \sqrt{D}/s^{3/2} \\ \langle |\hat{x}(s)|^3 \rangle_P &= 6D^{3/2}/s^{5/2}. \end{aligned} \quad (3.10)$$

Introducing these results into Eq. (3.6) and simplifying one finds $\langle x^2 \rangle_s = 2D/r$, so that the overall MSD in the large time limit does not depend on v . Note that in this case, condition (3.8) is fulfilled and the NESS distribution does not depend on v .

For a fBm, the propagator is given by $P(x, t) = [4\pi K t^\alpha]^{-1/2} \exp(-x^2/4K t^\alpha)$ and the moments we are interested in are

$$\begin{aligned} \langle \hat{x}(s)^2 \rangle_P &= 2K\Gamma(1 + \alpha)/s^{1+\alpha} \\ \langle |\hat{x}(s)| \rangle_P &= \sqrt{4K}\Gamma\left(1 + \frac{\alpha}{2}\right) / \sqrt{\pi}s^{1+\frac{\alpha}{2}} \\ \langle |\hat{x}(s)|^3 \rangle_P &= (4K)^{\frac{3}{2}}\Gamma\left(1 + \frac{3\alpha}{2}\right) / \sqrt{\pi}s^{1+\frac{3\alpha}{2}} \end{aligned} \quad (3.11)$$

in the Laplace space. It is easy to check from (3.7)–(3.9) that, unlike the normal diffusion, the overall MSD increases with v when $0 < \alpha < 1$ while it decreases with v when $1 < \alpha < 2$. When $\alpha = 1$ we recover the normal diffusion case and the MSD does not depend on v . The overall MSD is found from Eq. (3.6) and Eq. (3.11), which leads to

$$\langle x^2 \rangle_s = \frac{2K\Gamma(1 + \alpha)}{r^\alpha} \frac{1 + \frac{2\Gamma(1 + \frac{3\alpha}{2})}{3\sqrt{\pi}\Gamma(1 + \alpha)} \frac{\sqrt{4K}r^{1-\frac{\alpha}{2}}}{v}}{1 + \frac{\Gamma(1 + \frac{\alpha}{2})}{\sqrt{\pi}} \frac{\sqrt{4K}r^{1-\frac{\alpha}{2}}}{v}}. \quad (3.12)$$

In Fig. 3 we show three representative cases of this result compared to stochastic simulations. There, one can see that for motion processes, which are prone to stay near the origin, as fBm with $\alpha < 1$, the stationary MSD increases with v .

Otherwise, for processes that quickly move away from the origin, as fBm with $\alpha > 1$, a larger returning velocity v makes the stationary MSD decrease. Finally, when $\alpha = 1$, which is the case of Gaussian propagator, the overall stationary MSD is shown to not depend on the returning velocity.

IV. SCALE-FREE RESETTING

In this section we consider a Gaussian propagator and a Pareto for the resetting time PDF. For practical examples of phenomena that may generate scale-free reset times we refer the reader to Ref. [14]. The interest of this distribution is that the exponent γ controls the existence of finite moments. When $0 < \gamma \leq 1$ the distribution lacks moments and behaves like a Mittag-Leffler distribution in the large time limit, i.e., it decays as $t^{-1-\gamma}$. However, when $1 < \gamma \leq 2$ only the first moment is finite and there exists a characteristic resetting rate, when $2 < \gamma \leq 3$ only the first and second moments exist and so on and so forth.

Our first goal is to study the large time behavior of the overall distribution. To this end we take the limit $s \rightarrow 0$ in Eq. (2.12). For a diffusive propagator for the exploring state and the resetting times PDF in Eq. (2.29) we obtain that the NESS is reached when $\gamma > 1$ and it reads

$$\begin{aligned} \rho_s(x) &= \frac{(\gamma - 1)\sqrt{\frac{4\pi D}{r}}}{1 + \frac{\sqrt{Dr}}{v} \frac{\Gamma(\gamma - \frac{1}{2})}{\Gamma(\gamma - 1)}} \left[\Gamma\left(\gamma - \frac{1}{2}\right) U\left(\gamma - \frac{1}{2}, \frac{1}{2}; \frac{rx^2}{4D}\right) \right. \\ &\quad \left. + \frac{r|x|}{2v} \Gamma\left(\gamma + \frac{1}{2}\right) U\left(\gamma + \frac{1}{2}, \frac{3}{2}; \frac{rx^2}{4D}\right) \right]. \end{aligned} \quad (4.1)$$

This has been shown to be in agreement with the results from stochastic simulations of the process [see inset in Fig. 4(a)]. As for the stationary state with Markovian resetting, this result shows that the returning state modifies the shape of the NESS. Particularly, in Fig. 4(a) one can see that the NESS becomes wider when increasing the velocity, showing an asymptotic tendency to the instantaneous resetting NESS.

Our second goal is to find the overall MSD by using Eq. (2.20). To this end we need to compute separately the Laplace transforms that appear in this equation. The Laplace transform of the Pareto PDF is

$$\hat{\varphi}_R(s) = \gamma U(1, 1 - \gamma; s/r). \quad (4.2)$$

Analogously,

$$\begin{aligned} \mathcal{L}[\varphi_R(t)\langle |x(t)| \rangle_P] &= \gamma \sqrt{\frac{D}{r}} U\left(\frac{3}{2}, \frac{3}{2} - \gamma; \frac{s}{r}\right) \\ \mathcal{L}[\varphi_R(t)\langle |x(t)|^3 \rangle_P] &= 6\gamma \left(\frac{D}{r}\right)^{\frac{3}{2}} U\left(\frac{5}{2}, \frac{5}{2} - \gamma; \frac{s}{r}\right), \end{aligned} \quad (4.3)$$

where we made use of Eq. (3.10). Finally, since the survival PDF is $\varphi_R^*(t) = (1 + rt)^\gamma$ we get

$$\mathcal{L}[\varphi_R^*(t)\langle x(t)^2 \rangle_P] = 2D/r^2 U(2, 3 - \gamma; s/r). \quad (4.4)$$

Taking into account the asymptotic expansions for small arguments of the Tricomi functions (see Sec. 13 in Ref. [27])

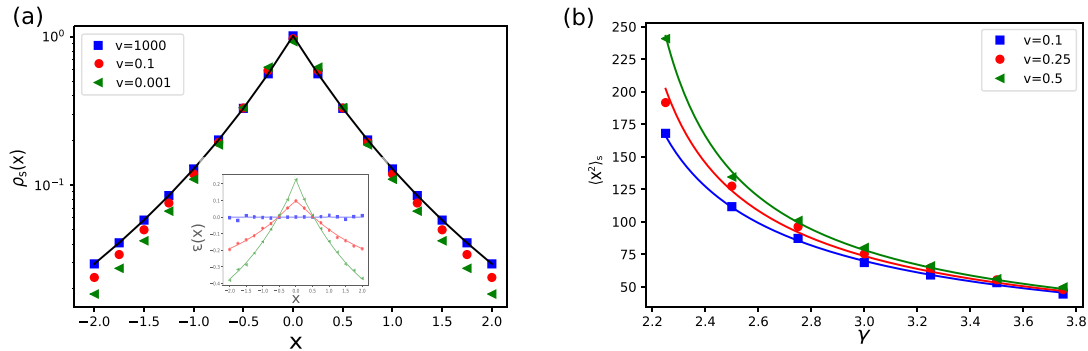


FIG. 4. Diffusive motion reset according to a Pareto PDF with $r = 0.2$ has been stochastically simulated. On the left (a), we show the NESS from simulations with exponent $\gamma = 2.25$ in the Pareto PDF, diffusion constant $D = 0.05$ and different returning velocities. The solid black line corresponds to the instantaneous resetting case, which can be obtained by taking the $v \rightarrow \infty$ limit in Eq. (4.1). As an inset, we include the relative distance between the different noninstantaneous resetting NESS and the instantaneous resetting NESS for simulations (squares, dots and triangles) and the corresponding analytical distribution from Eq. (4.1) (solid curves). On the right (panel B), the stationary MSD is plotted in terms of γ for three different values of the returning velocity and with diffusion constant $D = 5$.

for details) we find that, for $s/r \ll 1$,

$$1 - \hat{\varphi}_R(s) \sim \begin{cases} s^\gamma, & \gamma \leq 1 \\ s, & \gamma > 1 \end{cases} \quad (4.5)$$

and from (4.3) we obtain

$$\mathcal{L}[\varphi_R(t) \langle |x(t)| \rangle_P] \sim \begin{cases} s^{\gamma - \frac{1}{2}}, & \gamma \leq \frac{1}{2} \\ s^0, & \gamma > \frac{1}{2}, \end{cases} \quad (4.6)$$

$$\mathcal{L}[\varphi_R^*(t) \langle x(t)^2 \rangle_P] \sim \begin{cases} s^{\gamma - 2}, & \gamma \leq 2 \\ s^0, & \gamma > 2, \end{cases} \quad (4.7)$$

$$\mathcal{L}[\varphi_R(t) \langle |x(t)|^3 \rangle_P] \sim \begin{cases} s^{\gamma - \frac{3}{2}}, & \gamma \leq \frac{3}{2} \\ s^0, & \gamma > \frac{3}{2}. \end{cases} \quad (4.8)$$

Inserting the results (4.5)–(4.8) into Eq. (2.20) we find the overall MSD in the large time limit. The temporal scaling depends critically on the value of the exponent γ as follows:

$$\langle x^2(t) \rangle \sim \begin{cases} t, & 0 < \gamma \leq 1 \\ t^{2-\gamma}, & 1 < \gamma \leq 2, \\ t^0, & \gamma > 2 \end{cases} \quad (4.9)$$

where, for $\gamma > 2$ the following stationary value is reached:

$$\langle x^2 \rangle_s = \frac{2D}{r(\gamma - 2)} \frac{1 + \frac{\Gamma(\gamma - 3/2)}{v\Gamma(\gamma - 2)} \sqrt{rD}}{1 + \frac{1}{v} \frac{\Gamma(\gamma - 1/2)}{\Gamma(\gamma - 1)} \sqrt{rD}}. \quad (4.10)$$

Therefore, when $0 < \gamma \leq 1$ the overall MSD is diffusive, when $1 < \gamma < 2$ is subdiffusive and when $\gamma \geq 2$ there is stochastic localization, i.e., it saturates to a constant value with the consequent formation of a NESS. So that, as γ increases, the resetting PDF decays faster, i.e., the reset rate increases by hindering the overall transport process. It is interesting to note that if the instantaneous resetting limit ($v \rightarrow \infty$) is taken, the asymptotic scaling of the MSD remains the same. This can be explained with the result in Sec. IIB in which we have found that the resetting PDF always decays slower than the returning PDF. This means that, at long times, the former becomes more relevant than the latter and therefore the effect of the latter is negligible. Seeing this, the asymptotic equivalence of the

MSD scaling for instantaneous and noninstantaneous resetting is not surprising. In fact, this result resembles what has been recently found for a stochastic motion with a residence period after resetting [24]. There, it is shown that when both the resetting and the residence PDFs are long tailed, the residence only affects the asymptotic transport properties of the overall process when its PDF decays slower than the resetting PDF (i.e., it becomes more relevant at long times).

In Eq. (4.10) one can see that the stationary MSD is sensible to the returning velocity [see Fig. 4(b) for numerical confirmation] and in this case the MSD is always an increasing function of v . In addition, the Pareto PDF for resetting times makes possible the coexistence of a subdiffusive behavior [see the MSD in Eq. (4.9) for $1 < \gamma < 2$] with the existence of a NESS given by Eq. (4.1). This counterintuitive phenomenon is explained by noticing that the NESS for this case has divergent MSD. The subdiffusive scaling measures then the speed at which the second moment of $\rho(x, t)$ diverges. Actually, the NESS in Eq. (4.1) exhibits the asymptotic behavior $\rho_s(x) \sim 1/|x|^{2\gamma-1}$ when $x^2 \gg 2D/r$, which resembles the tail of a Lévy distribution precisely when $1 < \gamma < 2$.

V. CONCLUSIONS

We have developed a two-state model to describe resetting as a noninstantaneous movement towards the origin. In one of the states the walker is exploring and performs a random walk, while in the other it travels ballistically until it reaches the origin to start exploring again. In some way, the returning state can be seen as an exploration cost, which depends on both the type of movement in the exploring state and its duration.

We first focus on the case where the resetting (exploring) times are drawn from an exponential distribution and we derive an expression for the stationary distribution attained in this case. It is seen that it does not depend on the returning velocity for a diffusion process and the distribution for the exponential instantaneous resetting case is recovered [4]. Regarding the stationary value of the MSD, a general formula is found in terms of the first, second, and third absolute-value

moments of the propagator, the resetting rate and the returning velocity. It is seen to be an increasing function of the returning velocity for exploring motions, which are more likely to stay close to the origin (fBm with $\alpha < 1$) and a decreasing function when the exploring motion is more likely to occur away from it (fBm with $\alpha > 1$). Therefore, depending on the type of exploration, increasing the returning velocity may help or harm to have a bigger area of influence.

In the case of diffusion with resetting at times drawn from a Pareto PDFs, we find that the asymptotic scaling of the MSD in the noninstantaneous resetting model does not depend on the returning velocity and, consequently, is equivalent to the scaling observed in the instantaneous resetting limit. This is, the MSD scales linearly with time for $\gamma \leq 1$, when $1 < \gamma \leq 2$ the overall transport is subdiffusive and for $\gamma > 2$ the MSD reaches a stationary value. In this case there is a

NESS with a shape that depends explicitly on the returning velocity.

From a practical point of view, the results of this work may also help us to understand the underlying dynamics of certain processes. For instance, in a central-place foraging context where animals explore their environment and occasionally return to their nest, the model gives the particular relation between the dynamics of exploration and return to the nest, on one side, and the stationary distribution on the other. This relation could in principle be validated by empirical data.

ACKNOWLEDGMENTS

This research has been supported by the Ministerio de Economía y Competitividad through Grant No. CGL2016-78156-C2-2-R.

-
- [1] G. Orians and N. Pearson, in *Analysis of Ecological Systems*, edited by D. Horn, G. Stairs, and R. Mitchell (Ohio University Press, Columbus, 1979), pp. 157–177.
 - [2] J. Wolfe and T. Horowitz, *Nat. Hum. Behav.* **1**, 0058 (2017).
 - [3] L. Giuggioli, G. Abramson, V. M. Kenkre, R. Parmenter, and T. L. Yates, *J. Theor. Biol.* **240**, 126 (2006).
 - [4] M. R. Evans and S. N. Majumdar, *Phys. Rev. Lett.* **106**, 160601 (2011).
 - [5] M. Montero and J. Villarroel, *Phys. Rev. E* **87**, 012116 (2013).
 - [6] M. R. Evans and S. N. Majumdar, *J. Phys. A* **47**, 285001 (2014).
 - [7] X. Durang, M. Henkel, and H. Park, *J. Phys. A* **47**, 045002 (2014).
 - [8] A. Pal, *Phys. Rev. E* **91**, 012113 (2015).
 - [9] C. Christou and A. Schadschneider, *J. Phys. A* **48**, 285003 (2015).
 - [10] D. Campos and V. Méndez, *Phys. Rev. E* **92**, 062115 (2015).
 - [11] M. Montero and J. Villarroel, *Phys. Rev. E* **94**, 032132 (2016).
 - [12] V. Méndez and D. Campos, *Phys. Rev. E* **93**, 022106 (2016).
 - [13] A. Pal, A. Kundu, and M. R. Evans, *J. Phys. A* **49**, 225001 (2016).
 - [14] A. Nagar and S. Gupta, *Phys. Rev. E* **93**, 060102(R) (2016).
 - [15] M. Montero, A. Masó-Puigdellosas, and J. Villarroel, *Eur. Phys. J. B* **90**, 176 (2017).
 - [16] V. P. Shkilev, *Phys. Rev. E* **96**, 012126 (2017).
 - [17] Ł. Kuśmierz and E. Gudowska-Nowak, *Phys. Rev. E* **99**, 052116 (2019).
 - [18] A. Masó-Puigdellosas, D. Campos, and V. Méndez, *Front. Phys.* **7**, 112 (2019).
 - [19] S. Eule and J. J. Metzger, *New J. Phys.* **18**, 033006 (2016).
 - [20] A. Masó-Puigdellosas, D. Campos, and V. Méndez, *Phys. Rev. E* **99**, 012141 (2019).
 - [21] A. S. Bodrova, A. V. Chechkin, and I. M. Sokolov, *Phys. Rev. E* **100**, 012120 (2019).
 - [22] A. S. Bodrova, A. V. Chechkin, and I. M. Sokolov, *Phys. Rev. E* **100**, 012119 (2019).
 - [23] M. R. Evans and S. N. Majumdar, *J. Phys. A* **52**, 01LT01 (2018).
 - [24] A. Masó-Puigdellosas, D. Campos, and V. Méndez, *J. Stat. Mech.* (2019) 033201.
 - [25] S. Reuveni, M. Urbakh, and J. Klafter, *Proc. Natl. Acad. Sci. USA* **111**, 4391 (2014).
 - [26] T. Rotbart, S. Reuveni, and M. Urbakh, *Phys. Rev. E* **92**, 060101(R) (2015).
 - [27] M. Abramowitz, *Handbook of Mathematical Functions, With Formulas, Graphs, and Mathematical Tables* (Dover Publications, New York, 1974).

Appendix D

Fourth Article

Conditioned backward and forward times of diffusion with stochastic resetting: A renewal theory approach

Axel Masó-Puigdellosas, Daniel Campos and Vicenç Méndez

*Grup de Física Estadística. Departament de Física, Universitat Autònoma de
Barcelona, 08193 Bellaterra, Spain*

This paper has been published in *Phys. Rev. E* **106**, 034126

Conditioned backward and forward times of diffusion with stochastic resetting: A renewal theory approach

Axel Masó-Puigdellosas, Daniel Campos, and Vicenç Méndez

Grup de Física Estadística, Departament de Física, Universitat Autònoma de Barcelona, 08193 Bellaterra, Spain



(Received 3 May 2022; accepted 5 September 2022; published 16 September 2022)

Stochastic resetting can be naturally understood as a renewal process governing the evolution of an underlying stochastic process. In this work, we formally derive well-known results of diffusion with resets from a renewal theory perspective. Parallel to the concepts from renewal theory, we introduce the conditioned backward B and forward F times being the times since the last and until the next reset, respectively, given that the current state of the system $X(t)$ is known. These magnitudes are introduced with the paradigmatic case of diffusion under resetting, for which the backward and forward times are conditioned to the position of the walker. We find analytical expressions for the conditioned backward and forward time probability density functions (PDFs), and we compare them with numerical simulations. The general expressions allow us to study particular scenarios. For instance, for power-law reset time PDFs such that $\varphi(t) \sim t^{-1-\alpha}$, significant changes in the properties of the conditioned backward and forward times happen at half-integer values of α due to the composition between the long-time scaling of diffusion $P(x, t) \sim 1/\sqrt{t}$ and the reset time PDF.

DOI: [10.1103/PhysRevE.106.034126](https://doi.org/10.1103/PhysRevE.106.034126)

I. INTRODUCTION

The temporal dynamics of point processes are described by successive *events* in the time axis. At each of these events, an action is performed and the system is modified in some way. It may be the flip of a spin in a magnetic system, the breakdown of a machine in a factory, or lightning strikes during a storm.

In many cases, the time spotted between two successive events can be described by independent, identically distributed (iid) random variables. These type of processes are called *renewal processes* [1]. The statistics of renewal processes can be analyzed in terms of the density function of the time between two events, i.e., the holding time probability density function (PDF). Some examples of these properties are the number of events that occurred until time t or the occupation times of different states of the system [2,3]. Two important magnitudes in renewal theory are the forward and the backward times, being the time until the next and since the last event, respectively. The statistical properties of the forward and backward time PDFs depend on the properties of the holding time PDF. For instance, if the holding time PDF is exponential, the forward and backward times have been shown to be exponential too in the long t limit [2]. Fat-tailed holding time PDFs have also been investigated thoroughly in [2,3].

In the past few years, a particular type of renewal process has been studied exhaustively in the scientific literature: stochastic resetting [4,5]. Resets are usually treated as a renewal process forcing another stochastic process to start again. For instance, a diffusive random walker would follow its path until an event (reset) happens. Then, the walker is set to be at its initial position to diffuse until the next event (reset). Since diffusion with Markovian resets was studied in

[6], many stochastic processes have been analyzed when they are suddenly set to start again. For instance, resetting applied to Levy flights [7–9], run-and-tumble random walkers [10,11], and subdiffusive [12,13] random walkers has been studied, as well as other types of stochastic processes [14–21]. Also, different types of resetting mechanisms have been considered, apart from instantaneous Markovian resetting [22–27].

The vast majority of these works focus on two measures: the propagator and the mean first passage time of the process. While the first captures the spatial behavior, the latter provides information about the possible convenience of resetting to facilitate reaching certain interesting areas in a minimum amount of time. Their properties have been studied extensively for different dynamics and resetting mechanisms, as has recently been reviewed in [5]. Particularly, renewal equations have been employed to derive general features of stochastic search with resets [28,29]. Renewal theory may also provide supplementary tools to analyze stochastic dynamics with resets [11,30,31]. For instance, in [31] the forward time has been shown to be crucial to the understanding of resetting expediting first-passage times. In this work, we introduce the conditioned backward and forward times, which are the times since the last reset and until the upcoming reset, given that we know the current state of the process. For a random walker, this would be the backward and forward times conditioned on the walker being at position x . This is particularly interesting when asymptotically it does not depend on the measurement time t . In such cases, the properties of the backward and forward times may be induced from the current state only. This may be useful, for instance, in financial applications. Suppose a particular investor occasionally withdraws capital to accumulate profit. Then, from the current gains one could get statistics about the time until the next withdrawal. Also,

it may have industrial applications: by knowing the current state of a certain part of the assembly line, one may have information about its lifetime.

With this aim, in the following we consider a random walker described by a propagator $P(x, t)$, starting at $x = 0$, which resets its position at times given by the reset time PDF $\varphi(\tau)$. The resulting motion can be seen as a compound process from two individual stochastic processes: a temporal process for the resetting mechanism and a time-dependent spatial process for the position of the walker between two successive resets. In Sec. II we study the temporal dynamics of the process from a renewal theory perspective, and in Sec. III we include the spatial variable. In Sec. IV we introduce the conditioned backward and forward PDFs, and we conclude the article in Sec. V.

II. RENEWAL THEORY FOR STOCHASTIC RESETTING

A renewal process is a counting process where the times between successive events τ_i , happening at times t_i and t_{i+1} (i.e. $\tau_i = t_{i+1} - t_i$), are variables distributed according to a holding time distribution $\varphi(\tau_i)$. With this simple, general setup one can study multiple features in terms of the distribution $\varphi(\tau_i)$, as the number of events at a given time t , or the time of the last and the next event given that the measurement time is t . We refer the interested reader to Chap. 7 in [32] for a detailed viewpoint on renewal processes.

In the context of random walks, a renewal perspective has been extensively employed since [33]. In the current work, we are mainly interested in its applications to resetting, which has already been explored in recent articles [28,29]. The first step is to study the distribution of the times since the last reset and to the next one at a given time t , namely the backward (B) and forward (F) times, respectively. To do so, we derive an expression for the probability $Q_N(t)$ that the N th event happens at time t . For a renewal process, the probability of the N th event at time t is equal to the probability of the $(N - 1)$ th event happening at any past time $t - t'$, times the probability of a single event in the remaining time t' . This is

$$Q_N(t) = \int_0^t Q_{N-1}(t - \tau)\varphi(\tau)dt' \quad (1)$$

or

$$\hat{Q}_N(s) = \hat{Q}_{N-1}(s)\hat{\varphi}(s), \quad (2)$$

where $\hat{f}(s) = \mathcal{L}_s[f(t)] = \int_0^\infty e^{-st}f(t)dt$ is the Laplace transform of $f(t)$ with respect to the variable t . This recurrence equation can be easily solved with the initial condition $\hat{Q}_1(s) = \hat{\varphi}(s)$ to obtain

$$\hat{Q}_N(s) = \hat{\varphi}(s)^N. \quad (3)$$

Summing over N , we can get the overall PDF $Q(t)$ of the last event happening at time t . In the Laplace space, it reads

$$\hat{Q}(s) = \sum_{N=0}^{\infty} \hat{\varphi}(s)^N = \frac{1}{1 - \hat{\varphi}(s)}. \quad (4)$$

In renewal theory, $Q(t)$ is called the rate function. In the limit of long times, and assuming that the mean holding time is finite, we have that $Q(t) \sim 1/\langle\tau\rangle$. This is just the time deriva-

tive of the mean number of renewals in the interval $(0, t)$, i.e., $\langle N(t) \rangle \sim t/\langle\tau\rangle$ [3].

Now, the probability that exactly N events have happened before the measuring time t and the last reset happened at the previous time $t - B$ is thus

$$f^B(N, t, B) = \int_0^t dt' Q_N(t')\delta(t - t' - B) \int_B^\infty dy\varphi(y). \quad (5)$$

Now, summing over N , the PDF of the backward time B at the measurement time t reads

$$\begin{aligned} f^B(t, B) &= \sum_{N=0}^{\infty} \int_0^t dt' Q_N(t')\delta(t - t' - B) \int_B^\infty \varphi(y)dydt' \\ &= \varphi^*(B) \int_0^t Q(t - t')\delta(t' - B)dt' \\ &= Q(t - B)\varphi^*(B). \end{aligned} \quad (6)$$

$\varphi^*(t) = \int_t^\infty \varphi(t')dt'$ is the survival probability of the holding time, which in the Laplace space reads

$$\hat{\varphi}^*(s) = \frac{1 - \hat{\varphi}(s)}{s}.$$

Transforming Eq. (6) by Laplace in both t and B , with conjugate variables s and u , respectively, and using Eq. (3), one finds a formal expression for the backward time PDF in terms of the holding time PDF:

$$\hat{f}^B(s, u) = \frac{1}{1 - \hat{\varphi}(s)} \frac{1 - \hat{\varphi}(s + u)}{s + u}. \quad (7)$$

Let us now derive a similar expression for the forward time distribution $f^F(t, F)$, which is the PDF of the time until the next event F given that the measurement time is t . In this case,

$$f^F(N, t, F) = \int_0^t Q_N(\tau)\varphi(t + F - \tau)d\tau. \quad (8)$$

The forward time PDF is then

$$\begin{aligned} f^F(t, F) &= \sum_{N=0}^{\infty} f^F(N, t, F) \\ &= \sum_{N=0}^{\infty} \int_0^t Q_N(\tau)\varphi(t + F - \tau)d\tau, \end{aligned} \quad (9)$$

which after transforming by Laplace in t and F , and using Eq. (6), turns into

$$\hat{f}^F(s, u) = \frac{1}{1 - \hat{\varphi}(s)} \frac{\hat{\varphi}(u) - \hat{\varphi}(s)}{s - u}. \quad (10)$$

The forward waiting time plays an important role when studying aging phenomena in random walks (see Chap. 4 in [34]) or the first passage of random walks with resetting [31]. Equations (7) and (10) for the backward and forward time PDFs have already been derived and studied intensively in previous works [2,3].

III. PROPAGATOR

The temporal dynamics of a renewal process can be used to describe the resetting of a physical system. Resets are renewals of an underlying stochastic process. Here, we combine

the spatial dynamics of a diffusive random walker with the renewal benchmark presented in the previous section. For a general, stochastic process with a time-dependent PDF $P(x, t)$ and resets happening at random times distributed according to the PDF $\varphi(t)$, the overall propagator can be written as

$$\begin{aligned}\rho(x, t) &= \int_0^t f^B(t, B)P(x, B)dB \\ &= \int_0^t Q(t - B)\varphi^*(B)P(x, B)dB,\end{aligned}\quad (11)$$

where $f^B(t, B)$ is the distribution of the last reset (event) happening at time $t - B$, i.e., the backward time PDF as defined in Sec. II.

The propagator of a diffusive random walker is

$$P(x, t) = \frac{1}{\sqrt{4\pi Dt}} e^{-\frac{x^2}{4Dt}} \quad (12)$$

so that its Fourier transform for the spatial variable reads

$$\tilde{P}(k, t) = \int_{-\infty}^{\infty} e^{-ikx} P(x, t) dx = e^{-k^2 Dt}. \quad (13)$$

Introducing this expression into the Fourier transform of Eq. (11), we obtain

$$\tilde{\rho}(k, t) = \int_0^t Q(t - B)\varphi^*(B)e^{-k^2 DB} dB. \quad (14)$$

And performing the Laplace transform on the time variable, one gets the global propagator in the Fourier-Laplace space in terms of the reset time PDF:

$$\hat{\rho}(k, s) = \frac{1 - \hat{\varphi}(s + Dk^2)}{s + Dk^2} \frac{1}{1 - \hat{\varphi}(s)} = \frac{\hat{\varphi}^*(s + Dk^2)}{1 - \hat{\varphi}(s)}, \quad (15)$$

where we have used Eq. (4) to express the result in terms of the backward time PDF. Then, the behavior of $\rho(x, t)$ depends exclusively on the reset time PDF.

In the following, we study the overall propagator for different types of reset time PDFs. We first analyze distributions with a finite first moment to later consider distributions with all the moments diverging.

A. $\varphi(t)$ with a finite first moment

We start by considering reset time PDFs with a finite first moment. This includes the cases in which all the moments are finite [e.g., Markovian resetting $\varphi(t) = re^{-rt}$], but also the cases in which only the first moment converges [e.g., a power-law PDF decaying as $\varphi(t) \sim t^{-1-\alpha}$ for large t with $1 < \alpha < 2$]. In all these cases, the reset time PDF can be expanded in the Laplace space as $\hat{\varphi}(s) \approx 1 - \langle t \rangle_{\varphi} s + o(s)$. In the long-time limit (small s), Eq. (15) reads

$$\hat{\rho}(k, s) \simeq \frac{\hat{\varphi}^*(Dk^2)}{\langle t \rangle_{\varphi} s}. \quad (16)$$

Taking into account that

$$\hat{\varphi}^*(Dk^2) = \int_0^{\infty} e^{-Dk^2 t} \varphi^*(t) dt, \quad (17)$$

and applying the inverse Fourier and Laplace transforms for the spatial and time variables, respectively, the propagator

reads

$$\begin{aligned}\rho(x, t) &\simeq \frac{1}{2\pi \langle t \rangle_{\varphi}} \int_{-\infty}^{\infty} dk e^{ikx} \int_0^{\infty} dt' e^{-Dk^2 t'} \varphi^*(t') \\ &= \frac{1}{\langle t \rangle_{\varphi}} \int_0^{\infty} dt' \frac{\varphi^*(t')}{\sqrt{4\pi Dt'}} e^{-\frac{x^2}{4Dt'}}.\end{aligned}\quad (18)$$

Since this is time-independent, a stationary state is reached in this scenario, and the propagator is given by

$$\rho_s(x) = \frac{1}{\langle t \rangle_{\varphi}} \int_0^{\infty} dt' \frac{\varphi^*(t')}{\sqrt{4\pi Dt'}} e^{-\frac{x^2}{4Dt'}}. \quad (19)$$

This is general for any type of reset time PDF with a finite first moment. Therefore, under this condition, the resetting is always capable of stopping the expansion of the diffusion and reaching a stationary distribution in space. Let us consider specific types of resetting PDFs. To deal with Markovian resetting, we consider the exponential PDF, i.e.,

$$\varphi(t) = re^{-rt}, \quad (20)$$

where r is the constant reset rate. Inserting Eq. (20) into Eq. (19), one has

$$\rho_s(x) = \frac{1}{2} \sqrt{\frac{r}{D}} e^{-|x| \sqrt{r/D}}, \quad (21)$$

which is a well-known result in the resetting literature [6]. Otherwise, for non-Markovian resetting we consider a power-law reset time PDF of the form

$$\varphi(t) = \frac{\alpha/T}{(1 + t/T)^{1+\alpha}} \quad (22)$$

with $\alpha > 1$ (i.e., a Pareto type II or Lomax distribution), such that

$$\varphi^*(t) = \frac{1}{(1 + t/T)^{\alpha}}. \quad (23)$$

Then

$$\rho_s(x) = \frac{\alpha - 1}{\sqrt{4\pi DT}} \Gamma\left(\alpha - \frac{1}{2}\right) U\left(\alpha - \frac{1}{2}, \frac{1}{2}, \frac{x^2}{4DT}\right). \quad (24)$$

Here, $U(a, b, z)$ is Tricomi's (confluent hypergeometric) function (see Chap. 13 in [35]). This result was also found in [22] by similar means. In the limit $x \rightarrow 0$, the argument of the Tricomi function is small, and using the expansions from Sec. 13.1 in [35], we have

$$\rho_s(x) \simeq \frac{(\alpha - 1)\Gamma(\alpha - 1/2)}{\sqrt{4DT}\Gamma(\alpha)} - \frac{\alpha - 1}{2DT} |x|, \quad (25)$$

and at the resetting point it reaches a finite value

$$\rho_s(0) = \frac{(\alpha - 1)\Gamma(\alpha - 1/2)}{\sqrt{4DT}\Gamma(\alpha)}. \quad (26)$$

When the argument is large, i.e., $x^2 \gg 4DT$, using Eq. 13.1.8 of Ref. [35], we obtain

$$\rho_s(x) \simeq \frac{(\alpha - 1)\Gamma(\alpha - 1/2)}{\sqrt{4\pi DT}} \left(\frac{\sqrt{4DT}}{|x|}\right)^{2\alpha-1}. \quad (27)$$

Equations (21) and (24) are in agreement with numerical simulations of the process, as shown in Fig. 1. The stationary state in Eq. (24) is reached if $\alpha > 1$ and hence the solution

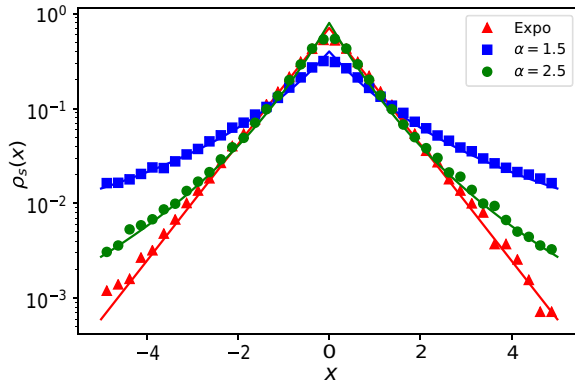


FIG. 1. Log-lin plot of the stationary distribution for diffusion with an exponential reset time distribution (red) and two Pareto reset time distributions with different decay exponents α (green and blue). The simulations have been performed for $N = 10^5$ trajectories with $D = 0.5$, $T = 1$ ($r = 1$ for the exponential), and measurement time $t = 10^4$. The solid curves show the analytical results in Eqs. (21) and (24).

is time-independent. However, when $\alpha < 1$ a natural steady state does not always exist, as we show below.

B. $\varphi(t)$ with all diverging moments

We consider now the scenario in which all the moments of the reset time diverge. We can express the distribution in the Laplace space as

$$\hat{\varphi}(s) \approx 1 - b_\alpha s^\alpha \quad \text{with } 0 < \alpha < 1 \quad (28)$$

for small s . This corresponds to a power-law decay of the form $t^{-1-\alpha}$ as $t \rightarrow \infty$. For a Pareto distribution, $b_\alpha = T^\alpha \Gamma(1 - \alpha)$ with $\alpha < 1$. Plugging this result into Eq. (4), we have that

$$\hat{Q}(s) \simeq \frac{1}{\Gamma(1 - \alpha)(sT)^\alpha}, \quad sT \ll 1. \quad (29)$$

Applying the inverse Laplace transform, we get

$$Q(t) \simeq \frac{T^{-\alpha}}{\Gamma(1 - \alpha)\Gamma(\alpha)t^{1-\alpha}}, \quad t \gg T, \quad (30)$$

which is decreasing with measurement time. Let us analyze $\rho(x, t)$ by studying the bulk of the distribution and its tail separately.

1. Bulk: $t \gg x^2/D$ and $t \gg T$

When the measurement time is much larger than the position, the integral in Eq. (11) can be simplified with Eq. (30). Working out the resulting integral, one arrives at the following expression for the propagator in this region:

$$\begin{aligned} \rho(x, t) &\simeq \frac{1}{\sqrt{4\pi D}} \frac{1}{\Gamma(1 - \alpha)\Gamma(\alpha)} \\ &\times \int_0^t \frac{e^{-\frac{x^2}{4DB}}}{\sqrt{B}(t - B)^{1-\alpha}(T + B)^\alpha} dB. \end{aligned} \quad (31)$$

If we analyze the long-time limit $t \gg T$, the propagator in the bulk region can be expressed as (see Appendix A 1 for further

details)

$$\rho(x, t) \simeq \begin{cases} \frac{\Gamma(\frac{1}{2} - \alpha)}{2\pi\Gamma(1 - \alpha)} \frac{1}{\sqrt{Dt}} & \text{if } 0 < \alpha < \frac{1}{2}, \\ \frac{\sin(\pi\alpha)\Gamma(2\alpha - 1)}{\pi\Gamma(\alpha)(Dt)^{1-\alpha}} \frac{1}{|x|^{2\alpha-1}} & \text{if } \frac{1}{2} < \alpha < 1. \end{cases} \quad (32)$$

It is worth noting that the long-time behavior of the propagator does not have a unique expression for all values of $\alpha < 1$. While for $\alpha > 1/2$ it decays as $t^{-1+\alpha}$, when $\alpha < 1/2$ it decays as $t^{-1/2}$, i.e., independent of the exponent α . This change of behavior below or above $\alpha = 1/2$ has been observed to appear for various measures of a diffusive process under resetting times drawn from the Pareto PDF given in Eq. (22). For instance, in [23], the mean first passage time is shown to converge only when $\alpha > 1/2$, and the PDF at the origin $\rho(0, t)$ has been seen to behave differently for $\alpha < 1/2$ and $\alpha > 1/2$ [25]. The two distinct behaviors of Eq. (32) have been numerically studied, and the results are presented in Fig. 2. There, it is shown that for $\alpha < 1/2$ the propagator tends to be flat when $x^2 \ll 4Dt$, while it behaves as $\rho(x, t) \sim 1/|x|^{2\alpha-1}$ when $\alpha > 1/2$.

2. Tail: $x^2 \propto 4Dt$ and $t \gg T$

When x^2 is comparable to Dt , one has to deal with Eq. (15) differently. In this scenario, both t and x^2/D are large, so s and $s + Dk^2$ are small enough to consider that

$$\hat{\varphi}(s + Dk^2) \simeq 1 - b_\alpha(s + Dk^2)^\alpha. \quad (33)$$

Then, the propagator in the Fourier-Laplace space can be approximated by

$$\hat{\rho}(k, s) \approx \frac{1}{s^\alpha(s + Dk^2)^\alpha} = \frac{1}{s} g\left(\frac{k}{\sqrt{s}}\right), \quad (34)$$

where we have introduced the scaling function

$$g(\chi) = \frac{1}{(1 + D\chi^2)^{1-\alpha}}. \quad (35)$$

In Appendix A 2, we analyze this expression following the same procedure as in [2]. Doing so, we get the formula for the propagator when $x^2 \propto 4Dt$ as

$$\rho(x, t) \simeq \frac{1}{\Gamma(1 - \alpha)} \frac{e^{-\frac{x^2}{4Dt}}}{\sqrt{4\pi Dt}} U\left(\alpha, \frac{1}{2} + \alpha, \frac{x^2}{4Dt}\right). \quad (36)$$

This result was found in [22] by different means. This has been compared to numerical simulations of the process for two distinct exponents α . The results are shown in Fig. 2.

IV. CONDITIONED BACKWARD AND FORWARD TIME

Renewal theory provides information about the backward and forward times of a temporal process given that the current absolute time (measurement time) since the dynamics started is known. Nevertheless, in some scenarios, the measurement time may not be an available quantity. For instance, for a random walker that occasionally resets its position by returning to the origin, it is clear how to determine the current position, while it may not be obvious how to determine the time since its motion started. With this in mind, in this section we introduce the concepts of *conditioned forward and backward time PDFs*, being the PDF for the forward and backward times

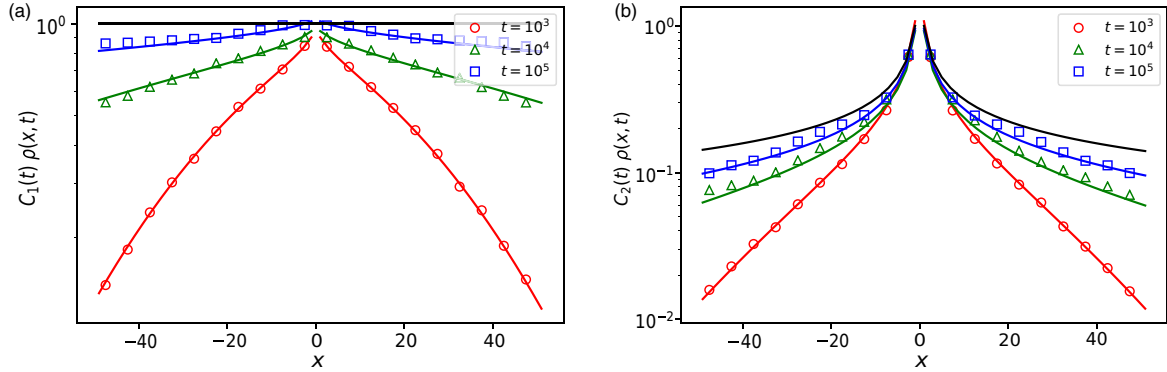


FIG. 2. (a) Propagator of diffusion with Pareto resetting ($\alpha = 0.25$) for the simulation of $N = 10^5$ trajectories at different measurement times t . The multiplicative factor in the y-axis is $C_1(t) = \frac{2\pi\Gamma(1-\alpha)}{\Gamma(1/2-\alpha)}\sqrt{Dt}$. As the time increases, the renormalized propagator tends to be flat as found in Eq. (32). (b) Propagator of diffusion with Pareto resetting ($\alpha = 0.75$) for the simulation of $N = 10^5$ trajectories at different measurement times t . The multiplicative factor in the y-axis is $C_2(t) = \frac{\pi\Gamma(\alpha)(Dt)^{1-\alpha}}{\sin(\pi\alpha)\Gamma(2\alpha-1)}$. As time increases, the propagator approaches this scaling limit. In both panels A and B, the diffusion constant is $D = 0.5$ and $T = 1$ in the Pareto reset distribution. The solid colored lines have been drawn from Eq. (36), while the dots, the triangles, and the squares correspond to the propagator obtained from the simulations. The solid black curves correspond to the asymptotic behavior found in Eq. (32). Both panels have been plotted on the log-lin axis.

given that the current state of the system x is known. We study this magnitude for different types of reset time PDF and determine the conditions under which a stationary form for long t is attained. This is particularly relevant since it permits the study of the backward and forward times by only knowing the current state, independently of the measurement time of the process. In the following, only the position of a diffusive random walker will be considered for an in-depth study of the conditioned forward and backward times, though some of the results herein derived are general for any stochastic process.

A. Conditioned backward time

Let us start by computing the time since the previous reset, given that the walker is currently at position $\mathbf{X}(t)$. This is,

$$p(B|x, t) = \frac{p(B, x|t)}{p(x|t)} = \frac{p(x|B, t)p(B|t)}{p(x|t)}, \quad (37)$$

where Bayes' law has been employed twice. Now, we define $f(B|x, t) = p(B|x, t)$ to be the conditioned backward time PDF. On the right-hand side, $p(B|t) = f^B(t, B)$ is the backward time PDF, $p(x|t) = \rho(x, t)$ is the propagator of the process with resets, and $p(x|B, t) = P(x, B)$ is the Gaussian propagator. Note that the latter is independent of t since the position of the walker only depends on the time elapsed since the last reset. Introducing the expression for the backward time PDF in Eq. (6), one gets

$$f(B|x, t) = \frac{p^B(B, x|t)}{\rho(x, t)} = \frac{Q(t-B)\varphi^*(B)P(x, B)}{\rho(x, t)}. \quad (38)$$

In the following, we derive $f(B|x, t)$ from a different perspective, which will be used afterwards to obtain the equivalent distribution for the conditioned forward time. We start by computing $p(B, x|t)$ in Eq. (37). This is the joint PDF of the walker being at position x and that the last reset happened at a previous time $t-B$, given that measurement time is t . As for the usual backward time, we start by finding the equation when

exactly N resets have happened before the measuring time, i.e.,

$$p^B(N, B, x|t) = \int_0^t Q_N(\tau)\delta(t-\tau-B)\varphi^*(B)P(x, B)d\tau, \quad (39)$$

where we have included the condition that the walker must be at position $\mathbf{X}(B)$ at the measurement time t . Adding all the contributions for N , we get

$$p^B(B, x|t) = \sum_{N=0}^{\infty} \int_0^t Q_N(\tau)\delta(t-\tau-B)\varphi^*(B)P(x, B)d\tau. \quad (40)$$

Applying the Laplace transform and using Eq. (3), one obtains

$$\begin{aligned} \hat{p}^B(B, x|s) &= \varphi^*(B)P(x, B)e^{-sB} \sum_{N=0}^{\infty} \hat{Q}_N(s) \\ &= \frac{e^{-sB}}{1-\hat{\varphi}(s)}\varphi^*(B)P(x, B), \end{aligned} \quad (41)$$

and applying the inverse Laplace transform to the result back to t , taking Eq. (4) into account, we readily obtain

$$p^B(B, x|t) = Q(t-B)\varphi^*(B)P(x, B). \quad (42)$$

It is easy to see that integrating Eq. (42) over x one obtains the marginal PDF for B given in Eq. (6). On the other hand, the marginal PDF obtained by integrating $\hat{p}^B(B, x|s)$ over B is the propagator of a process with resets given by Eq. (11). Now, the backward time distribution conditioned on the walker being at position x at time t reads

$$f(B|x, t) = \frac{p^B(B, x|t)}{\rho(x, t)} = \frac{Q(t-B)\varphi^*(B)P(x, B)}{\rho(x, t)}, \quad (43)$$

which is the same as Eq. (38).

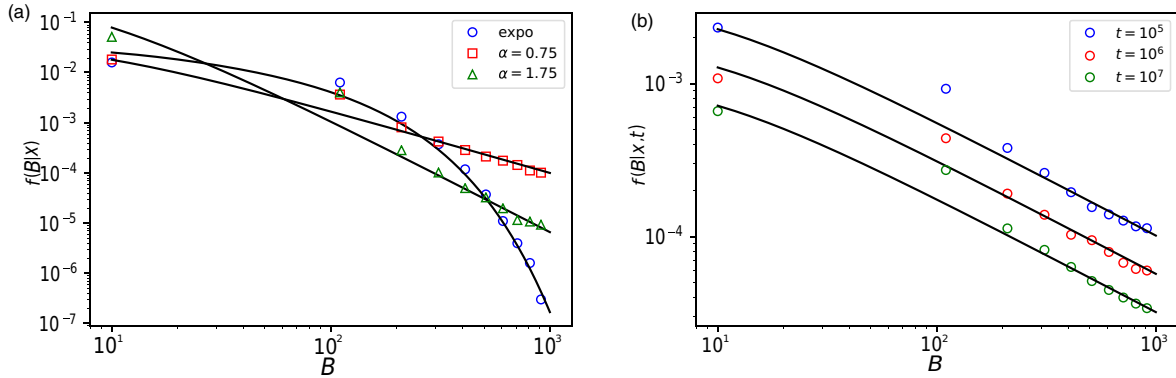


FIG. 3. (a) Stationary conditioned backward time distribution for diffusion and exponential resetting with $r = 0.05$ and Pareto resetting with $T = 5$ and two different values of the decay exponent α . The solid lines have been drawn from the behaviors in Eqs. (46) and (47) for the exponential and Pareto cases, respectively. (b) Conditioned backward time PDF for diffusion and Pareto resetting with $T = 5$ and $\alpha = 0.25$. Three different measurement times have been plotted, showing that $f(B|x, t)$ does not reach a stationary shape. The solid lines correspond to the behavior in Eq. (47) with the time-dependent normalization defined in Eq. (49). Both panels (a) and (b) have been obtained averaging $N = 10^6$ different trajectories with diffusion constant $D = 0.1$.

Let us study the long-time limit ($t \gg B$) of this expression, where we have that $Q(t - B) \simeq Q(t)$. This approximation is accurate for systems where the measurement time scale of the process is many orders of magnitude smaller than the time elapsed since it started. Thus, in this scenario,

$$f(B|x, t) \simeq \frac{Q(t)}{\rho(x, t)} \varphi^*(B) P(x, B). \quad (44)$$

The time dependence of $f(B|x, t)$ comes from the normalization factor only. So, if $Q(t)/\rho(x, t)$ attains a stationary value for long t , then a stationary conditioned backward time PDF $f(B|x)$ exists that only depends on the current position x . Despite focusing on the position of a random walk, let us recall that this expression is general for any stochastic process $\xi(t)$ with propagator $P(\xi, t)$ and resets happening at times given by $\varphi(t)$. In the following, we analyze the characteristics of the conditioned backward time PDF for different reset time distributions.

1. $\varphi(t)$ with a finite first moment

When the reset time PDF has a finite first moment, the diffusion process attains the stationary state given by Eq. (19). Also, in the asymptotic limit $t \gg T$, one has $Q(t) \simeq 1/\langle t \rangle_\varphi$. Therefore, the ratio $Q(t)/\rho(x, t)$ reaches a stationary value, and from Eq. (44) the conditioned backward time PDF tends to

$$f(B|x) \simeq \frac{\frac{\varphi^*(B)}{\sqrt{B}} e^{-\frac{x^2}{4DB}}}{\int_0^\infty dt' \frac{\varphi^*(t')}{\sqrt{t'}} e^{-\frac{x^2}{4Dt'}}}, \quad t \gg T, B \quad (45)$$

considering a diffusive process [Eq. (12)].

When the resetting PDF is exponential, the stationary PDF behaves as

$$f(B|x) \sim \frac{e^{-rB - \frac{x^2}{4DB}}}{\sqrt{B}}, \quad t \gg T, B. \quad (46)$$

Thus, the PDF of the conditioned backward time explicitly depends on the position of the walker even if the resetting is a Markov process. In Fig. 3(A) we compare Eq. (46) (solid line) with numerical simulations (circles). An excellent agreement is observed.

If the reset time PDF is a Pareto distribution with $\alpha > 1$, the behavior of the stationary PDF with B is as follows:

$$f(B|x) \sim \frac{e^{-\frac{x^2}{4DB}}}{\sqrt{B}(1 + B/T)^\alpha}, \quad t \gg T, B, \quad (47)$$

which has been corroborated by numerical simulations of the process in Fig. 3(a) (triangles). We can identify two different regimes. For small B , such that $B \propto x^2/4D$, the diffusion process dominates the behavior of $f(B|x)$ and its shape is Gaussian. However, when $B \gg x^2/4D$, the effect of the resetting becomes more important and the resulting conditioned backward time PDF is a power law of the form

$$f(B|x) \sim \frac{1}{B^{\alpha+1/2}} \quad \text{as } B \gg x^2/4D. \quad (48)$$

Note that when $1 < \alpha < 3/2$, while the reset time PDF has a finite mean, the conditional mean $\langle B|x \rangle$ apparently diverges. Nevertheless, $f(B|x)$ is the asymptotic distribution of $f(B|x, t)$, which has a cutoff at t . Therefore, even when t is large, the cutoff prevents the first moment of the conditioned backward time PDF from diverging.

2. $\varphi(t)$ with all diverging moments

Let us study the behavior of the conditioned backward time PDF for power-law resets of the form Eq. (23) with infinite first moment ($\alpha < 1$). In this case, if $t \gg x^2/DB$, we have

$$\frac{Q(t)}{\rho(x, t)} \simeq \begin{cases} \frac{2\pi}{\Gamma(\alpha)\Gamma(\frac{1}{2}-\alpha)} \frac{\sqrt{D}}{t^{\alpha+\frac{1}{2}-\alpha}} & \text{if } 0 < \alpha < \frac{1}{2}, \\ \frac{\Gamma(\alpha)}{\Gamma(2\alpha-1)} \frac{|x|^{2\alpha-1}}{D^{1-\alpha}T^\alpha} & \text{if } \frac{1}{2} < \alpha < 1. \end{cases} \quad (49)$$

So, for $\alpha \leq 1/2$, it decays as $t^{\alpha-1/2}$ and consequently $f(B|x, t)$ does not reach a stationary distribution in this case.

In Fig. 3(b) we show numerical simulations on which the conditioned backward time PDF varies with t even in the long t limit. However, it does reach a stationary distribution when $1/2 < \alpha < 1$. This case is shown in Fig. 3(a), where we compare the result in Eq. (47) with the numerical simulations for $\alpha = 0.75$ (squares). Here, the ratio $Q(t)/\rho(x, t)$ is finite when $t \rightarrow \infty$ and therefore $f(B|x, t)$ converges to the distribution in Eq. (47) as when $\alpha > 1$ [see Fig. 3(b)].

B. Conditioned forward time

We can proceed similarly for the forward time PDF. In this case, we are interested in knowing the time F until the upcoming reset, given that we know the position of the walker and the measurement time t . We start again by computing the joint PDF of the walker being at position x at time t and the following reset happening at time $t + F$. Given that exactly N resets have occurred since the process started, the joint PDF reads

$$p^F(N, F, x|t) = \int_0^t Q_N(t') \varphi(t + F - t') P(x, t - t') dt', \quad (50)$$

which is similar to Eq. (8) introducing the probability of being at x at time t . Summing over N , we have that

$$p^F(F, x|t) = \sum_{N=0}^{\infty} \int_0^t Q_N(t') \varphi(t + F - t') P(x, t - t') dt', \quad (51)$$

and performing the Laplace transform on t , we obtain

$$\hat{p}^F(F, x|s) = \frac{\mathcal{L}_s[\varphi(t + F)P(x, t)]}{1 - \hat{\varphi}(s)}, \quad (52)$$

where we have used Eq. (3). Using Eq. (4), the above equation can be inverted by Laplace to obtain

$$p^F(F, x|t) = \int_0^t Q(t - t') \varphi(t' + F) P(x, t') dt'. \quad (53)$$

Now, one can recover the general propagator $\rho(x, t)$ in Eq. (11) by integrating over F . The PDF for F is thus

$$f(F|x, t) = \frac{p^F(F, x|t)}{\rho(x, t)} = \frac{\int_0^t Q(t - t') \varphi(t' + F) P(x, t') dt'}{\rho(x, t)}. \quad (54)$$

Again, this expression has been derived for the position of a random walker, but it is general for any stochastic process $\xi(t)$ with resets. As we have done for the backward, in the following we study the behavior of this PDF for different types of reset time distributions.

1. $\varphi(t)$ with finite first moment

Let us first consider resets happening with a finite mean time. In Sec. III we have seen that the system reaches a stationary state under this condition. So, in the long t limit,

$$f(F|x, t) \simeq \frac{\int_0^t Q(t - t') \varphi(t' + F) P(x, t') dt'}{\rho_s(x)} \quad (55)$$

and, applying the Laplace transform for t ,

$$\hat{f}(F|x, s) \simeq \frac{\hat{Q}(s) \mathcal{L}[\varphi(t' + F)P(x, t')]}{\rho_s(x)}. \quad (56)$$

Now, recalling that $\hat{Q}(s) \sim 1/\langle t \rangle_\varphi s$ for small s (large t), we have that

$$f(F|x) = \lim_{t \rightarrow \infty} f(F|x, t) \simeq \frac{\int_0^\infty \varphi(t' + F) P(x, t') dt'}{\langle t \rangle_\varphi \rho_s(x)}. \quad (57)$$

If the resets are exponentially distributed as in Eq. (20), the conditioned forward time PDF approximation takes the same exponential form,

$$f(F|x) \simeq r e^{-rF}, \quad (58)$$

which does not depend on the position of the walker x . This is due to the Markovianity of the resetting process. Regardless of the moment (or position) we consider, the time until the next reset is equally distributed.

If, instead, the reset times are drawn from a Pareto PDF according to Eq. (22) with $\alpha > 1$, the stationary conditioned forward time PDF can be approximated by

$$f(F|x) \simeq \frac{\alpha(\alpha - \frac{1}{2})}{T(1 + \frac{F}{T})^{\frac{1}{2} + \alpha}} \frac{U(\alpha + \frac{1}{2}, \frac{1}{2}, \frac{x^2}{4D(T+F)})}{U(\alpha - \frac{1}{2}, \frac{1}{2}, \frac{x^2}{4DT})}. \quad (59)$$

We refer the reader to Appendix B for the detailed derivation. For small arguments, the Tricomi function tends to a constant value. Therefore, in the limit $F \gg x^2/4D$, the only dependence on the forward time comes from the power-law factor, and the conditioned forward-time PDF scales with F as

$$f(F|x) \sim \frac{T^{\alpha - \frac{1}{2}}}{F^{\frac{1}{2} + \alpha}} \quad \text{as } F \gg x^2/4D, \quad (60)$$

as can be seen in Fig. 4(a), where we show some examples of the distribution obtained from numerical simulations of the process. It is worth noting that the conditioned forward time PDF seems to have a long tail when the reset time PDF scales as $\varphi(t) \sim t^{-1-\alpha}$ with $\alpha > 1$. This happens for $\alpha < 3/2$. So apparently for $1 < \alpha < 3/2$, the mean conditioned forward time is finite while the mean reset time diverges. This strangeness comes from the nonvalidity of the approximation when $F \propto t$. In Eq. (57), when eliminating the current time by taking $t \rightarrow \infty$, we are implicitly considering the $F \ll t$ limit, where the scaling in Eq. (60) is valid. Nevertheless, this behavior varies when $F \propto t$, where the properties of the forward time are significantly different (see [3] for further details). Thus, the approximation employed herein to describe the conditioned forward time is only valid for $F \ll t$. This explains the apparent paradox of having a finite mean conditioned forward time when the mean reset time is finite.

2. $\varphi(t)$ with all diverging moments

Finally, we study the conditioned forward time PDF when all the moments of the reset time distribution diverge. Introducing Eq. (31) into Eq. (54) and proceeding analogously, we

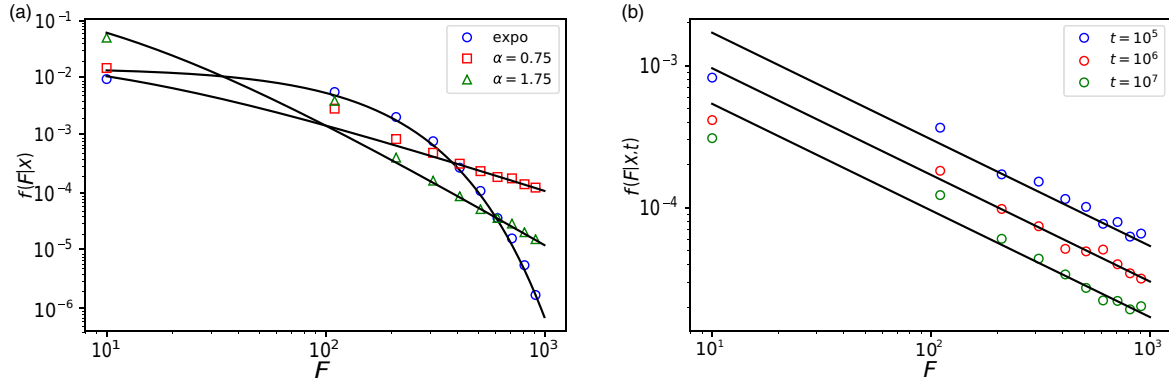


FIG. 4. (a) Stationary conditioned forward time distribution for diffusion under exponential resetting with $r = 0.05$ (circles) and under Pareto resetting with $T = 5$ and two different values of the decay exponent: $\alpha = 0.75$ (squares) and $\alpha = 1.75$ (triangles). The solid lines have been drawn from the behaviors in Eqs. (58) and (59) for the exponential and Pareto cases respectively. (b) Conditioned forward time PDF for diffusion and Pareto resetting with $T = 5$ and $\alpha = 0.25$. Three different measurement times have been plotted, showing that $f(B|x, t)$ does not reach a stationary shape. The solid lines correspond to the power-law behavior in Eq. (60) for $\alpha < 1/2$. Both panels (a) and (b) have been obtained averaging $N = 10^6$ different trajectories with diffusion constant $D = 0.1$.

obtain (see Appendix A for detailed calculations)

$$f(F|x, t) \simeq \frac{1}{T} \frac{\sum_{n=0}^{\infty} \frac{\Gamma(n+\alpha+1)}{n!} \left(-\frac{t}{T+F}\right)^n U\left(\alpha, \frac{1}{2} - n, \frac{x^2}{4Dt}\right)}{\left(1 + \frac{F}{T}\right)^{1+\alpha} \sum_{n=0}^{\infty} \frac{\Gamma(n+\alpha)}{n!} \left(-\frac{t}{T}\right)^n U\left(\alpha, -n, \frac{x^2}{4Dt}\right)}. \quad (61)$$

Similarly to what we have done for the propagator, we can get the long-time limit $t \gg T$, $t \gg F$, and $F \gg x^2/4D$ is the scaling behavior of the conditioned forward time PDF with F in terms of α to be

$$f(F|x, t) \sim \begin{cases} \frac{t^{\alpha-\frac{1}{2}}}{F^{\frac{1}{2}+\alpha}} & \text{for } 0 < \alpha < \frac{1}{2}, \\ \frac{T^{\alpha-\frac{1}{2}}}{F^{\frac{1}{2}+\alpha}} & \text{for } \frac{1}{2} < \alpha < 1. \end{cases} \quad (62)$$

As in the finite-moment scenario, the conditioned forward time PDF attains a stationary shape when $\alpha > 1/2$. However, when the tail of the resetting distribution is wider ($\alpha < 1/2$), the conditioned forward time PDF depends explicitly on time even in the $t \rightarrow \infty$ limit, similarly to what happens with the conditioned backward time PDF. This has been checked numerically, and the results are shown in Fig. 4(b). Once again, the value $\alpha = 1/2$ is relevant to describe both the conditioned forward and backward time PDFs.

V. CONCLUSIONS

In this work, we have introduced the conditioned forward and backward times for stochastic processes with resetting. Interestingly, for a diffusive process with resets, under certain conditions (see Sec. IV) we are able to find a PDF for the forward and backward times that is independent of the measurement time t , depending only on the position of the walker. This result may be of particular relevance when considering processes for which the measurement time is inaccessible. In such cases, one can have statistical information about the forward and backward times by only knowing the current position of the walker. It may be interesting to study the con-

ditioned backward and forward times for dynamics different from the diffusive random walker.

We have found that the behavior of the conditioned backward and forward time PDFs for Pareto distributed reset times is different for $\alpha < 1/2$ than when $\alpha > 1/2$. The appearance of $\alpha = 1/2$ as a turning point is not new in the resetting literature [23,25], and it appears to be a general characteristic of diffusion with power-law resetting. Particularly, it arises when studying temporal features of the process. Somehow, the long-time behavior of diffusion $P(x, t) \sim 1/\sqrt{t}$ adds on the reset time PDF scaling $\varphi(t) \sim t^{-1-\alpha}$ when the focus is put on the time variable. As a result, for diffusion with power-law resetting, significant changes on the dynamics occur when α is a half-integer instead of an integer. It would be interesting to study this aspect in much more detail to acquire more knowledge on the precise mechanism behind the junction of the temporal behavior of diffusion and the resetting.

ACKNOWLEDGMENTS

The authors would like to thank Eli Barkai for his comments and suggestions, which have been of significant help. This research was partially supported by the Ministerio de Economía y Competitividad through Grant No. CGL2016-78156-C2-2-R.

APPENDIX A: PROPAGATOR WITH INFINITE-MEAN RESETTING

1. Bulk $x^2/4D \ll t$

Computing the Fourier transform of Eq. (31), we obtain

$$\tilde{\rho}(k, t) = \frac{\alpha^\alpha e^{-Dk^2 t}}{\Gamma(\alpha)\Gamma(1-\alpha)} \int_0^1 \frac{e^{Dk^2 t y}}{y^{1-\alpha}(1-ay)^\alpha} dy,$$

where we have introduced the new variable $y = 1 - B/t$, and we have defined

$$a = \frac{t/T}{1 + t/T}.$$

In the long-time limit $t \gg T$ one has $a \simeq 1$, and the integral can be expressed in terms of Kummer's M function as

$$\tilde{\rho}(k, t) \simeq e^{-Dk^2 t} M(\alpha, 1, Dk^2 t) \text{ if } 0 < \alpha < 1. \quad (\text{A1})$$

Since we are interested in obtaining the expression of the propagator in the bulk region, we consider $x^2 \ll Dt$, which is equivalent to $Dtk^2 \gg 1$. Kummer's M function $M(a, c, z)$ admits the asymptotic expansion for a large argument (see Eq. 13.1.4 in [35]),

$$M(a, c, z) \simeq \frac{\Gamma(b)e^z z^{a-b}}{\Gamma(a)} [1 + O(|z|^{-1})].$$

Thus, from (A1),

$$\tilde{\rho}(k, t) \simeq \frac{(Dt)^{\alpha-1}}{\Gamma(\alpha)|k|^{2(1-\alpha)}},$$

which after Fourier inversion yields

$$\begin{aligned} \rho(x, t) &\simeq \frac{1}{\pi \Gamma(\alpha)(Dt)^{1-\alpha}} \int_0^\infty \frac{\cos(kx)}{|k|^{2(1-\alpha)}} dk \\ &= \frac{\sin(\pi\alpha)\Gamma(2\alpha-1)}{\pi \Gamma(\alpha)(Dt)^{1-\alpha}} \frac{1}{|x|^{2\alpha-1}} \text{ if } \frac{1}{2} < \alpha < 1. \end{aligned} \quad (\text{A2})$$

Alternatively, we can make use of the power-series expansion of Kummer's M function (see Eq. 13.1.2 in [35]) before inverting by Fourier. Hence, inserting

$$M(\alpha, 1, Dk^2 t) = \frac{1}{\Gamma(\alpha)} \sum_{n=0}^{\infty} \frac{\Gamma(\alpha+n)}{(n!)^2} (Dk^2 t)^n$$

into Eq. (A1), we find

$$\begin{aligned} \rho(x, t) &\simeq \frac{1}{\pi \Gamma(\alpha)} \sum_{n=0}^{\infty} \frac{\Gamma(\alpha+n)}{(n!)^2 (Dt)^{-n}} \int_0^\infty k^{2n} \cos(kx) e^{-Dk^2 t} dk \\ &= \frac{e^{-\frac{x^2}{4Dt}}}{2\pi \Gamma(\alpha) \sqrt{Dt}} \sum_{n=0}^{\infty} \frac{\Gamma(\alpha+n)\Gamma(n+\frac{1}{2})}{(n!)^2} \\ &\quad \times M\left(-n, \frac{1}{2}, \frac{x^2}{4Dt}\right). \end{aligned} \quad (\text{A3})$$

In the bulk region, $x^2 \ll 4Dt$ and then $e^{-\frac{x^2}{4Dt}} \simeq 1 + O(x^2/Dt)$ and $M(-n, \frac{1}{2}, \frac{x^2}{4Dt}) \simeq 1 + O(x^2/Dt)$. On the other hand,

$$\sum_{n=0}^{\infty} \frac{\Gamma(\alpha+n)\Gamma(n+\frac{1}{2})}{(n!)^2} = \frac{\Gamma(\frac{1}{2}-\alpha)\Gamma(\alpha)}{\Gamma(1-\alpha)} \text{ if } 0 < \alpha < \frac{1}{2}.$$

Finally, from this result and (A3) one readily finds

$$\rho(x, t) \simeq \frac{\Gamma(\frac{1}{2}-\alpha)}{2\pi \Gamma(1-\alpha)} \frac{1}{\sqrt{Dt}} \text{ if } 0 < \alpha < \frac{1}{2}. \quad (\text{A4})$$

2. Tail $x^2 \propto Dt$

To derive the expression for the propagator when $x^2/4D \propto t$, we will demonstrate the four points enumerated in Appendix B from [2] for the unconditioned backward time PDF. Here, we reproduce the derivation for the propagator $\rho(x, t)$.

a. Existence of a limiting distribution

To demonstrate that a limiting distribution exists, we study the asymptotic behavior of the moments of the global propagator $\rho(x, t)$. To do so, we employ the well-known formula for the n th moment in terms of the Fourier transform of the propagator,

$$\langle x^n(s) \rangle = t^n \left[\frac{\partial^n \hat{\rho}(k, s)}{\partial k^n} \right]_{k=0} \quad (\text{A5})$$

in the Laplace space. The n th derivative of (A5) can be expressed in terms of the Bell polynomials by using the Faà di Bruno formula [36]

$$\left[\frac{\partial^n \hat{\rho}(k, s)}{\partial k^n} \right]_{k=0} = \frac{\sum_{l=1}^n \hat{\phi}^{*(l)}(s) B_{n,l}(0, 2D, 0, \dots, 0)}{1 - \hat{\phi}(s)}, \quad (\text{A6})$$

where the exponent (l) means derivative of order l . Note that the Bell polynomials $B_{n,l}(0, 2D, 0, \dots, 0) \neq 0$ only when n is even. Thus, the $(2n-1)$ th derivative of the propagator and, therefore, the $(2n-1)$ th moments are 0 as expected due to the symmetry of the process. Then for even n , only the term $l = n/2$ is different from 0. In particular, $B_{n,n/2}(0, 2D, 0, \dots, 0) = n! D^{n/2} / (n/2)!$. Therefore, from (A5) and (A6),

$$\begin{aligned} \langle x^{2n}(s) \rangle &= \frac{(-1)^n}{1 - \hat{\phi}(s)} \hat{\phi}^{*(n)}(s) B_{2n,n}(0, 2D, 0, \dots, 0) \\ &= (-1)^n D^n \frac{2n! \hat{\phi}^{*(n)}(s)}{n! s \hat{\phi}^*(s)}, \end{aligned} \quad (\text{A7})$$

where we have used that $1 - \hat{\phi}(s) = s \hat{\phi}^*(s)$. In the small s limit (or long t), this can be inverted by Laplace to yield

$$\langle x^{2n}(t) \rangle \approx (-1)^n \frac{\Gamma(\alpha)}{\Gamma(\alpha-n)\Gamma(n)} D^n t^n \text{ as } t \rightarrow \infty. \quad (\text{A8})$$

In this limit, all the even moments of the global propagator scale as $\langle x^{2n}(t) \rangle \sim t^n$. Therefore, there must exist a limiting distribution $\rho_Y(y)$ for the variable $y = x/\sqrt{t}$.

b. Expression of the scaling function $g(\chi)$ in terms of the limiting distribution $\rho_Y(y)$

Let us find the integral expression of the scaling function in terms of the (yet unknown) limiting distribution of the previously defined variable y . In the Fourier-Laplace space, the global propagator can be expressed as

$$\hat{\rho}(k, s) = \int_0^\infty dt e^{-st} \langle e^{-ikx} \rangle_X = \int_0^\infty dt e^{-st} \langle e^{-ik\sqrt{t}y} \rangle_Y, \quad (\text{A9})$$

where, in the second equality, the expected value is computed with respect to the new variable y instead of the original position variable x . Taking the expected value out of the integral and performing the Laplace transform within the brackets, one gets

$$\hat{\rho}(k, s) = \frac{1}{s} - \frac{k\sqrt{\pi}}{2s^{3/2}} \left[y e^{-\frac{k^2 y^2}{4s}} \left[i + \operatorname{erfi} \left(\frac{ky}{2\sqrt{s}} \right) \right] \right]_Y. \quad (\text{A10})$$

The expected value has to be taken with the limiting distribution $\rho_Y(y)$.

Now, in the long-time limit (small s), the propagator can be described by the scaling function defined in Eq. (35), as shown in Eq. (34). From this relation, one can isolate the scaling function to be

$$g(\chi) = 1 - \frac{\sqrt{\pi}}{2} \chi \left\langle y e^{-\frac{\chi^2 y^2}{4}} \operatorname{erfi} \left(\frac{\chi y}{2} \right) \right\rangle_Y, \quad (\text{A11})$$

where we have used that $\langle y e^{-\chi^2 y^2/4} \rangle_Y = 0$ due to symmetry.

c. Expression of the moments of the limiting distribution

Let us now expand the expressions of $g(\chi)$ from Eqs. (35) and (A11), and compare to get the moments of $\rho_Y(y)$. Starting from the first, its Taylor series for χ gives

$$g(\chi) = \sum_{n=0}^{\infty} (-1)^n \frac{\Gamma(n+1-\alpha)}{n! \Gamma(1-\alpha)} D^n \chi^{2n}, \quad (\text{A12})$$

while by expanding the derivative of the imaginary error function in the expected value of Eq. (A11), we obtain

$$g(\chi) = \sum_{n=0}^{\infty} (-1)^n \frac{\chi^{2n}}{2^n (2n-1)!!} \langle y^{2n} \rangle. \quad (\text{A13})$$

Now, comparing both expressions term by term, one can isolate the even moments of the limiting distribution to be

$$\langle y^{2n} \rangle = (4D)^n \frac{\Gamma(n+\frac{1}{2}) \Gamma(n+1-\alpha)}{\sqrt{\pi} \Gamma(1-\alpha)}. \quad (\text{A14})$$

The odd moments are null due to the symmetry of the process.

d. Expression of the limiting distribution $\rho_Y(y)$

Finally, we can gather the information in the moments of $\rho_Y(y)$ to get an expression for it. The characteristic function of the limiting distribution can then be computed from the moments

$$\rho_Y(k) = \langle e^{iky} \rangle = \sum_{n=0}^{\infty} \frac{(-k^2)^n}{(2n)!} \langle y^{2n} \rangle \quad (\text{A15})$$

so that

$$\begin{aligned} \rho_Y(k) &= \frac{1}{\Gamma(1-\alpha)} \sum_{n=0}^{\infty} \frac{(-Dk^2)^n}{n!} \Gamma(n+1-\alpha) \\ &= M(1-\alpha, 1, -Dk^2), \end{aligned}$$

where $M(a, b, z)$ is Kummer's M function. To invert by Fourier, we express Kummer's M function in integral form,

$$M(1-\alpha, 1, -Dk^2) = \frac{1}{\Gamma(\alpha) \Gamma(1-\alpha)} \int_0^1 \frac{e^{-Dk^2 u}}{u^\alpha (1-u)^{1-\alpha}} du.$$

Then

$$\begin{aligned} \rho(y) &= \frac{1}{\Gamma(\alpha) \Gamma(1-\alpha)} \frac{1}{\sqrt{4\pi D}} \int_1^\infty \frac{e^{-\frac{y^2}{4D} z}}{\sqrt{z} (z-1)^{1-\alpha}} dz \\ &= \frac{1}{\Gamma(1-\alpha)} \frac{e^{-\frac{y^2}{4D}}}{\sqrt{4\pi D}} U \left(\alpha, \frac{1}{2} + \alpha, \frac{y^2}{4D} \right), \end{aligned}$$

where $U(a, b, z)$ is Kummer's U function. If we undo the change of variable $y = x/\sqrt{t}$, we get the PDF

$$\rho(x, t) = \frac{1}{\Gamma(1-\alpha)} \frac{e^{-\frac{x^2}{4Dt}}}{\sqrt{4\pi Dt}} U \left(\alpha, \frac{1}{2} + \alpha, \frac{x^2}{4Dt} \right). \quad (\text{A16})$$

APPENDIX B: DERIVATION OF EQ. (59)

Inserting Eqs. (12) and (22) in the integral of Eq. (57), one has

$$\begin{aligned} &\int_0^\infty \varphi(t'+F) P(x, t') dt' \\ &= \frac{\alpha}{\sqrt{4\pi DT}} \frac{1}{\left(1 + \frac{F}{T}\right)^{\frac{1}{2} + \alpha}} \\ &\quad \times \int_0^\infty u^{\alpha - \frac{1}{2}} (1+u)^{-1-\alpha} e^{-\frac{x^2}{4D(T+F)} u} du \\ &= \frac{\alpha}{\sqrt{4\pi DT}} \frac{\Gamma(\alpha + \frac{1}{2})}{\left(1 + \frac{F}{T}\right)^{\frac{1}{2} + \alpha}} U \left(\alpha + \frac{1}{2}, \frac{1}{2}, \frac{x^2}{4D(T+F)} \right), \end{aligned} \quad (\text{B1})$$

where we have introduced the variable $u = (T+F)/t'$. Combining Eqs. (24) and (B1), we finally obtain Eq. (59).

APPENDIX C: DERIVATION OF EQ. (61)

Let us begin with the calculation of the numerator in Eq. (54) in the limit $t \gg T$. Introducing Eqs. (12), (22), and (30) into the integral of Eq. (54), we obtain

$$\begin{aligned} &\int_0^t Q(t-t') \varphi(t'+F) P(x, t') dt' \\ &\simeq \frac{\alpha}{t^{3/2} \sqrt{4\pi D} \Gamma(\alpha) \Gamma(1-\alpha)} \\ &\quad \times \int_1^\infty \frac{e^{-\frac{x^2}{4Dt} y} \left(\frac{T+F}{t} + y^{-1}\right)^{-1-\alpha}}{y^{\frac{1}{2} + \alpha} (y-1)^{1-\alpha}} dy, \end{aligned} \quad (\text{C1})$$

where we have defined the variable $y = t/t'$. It is useful to write the factor as

$$\left(\frac{T+F}{t} + y^{-1} \right)^{-1-\alpha} = \sum_{n=0}^{\infty} \lambda_n y^{-n} \quad (\text{C2})$$

as power series of y^{-1} , where λ_n are the corresponding coefficients of the Maclaurin expansion:

$$\lambda_n = \left(\frac{t}{F+T} \right)^{1+\alpha} \frac{\Gamma(1+n+\alpha)}{\Gamma(1+\alpha) n!} \left(-\frac{t}{F+T} \right)^n.$$

Plugging the above expansion into Eq. (C1), we express the integral in the following form:

$$\begin{aligned} &\int_0^t Q(t-t') \varphi(t'+F) P(x, t') dt' \\ &\simeq \frac{\alpha e^{-\frac{x^2}{4Dt}}}{t^{3/2} \sqrt{4\pi D} \Gamma(1-\alpha)} \sum_{n=0}^{\infty} \lambda_n U \left(\alpha, \frac{1}{2} - n, \frac{x^2}{4Dt} \right), \end{aligned} \quad (\text{C3})$$

where we have made use of Eq. 13.2.6 in [35]. The denominator in Eq. (54) is merely the propagator. It can be obtained

by inserting Eqs. (12), (23), and (30) into (11). After defining the new variable $y = t/B$, one has

$$\rho(x, t) \simeq \frac{1}{T^{\alpha} t^{1/2-\alpha} \sqrt{4\pi D} \Gamma(\alpha) \Gamma(1-\alpha)} \times \int_1^{\infty} \frac{e^{-\frac{x^2}{4Dt} y} \left(\frac{T}{t} + y^{-1}\right)^{-\alpha}}{y^{1+\alpha} (y-1)^{1-\alpha}} dy, \quad (\text{C4})$$

which holds in the limit $t \gg T$. Making use of the Maclaurin expansion, the factor $\left(\frac{T}{t} + y^{-1}\right)^{-\alpha}$ reads

$$\left(\frac{T}{t} + y^{-1}\right)^{-\alpha} = \frac{1}{\Gamma(\alpha)} \sum_{n=0}^{\infty} \frac{\Gamma(n+\alpha)}{n!} \left(-\frac{t}{T}\right)^n y^{-n},$$

and the integral in Eq. (C4) can be computed using again Eq. 13.2.6 in [35]. One readily finds

$$\rho(x, t) \simeq \frac{e^{-\frac{x^2}{4Dt}}}{T^{\alpha} t^{1/2-\alpha} \sqrt{4\pi D} \Gamma(\alpha) \Gamma(1-\alpha)} \times \sum_{n=0}^{\infty} \frac{\Gamma(n+\alpha)}{n!} \left(-\frac{t}{T}\right)^n U\left(\alpha, -n, \frac{x^2}{4Dt}\right). \quad (\text{C5})$$

Dividing Eqs. (C1) and (C5), we finally find Eq. (61) in the main text.

- [1] D. Cox, *Renewal Theory*, Methuen's Monographs on Applied Probability and Statistics (Wiley, New York, 1962)
- [2] C. Godreche and J.-M. Luck, Statistics of the occupation time of renewal processes, *J. Stat. Phys.* **104**, 489 (2000).
- [3] W. Wang, J. H. P. Schulz, W. Deng, and E. Barkai, Renewal theory with fat-tailed distributed sojourn times: Typical versus rare, *Phys. Rev. E* **98**, 042139 (2018).
- [4] M. Montero, A. Masó-Puigdellosas, and J. Villarroel, Continuous-time random walks with reset events: Historical background and new perspectives, *Eur. Phys. J. B* **90**, 176 (2017).
- [5] M. R. Evans, S. N. Majumdar, and G. Schehr, Stochastic resetting and applications, *J. Phys. A* **53**, 193001 (2020).
- [6] M. R. Evans and S. N. Majumdar, Diffusion with Stochastic Resetting, *Phys. Rev. Lett.* **106**, 160601 (2011).
- [7] L. Kusmierz, S. N. Majumdar, S. Sabhapandit, and G. Schehr, First Order Transition for the Optimal Search Time of Lévy Flights with Resetting, *Phys. Rev. Lett.* **113**, 220602 (2014).
- [8] Ł. Kuśmierz and E. Gudowska-Nowak, Optimal first-arrival times in Lévy flights with resetting, *Phys. Rev. E* **92**, 052127 (2015).
- [9] V. Méndez and D. Campos, Characterization of stationary states in random walks with stochastic resetting, *Phys. Rev. E* **93**, 022106 (2016).
- [10] M. R. Evans and S. N. Majumdar, Run and tumble particle under resetting: a renewal approach, *J. Phys. A* **51**, 475003 (2018).
- [11] P. C. Bressloff, Occupation time of a run-and-tumble particle with resetting, *Phys. Rev. E* **102**, 042135 (2020).
- [12] Ł. Kuśmierz and E. Gudowska-Nowak, Subdiffusive continuous-time random walks with stochastic resetting, *Phys. Rev. E* **99**, 052116 (2019).
- [13] J. Masoliver and M. Montero, Anomalous diffusion under stochastic resettings: A general approach, *Phys. Rev. E* **100**, 042103 (2019).
- [14] M. Montero and J. Villarroel, Directed random walk with random restarts: The sisyphus random walk, *Phys. Rev. E* **94**, 032132 (2016).
- [15] C. Maes and T. Thiery, The induced motion of a probe coupled to a bath with random resettings, *J. Phys. A* **50**, 415001 (2017).
- [16] S. Belan, Restart Could Optimize the Probability of Success in a Bernoulli Trial, *Phys. Rev. Lett.* **120**, 080601 (2018).
- [17] G. Mercado-Vásquez and D. Boyer, Lotka–volterra systems with stochastic resetting, *J. Phys. A* **51**, 405601 (2018).
- [18] J. Masoliver, Telegraphic processes with stochastic resetting, *Phys. Rev. E* **99**, 012121 (2019).
- [19] M. Magoni, S. N. Majumdar, and G. Schehr, Ising model with stochastic resetting, *Phys. Rev. Res.* **2**, 033182 (2020).
- [20] T. Sandev, V. Domazetoski, L. Kocarev, R. Metzler, and A. Chechkin, Heterogeneous diffusion with stochastic resetting, *J. Phys. A* **55**, 074003 (2022).
- [21] M. R. Evans, S. N. Majumdar, and G. Schehr, An exactly solvable predator prey model with resetting, *J. Phys. A: Math. Theor.* **55**, 274005 (2022).
- [22] A. Nagar and S. Gupta, Diffusion with stochastic resetting at power-law times, *Phys. Rev. E* **93**, 060102(R) (2016).
- [23] A. Masó-Puigdellosas, D. Campos, and V. Méndez, Transport properties and first-arrival statistics of random motion with stochastic reset times, *Phys. Rev. E* **99**, 012141 (2019).
- [24] A. Masó-Puigdellosas, D. Campos, and V. Méndez, Transport properties of random walks under stochastic noninstantaneous resetting, *Phys. Rev. E* **100**, 042104 (2019).
- [25] A. S. Bodrova, A. V. Chechkin, and I. M. Sokolov, Scaled Brownian motion with renewal resetting, *Phys. Rev. E* **100**, 012120 (2019).
- [26] A. S. Bodrova, A. V. Chechkin, and I. M. Sokolov, Nonrenewal resetting of scaled Brownian motion, *Phys. Rev. E* **100**, 012119 (2019).
- [27] Ł. Kuśmierz and T. Toyozumi, Robust random search with scale-free stochastic resetting, *Phys. Rev. E* **100**, 032110 (2019).
- [28] A. Pal and S. Reuveni, First Passage under Restart, *Phys. Rev. Lett.* **118**, 030603 (2017).
- [29] A. Chechkin and I. M. Sokolov, Random Search with Resetting: A Unified Renewal Approach, *Phys. Rev. Lett.* **121**, 050601 (2018).
- [30] B. De Bruyne, J. Randon-Furling, and S. Redner, Optimization in First-Passage Resetting, *Phys. Rev. Lett.* **125**, 050602 (2020).
- [31] A. Pal, S. Kostinski, and S. Reuveni, The inspection paradox in stochastic resetting, *J. Phys. A* **55**, 021001 (2022).
- [32] S. M. Ross, *Introduction to Probability Models* (Academic, San Francisco, CA, 2014).
- [33] W. Feller, Diffusion processes in one dimension, *Trans. Am. Math. Soc.* **77**, 1 (1954).
- [34] J. Klafter and I. M. Sokolov, *First Steps in Random Walks: From Tools to Applications* (Oxford University Press, Oxford, 2011).
- [35] M. Abramovitz and I. A. Stegun, *Handbook of Mathematical Functions. With Formulas, Graphs and Mathematical Tables* (Dover, New York, 1964).
- [36] C. A. Charalambides, *Enumerative Combinatorics* (CRC, Boca Raton, FL, 2018).